THE ROLE OF FREE RADICALS, IRON, AND ANTIOXIDANTS IN ULTRAVIOLET RADIATION-INDUCED SKIN DAMAGE

by

Beth Anne Jurkiewicz

An Abstract

Of a thesis submitted in partial fulfillment
of the requirements for the Doctor of
Philosophy degree in Radiation Biology
in the Graduate College of
The University of Iowa

August 1995

Thesis supervisor: Adjunct Associate Professor Garry R. Buettner

ABSTRACT

Ultraviolet radiation (UV) is thought to cause premature skin aging and cancer through the production of free radical species. However, evidence for UV-induced free radical production in skin is circumstantial. The goal of this research was direct detection of these proposed UV-induced free radicals by electron paramagnetic resonance (EPR) spectroscopy.

Using room temperature EPR, a low steady-state level of the ascorbate radical is detectable in mouse skin; upon exposure to UV this ascorbate free radical signal intensity increases, indicating free radical-mediated oxidative stress. The ascorbate radical is resonance-stabilized and easily detectable by EPR. However, the nonresonance-stabilized radicals produced initially by UV would have very short lifetimes at room temperature. Thus, EPR spin trapping techniques were used to detect these radicals. Using the spin trap α-[4-pyridyl-1-oxide]-N-*tert*-butyl nitrone (POBN), a UV-induced, carbon-centered free radical adduct is observable in mouse skin, characteristic of spin trapped alkyl radicals generated from membrane lipids.

Chronic exposure of skin to UV increases levels of non-hemoglobin iron. Iron can act as a catalyst in oxidative reactions, promoting lipid peroxidation. Topical application of Desferal®, a metal chelator, prior to UV exposure results in a significant reduction in the spin

trapped POBN radical adduct EPR signal, consistent with a role for iron in UV-produced free radical damage in skin.

If free radicals are involved in UV-induced photodamage, then supplementation with antioxidants should prevent this damage. Indeed, topical application of tocopherols reduces UV-induced free radical flux, skin wrinkling, and tumor formation. Tocopherol sorbate is more protective against UV-induced free radical formation and photodamage than α-tocopherol and tocopherol acetate.

The Skh-1 mouse skin model was compared with human skin biopsies for UV-induced free radical formation. In human skin, the ascorbate free radical is also naturally observable by EPR, and increases upon UV exposure. Using spin trapping techniques, other UV-induced radicals are also observable, indicating that the mouse skin model has similarities to human skin.

Due to escalating skin cancer incidence, and an influx of patients seeking care for noncancerous lesions and youth-restorative surgery, the development of the innovative photoprotective concepts addressed in this thesis is imperative.

Abstract approved: _____

Thesis supervisor

_____

Title and department

_____

Date

THE ROLE OF FREE RADICALS, IRON, AND ANTIOXIDANTS IN ULTRAVIOLET RADIATION-INDUCED SKIN DAMAGE

by

Beth Anne Jurkiewicz

A thesis submitted in partial fulfillment
of the requirements for the Doctor of
Philosophy degree in Radiation Biology
in the Graduate College of
The University of Iowa

August 1995

Thesis supervisor: Adjunct Associate Professor Garry R. Buettner

Graduate College
The University of Iowa
Iowa City, Iowa

CERTIFICATE OF APPROVAL

_____

PH.D. THESIS

_____

This is to certify that the Ph.D. thesis of

Beth Anne Jurkiewicz

has been approved by the Examining Committee
for the thesis requirement for the Doctor of
Philosophy degree in Radiation Biology at the
August 1995 graduation.

Thesis committee: _____
Thesis supervisor

_____
Member

_____
Member

_____
Member

_____
Member

ACKNOWLEDGMENTS

I would like to thank Dr. Garry R. Buettner for introducing me to 'the world of free radicals'. He has provided me with guidance, independence, motivation, friendship, and a positive outlook on science and life.

I would like to thank my committee members Drs. Bradley Britigan, C. Patrick Burns, Larry Oberley, and Mike Robbins for their critical evaluation of this work, and more importantly, their time.

I also would like to thank Drs. Donald Bissett, Neil Hogg, Ernest Lam for their critical scientific input and interest in this research project.

This investigation was supported in part by The Procter and Gamble Company, the Center for Global and Regional Environmental Research, and the Center on Aging at The University of Iowa.

TABLE OF CONTENTS

LIST OF TABLES

LIST OF FIGURES

LIST OF ABBREVIATIONS

a	hyperfine constant
AAPH	2,2′-azo-*bis* (2-amidinopropane) dihydrochloride
$Asc^{\bullet-}$	ascorbate free radical
$AscH^-$	ascorbate monoanion
A.U.	arbitrary units
B_e	electron Bohr magneton
BHT	butylated hydroxytoluene
CAT	catalase
DHA	dehydroascorbic
Desferal®	trade name for deferrioxamine mesylate
DETAPAC	diethylenetriaminepentaacetic acid
DMPO	5,5-dimethyl-pyrroline-1-oxide
EDTA	ethylenediaminetetraacetic acid
EPR	electron paramagnetic resonance
ESR	electron spin resonance
FDO	2-furildioxime

Fe(II)	ferrous iron
Fe(III)	ferric iron
g_o	g factor
G	Gauss
GPx	glutathione peroxidase
GSH	glutathione
GSSG	oxidized glutathione
GR	glutathione reductase
Gy	Gray
H_o	magnetic field strength
$HO^{\bullet}$	hydroxyl radical
$HOO^{\bullet}$	hydroperoxyl radical
H_2O_2	hydrogen peroxide
HX	hypoxanthine
IPA	isopropyl alcohol
IR	infrared radiation (0.76 μm - 1000 μm)
J	Joule
$L^{\bullet}$	lipid radical
$LO^{\bullet}$	lipid alkoxyl radical
$LOO^{\bullet}$	lipid peroxyl radical

LOOH	lipid hydroperoxide
MDA	malondialdehyde
MED	minimum erythemal dose
MGD	*N*-Methyl-D-glucamine dithiocarbamate
$O_2^{\bullet-}$	dioxide(1-), superoxide anion radical
PABA	*para*-aminobenzoic acid
PHGPx	phospholipid hydroperoxide glutathione peroxidase
POBN	α-[4-pyridyl 1-oxide]-N-*tert*-butyl nitrone
PUFA	polyunsaturated fatty acid
Rib	riboflavin
TBARS	thiobarbituric acid reactive substances
TOH	tocopherol
SOD	superoxide dismutase
UV	ultraviolet radiation
UVA	320 - 400 nm
UVB	280 - 320 nm
UVC	200 - 280 nm
W	watt
XO	xanthine oxidase

CHAPTER I

INTRODUCTION

Statement of Problem

The free radical theory of aging, first proposed by Denham Harmon at the University of Nebraska, suggests that damage caused by free radicals is responsible for many of the bodily changes that come with aging [Harmon, 1992]. Aging is the accumulation of changes responsible for both the sequential alterations that accompany advancing age and associated progressive increases in the chance of disease and death.

Photoaging, or accelerated skin aging due to ultraviolet (UV) radiation damage in skin, produces wrinkles, loss of elasticity, and premalignant lesions. Non-melanoma skin cancer is the most prevalent form of cancer in the United States [Boring *et al.*, 1993]; more than one million cases are reported each year and projections indicate that 50% of Americans will have skin cancer at least once in their lifetime [Miller and Weinstock, 1994]. This results in substantial cost and impact on the health care system, with a million patients a year, and considerably more seeking care for noncancerous lesions and cosmetic changes to reduce signs of photoaging.

The principal risk factor for photoaging and skin cancer is exposure to ultraviolet radiation (UV); making UV radiation the primary environmental health carcinogen. To

exacerbate the problem, stratospheric ozone, our primary protective screen from UV radiation, is being depleted. Depletion of ozone leaves the upper atmosphere more transparent to UV radiation, thereby increasing our potential for UV exposure and subsequent dermatopathology.

Theoretical Framework

Both acute and chronic exposure of skin to UV radiation results in biochemical changes leading to photoaging and skin cancer. The overall objective of this research program was to provide a better understanding of the initial mechanisms by which UV radiation damages skin. The working paradigm of this research is that UV radiation results in dermatopathology that can lead to accelerated aging and even skin cancer. The working hypothesis of this research is that this damage results from oxidative events in the skin that are mediated by free radical mechanisms, *i.e.*, UV radiation produces free radical species in skin, leading to premature aging. A corollary of this is that application of antioxidants should reduce free radical-initiated injury and protect against photodamage. In addition, it is further hypothesized that UV radiation exposure increases iron levels in the skin thereby enhancing free radical-mediated oxidative reactions in the skin.

These hypotheses were tested by investigating the following specific aims:

1. Examine the use of the ascorbate free radical as a marker of oxidative stress in chemical and biochemical systems (Chapter III);

and then apply this ascorbate radical model to the study of UV radiation-induced free radical formation in Skh-1 mouse skin:

2. Detect and identify by EPR spectroscopy the free radical species produced in UV irradiated skin (Chapter IV);

3. Measure levels of catalytic iron in chronic UV radiation exposed mouse skin and correlate levels of catalytic iron with free radical formation induced by acute UV radiation exposure (Chapter V);

4. Study the effects of topically applied iron chelators on free radical production in acute UV radiation-exposed mouse skin (Chapter V);

5. Determine whether the elimination or reduction of UV radiation-induced free radicals through topical application of antioxidants to skin will protect against photodamage (Chapter VI);

6. Compare UV radiation-induced free radical production in the Skh-1 mouse model to human skin biopsies (Chapter VII).

This research program probes the fundamental mechanism of UV radiation-induced skin damage. Understanding this mechanism will allow us to develop new approaches to protection of skin from UV radiation.

Skin Basics

The Structure and Function of Human Skin

Human skin is well-designed to serve many functions[1]. It is the farthest outpost of the immune system, and acts as a barrier against UV radiation, toxins, chemicals, and pollutants. The skin regulates heat loss and works with other organs to maintain a constant body temperature. It is also of unique importance in the production, storage, and release of vitamin D, which is essential for the absorption of calcium and phosphorous.

The skin is composed of two layers: the epidermis and beneath it, the dermis. The epidermis is the outer layer of the skin. The top layer of the epidermis, the stratum corneum, is comprised of overlapping cells that create a network of protection from the environment. The epidermis is replaced approximately every 28 days as older cells shed from the surface and newer cells move up from the lower level basal cell layer. As basal cells divide and move upwards from the basal cell layer towards the surface of the skin, they become progressively flatter and harder. Eventually, they become part of the stratum corneum as the dead cells in the outermost layer are shed.

Beneath the epidermis is the second layer of skin, the dermis. This layer contains blood vessels, lymph vessels, and nerves. The dermis has two sections, an upper level called the papillary dermis and a lower reticular dermis. The dermis is composed primarily of collagen and elastin. Structural changes occur in these dermal components during normal skin aging. It is

well accepted that the majority of the degradative skin changes that occur with age are the direct result of cumulative UV radiation exposure [Klingman and Gebre, 1991]. Elastosis, wrinkling, and premature aging of the skin are associated with cumulative damage from actinic radiation. Thus, changes that occur with UV radiation-induced accelerated skin aging can provide clues to the natural aging processes because many of the same events occur with normal cell aging, although at a slower rate.

UV Radiation and Skin Cancer

The causal relationship between skin cancer and sun exposure was proposed as early as 1884 [Unna, 1894]. Early studies determined that skin cancer is due to the UV radiation component in sunlight [Findlay, 1928; Roffo, 1934]. UV radiation is thought to be a complete carcinogen, which means it both initiates the malignant process and promotes its growth.

The UV spectrum consists of three specific regions: UVA (320 - 400 nm), UVB (280 - 320 nm), and UVC (200 - 280 nm). Although the UV radiation spectrum at the Earth's surface consists mainly of UVA radiation, it is the UVB wavelength range that is thought to be primarily responsible for the solar carcinogenic effects [Davies and Forbes, 1986]. UVC as well as portions of the UVB wavelengths are filtered out in the upper stratosphere by the ozone layer, which acts as a natural sunscreen.

Depletion of the ozone layer makes the upper atmosphere more transparent to UVB radiation resulting in increased human exposure and consequent elevated incidence of non-

---

[1] For a more extensive review of skin structure and biochemistry see Goldsmith, 1982.

melanoma and melanoma skin cancers. Using kinetic modeling, it has been estimated that for every 1% decrease in stratospheric ozone, UVB radiation exposure will increase by 2.3% [Zurer, 1993], resulting in approximately a 4% increase in skin cancer incidence [Moan *et al.*, 1989]. As can be seen in Figure 1, the percentage change in ultraviolet radiation due to ozone depletion sharply increases in the shorter wavelengths of the UVB spectrum, those wavelengths that are known to be the most biologically effective. The increasing threat of this environmental carcinogen emphasizes the imperative need for a better understanding of the mechanism by which UV radiation induces dermatopathology.

The different wavelengths of UV radiation penetrate with varying efficiencies into the skin; each elicits distinct biological responses. As mentioned previously, UVC wavelengths are primarily absorbed by the ozone layer, and thus are biologically insignificant. UVB wavelengths are most efficient at producing sunburn formation and skin cancer. UVA wavelengths contribute to skin wrinkling and sagging, which contribute to photoaging. The effects of these different wavelengths on free radical formation in skin are examined in Chapter IV.

Free Radicals and Skin

Production of Reactive Oxygen Species by UV Radiation

UVA and UVB radiation are proposed to exert many of their adverse biological effects (*i.e.*, membrane and DNA damage) as a result of the generation of reactive oxygen species [Black, 1987]. These species can be generated both directly and indirectly through photochemical or photosensitization reactions. Cellular photosensitizers absorb UV radiation

leaving the sensitizer in an excited state that can then react with ground state molecular oxygen, converting it to various reactive oxygen species. Chromophores, and possible photosensitizers, in skin include urocanic acid, porphyrins, carotenoids,

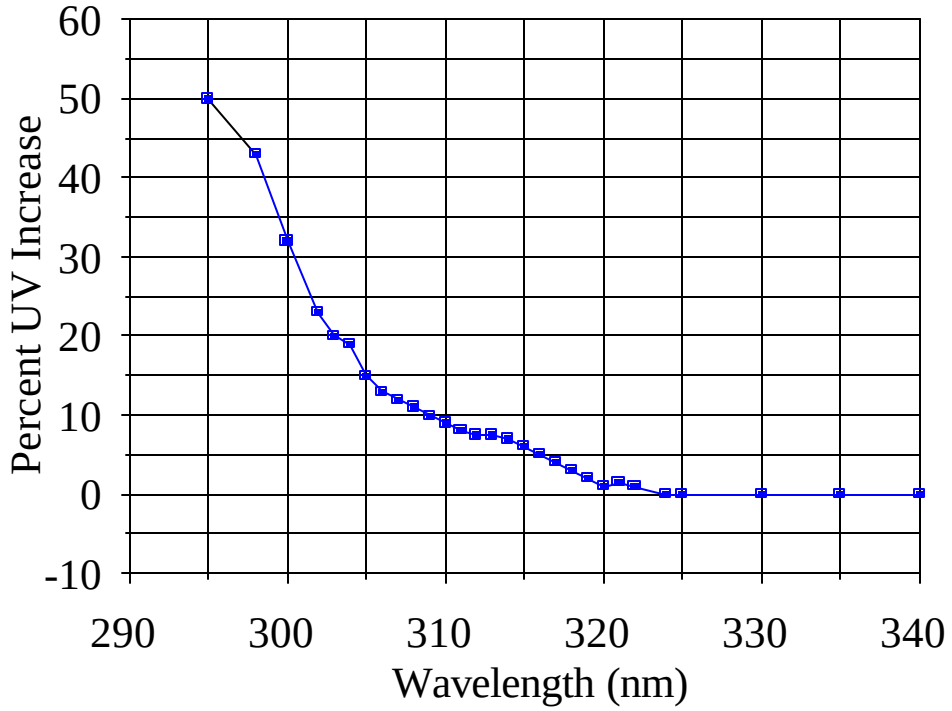

Figure 1. Predicted wavelength dependent changes in ground level UV radiation in Iowa due to depletion of the stratospheric ozone layer.
These changes are calculated for the year 2004 with 1984 as a reference. The largest increase is at the shorter wavelengths, which correspond to the wavelengths of greatest biological response. (This figure was adapted from work done by colleagues at The University of Iowa in the Center for Global and Regional Environmental Research [Crist, 1994].

steroids, NADPH, and flavins [Cadet *et al.*, 1986]. The possible reactive oxygen species formed through photoreactions include free radicals, such as superoxide anion, hydroperoxyl, and hydroxyl radicals, and the non-radical oxidants singlet oxygen and hydrogen peroxide.

Free radicals are generally reactive chemical species that contain one or more unpaired electrons. The hydroxyl radical ($HO^{\bullet}$) is a strongly oxidizing species that can react with almost any type of molecule found in biology at close to diffusion limited rates. However, due to its high reactivity, the hydroxyl radical is a non-selective oxidant and the specificity of its reactions are dictated by the site of radical generation. Hydroxyl radicals also can be produced from the superoxide anion radical. Superoxide anion radical ($O_2^{\bullet -}$) is not considered to be very reactive; however, superoxide may to exert many of its biological effects indirectly through other mechanisms, such as dismutation in water forming singlet oxygen [Corey *et al.*, 1987] and perhaps more importantly hydrogen peroxide [Borg *et al.*, 1978]. Hydrogen peroxide in the presence of catalytic transition metals can be reduced to form extremely damaging $HO^{\bullet}$.

Of the possible oxidants produced in skin by UV radiation, hydrogen peroxide (H_2O_2) is the most stable of the oxygen products. This species is capable of directly oxidizing sulfhydryl groups and can indirectly oxidize polyunsaturated fatty acids. The cytotoxicity of hydrogen peroxide is thought to result from the formation of hydroxyl radicals formed through the Fenton reaction. Singlet oxygen ($^1O_2$), an electronically excited form of oxygen, has a relatively long half-life in aqueous solution (compared with $HO^{\bullet}$) and is thought to be capable of diffusing

appreciable distances before reacting with and damaging lipids, amino acids, and DNA [Ito, 1978; Kasha and Kahn, 1970].

These reactive oxygen species are hypothesized to be responsible for some of the deleterious effects of UV radiation on skin, including photoaging and skin cancer induction [Black, 1987; Chatterjee *et al.*, 1990]. Reactive oxygen species are believed to mediate these effects through membrane lipid peroxidation, chromosomal aberrations, and mutations [Cerutti, 1985; Oberley and Oberley, 1981].

Direct Evidence of Free Radical Production in Skin

Direct detection of UV radiation-induced free radical formation in the skin has been difficult because of the high reactivity and low steady-state concentrations of these putative free radicals. As a result, the majority of evidence for free radical production is circuitous [Meffert *et al.*, 1976; Fuchs *et al.*, 1989; Schallreuter and Wood, 1989]. The only method currently available to directly detect free radicals is electron paramagnetic resonance (EPR) spectroscopy. A more detailed explanation of EPR techniques is discussed in Chapter II.

In 1962, using low temperature EPR (77 K), Norins was the first to show direct evidence of UV radiation-induced free radical formation in skin [Norins, 1962]. The radical was not seen at room temperature, nor was it detectable prior to UV irradiation. He described it as having a broad EPR signal; however, insufficient information was provided to identify the radical species. In 1964, Blois *et al.* also using low temperature EPR reported finding in mouse skin a melanin radical having a line-width of 4 to 8 Gauss, at g = 2.003 [Blois *et al.*, 1964].

This g-value is consistent with similar measurements of other natural melanin samples obtained by EPR spectroscopy. Pathak and Stratton also found melanin radicals in pigmented human skin (77 K) at g = 2.003 and a line-width of 5-6 Gauss [Pathak and Stratton, 1968]. The melanin radical signal intensity was found to increase when the pigmented skin was exposed to UV radiation. In non-pigmented skin, the melanin radical signal was absent before and during irradiation; there were no detectable radicals at room temperature.

At room temperature, near physiologic conditions, the only radical directly detectable in the skin is the ascorbate free radical [Buettner *et al.*, 1987]. This is consistent with ascorbate's role as the terminal small-molecule antioxidant [Buettner, 1993; Frei *et al.*, 1989]. The use of ascorbate as a marker of oxidative stress in chemical and biochemical systems will be examined in Chapter III, and in skin in Chapter IV.

Indirect Evidence of Free Radical Production in Skin

Indirect evidence for the formation of reactive oxidants in epidermal and dermal cell homogenates can be obtained by the quantitation of oxidation products such as thiobarbituric acid reactive substances (TBARS), measurement by chemiluminescence, or detection of radicals by spin trapping. Numerous data in the literature concerning UV radiation-induced oxidative stress are derived from TBARS measurements of lipid peroxidation products [Meffert *et al.*, 1976]. Although this assay is sensitive, it is not specific. In addition to measuring the products of lipid peroxide breakdown, TBARS also measures ketoacid products and some nucleic acid base conjugates, and thus cannot be used to directly measure peroxidation kinetics

[Gutteridge, 1986]. Estimations of chemiluminescence also have considerable drawbacks in practical applicability since only end-products of lipid peroxidation are measured [Iwaoka *et al.*, 1987].

Spin Trapping of Free Radicals in Skin Homogenates

Spin trapping techniques have been used to study UV radiation-induced free radical production in skin cells and homogenates. Using the spin trap 5,5-dimethyl-pyrroline-1-oxide (DMPO), Ogura and Nishi detected a UV radiation-induced free radical adduct in a mouse skin homogenate. They reported lipid-derived radicals detected as a DMPO/L$^{\bullet}$ adduct, with g = 2.0064 and hyperfine splittings, a^N = 15.5 G, a^H =22.7 G [Nishi *et al.*, 1991; Ogura *et al.*, 1987; Ogura *et al.*, 1991], as well as the hydroxyl radical adduct DMPO/$^{\bullet}$OH, $a^N = a^H$=15.5 G [Nishi *et al.*, 1991; Ogura *et al.*, 1987; Ogura *et al.*, 1991; Taira *et al.*, 1992] in skin following UV radiation exposure. Although these experiments indicate that UV radiation produces free radicals, the use of homogenized tissue is prone to production of artifacts [Draper *et al.*, 1993; Kozlov *et al.*, 1992].

Proposed Free Radical Targets in Skin

Almost every cellular constituent is a potential free radical target [Black, 1987]. The main targets of UV radiation-induced free radical attacks in skin are the lipids, proteins, and nucleic acids [Freeman and Carpo, 1982]. Photooxidation of membrane lipids, crosslinking of collagen and elastin [Monboisse and Borel, 1992], and DNA damage all contribute to UV radiation-induced damage of skin. Although DNA has been proposed to be both a possible

target and chromophore for UV radiation damage, nucleic acids absorb chiefly in the UVC region (260 nm). Thus, the most biologically effective wavelengths of solar radiation can not be absorbed significantly by DNA [Fuchs, 1992]. It is likely, therefore, that the pyrimidine dimers, DNA strand breaks, and base modifications that are present in UV radiation exposed skin occur indirectly as a result of free radical attack [Beehler *et al.*, 1992] or from lipid peroxidation.

Photooxidation of membrane lipids may be the most important contributor to the pathogenesis of UV radiation-induced damage [Miyachi *et al.*, 1988; Fuchs and Schurer, 1991]. In skin, approximately 25% of the total surface lipids are unsaturated [Sugiura *et al.*, 1985; Sugiura *et al.*, 1986]; polyunsaturated lipids are vulnerable targets in lipid peroxidation, as *bis*-allylic hydrogens are prone to hydrogen abstraction [Buettner, 1993]. There is considerable circumstantial evidence for UV radiation-induced lipid peroxidation in skin cells and homogenates [Punnonen *et al.*, 1991; Meffert *et al.*, 1976]. UV radiation-induced lipid peroxidation in skin will be examined in Chapter IV.

Lipid peroxidation has three main components: an initiation step, propagation of radical chain reactions, and termination [Halliwell and Gutteridge, 1989]. The initiation step requires the production of an initiating species ($X^{\bullet}$), such as the hydroxyl radical (Equation I- 1). This species then abstracts a hydrogen atom from the methylene carbon located between two adjacent double bonds in a polyunsaturated fatty acid beginning a complex free radical chain

reaction. This results in a reduced species, XH, and a carbon-centered lipid radical, $L^{\bullet}$ (Equation I- 2).

$$X + h\nu \longrightarrow X^{\bullet} \quad \text{(I-1)}$$

$$LH + X^{\bullet} \longrightarrow L^{\bullet} + XH \quad \text{(I-2)}$$

If oxygen is present, $L^{\bullet}$ can form a lipid peroxyl radical, $LOO^{\bullet}$ (Equation I- 3) [Hasegawa and Patterson, 1978].

$$L^{\bullet} + O_2 \longrightarrow LOO^{\bullet} \quad k = 3 \times 10^8 \ M^{-1}s^{-1} \quad \text{(I-3)}$$

The lipid peroxyl radical can then abstract the methylene hydrogen from a neighboring fatty acid forming other lipid radicals (Equation I- 4), while itself generating a lipid hydroperoxide, LOOH. Equation I-3 and I-4 represent the propagation of lipid peroxidation and effectively converts LH into LOOH [Buettner, 1993].

$$LOO^{\bullet} + L'H \longrightarrow LOOH + L'^{\bullet} \quad k = 10 \text{ to } 50 \ M^{-1}s^{-1} \quad \text{(I-4)}$$

This reaction is very slow compared to the addition of oxygen to a lipid radical; however, the lipid hydroperoxides can be transformed into highly reactive species ($LO^{\bullet}$, $LOO^{\bullet}$, $HO^{\bullet}$) by transition metals, other free radicals, thermolysis, photolysis, and dismutation [Meffert *et al.*, 1976]. Because reaction I- 4 is the rate-limiting step in lipid peroxidation, antioxidants such as tocopherol have a chance to compete with oxidizable substrates for the lipid hydroperoxyl radical and thereby break the chain of propagation. Termination of lipid peroxidation occurs when the radicals formed during the propagation step react to form non-radical products. The chemistry of this process is complex and can ultimately give rise to

compounds such as malondialdehyde, 4-hydroxynonenal, ethane, and pentane. Although these decomposition products are non-radicals, they are known to be mutagenic [Mukai and Goldstein, 1976; Esterbauer *et al.*, 1990] and may also act as biological messengers for UV radiation-induced immunological effects, such as contact hypersensitivity [Picardo *et al.*, 1991].

Iron in Skin

Iron can act as a catalyst in lipid peroxidation [Miller *et al.*, 1990]. By reacting with lipid hydroperoxides (Equation I- 5), iron mediates the production of lipid alkoxyl radicals, $LO^{\bullet}$, in a Fenton-like reaction.

$$LOOH + Fe(II) \longrightarrow LO^{\bullet} + HO^{-} + Fe(III) \qquad (I\text{-}5)$$

Alkoxyl radicals can then participate in the initiation of further chain propagation reactions generating lipid and lipid peroxyl radicals (Equations I- 6, I- 7) or can undergo β-scission to form aldehydes, RCH=O, and short chain alkyl radicals, such as ethyl and pentyl radicals, $RCH_2^{\bullet}$ (Equation I- 8).

$$LO^{\bullet} + LH \longrightarrow LOH + L^{\bullet} \qquad (I\text{-}6)$$

$$LO^{\bullet} + LOOH \longrightarrow LOH + LOO^{\bullet} \qquad (I\text{-}7)$$

$$LO^{\bullet} \longrightarrow RCH_2^{\bullet} + RCH{=}O \qquad (I\text{-}8)$$

Skin is a significant site of iron excretion with 0.24 - 0.6 mg lost daily by epithelial cell desquamation, as well as by gland and sweat secretions [Green *et al.*, 1968]. Therefore in hyper-proliferative disease, such as psoriasis, an increase in iron is found in psoriatic lesions

compared with normal skin [Molin and Wester, 1973]. In human skin the iron content of the epidermis from high sun exposure sites (forehead, cheek) versus low sun exposure sites (buttocks, thighs) are as follows: high sun mean 53.0 ± 34.4 ppm (n = 7); low sun mean 17.8 ± 9.3 ppm (n = 9). Data is based on dry weight [Bissett *et al.*, 1991]. In Skh-1 mouse skin, chronic exposure to UV radiation leads to significantly increased basal amounts of non-hemoglobin iron [Bissett *et al.*, 1991]. The localization and quantitation of iron in chronic UVB exposed mouse skin will be examined in Chapter V.

Chelation of iron should prevent iron-mediated free radical production and consequently reduce oxidative damage. Topical application of iron chelators to mouse skin has been found to be photoprotective during chronic UV exposure by decreasing photowrinkling and increasing the exposure time necessary for tumor induction [Bissett *et al.*, 1991]. In Chapter V topical application of the metal chelator Desferal® is examined for its effects on UV radiation-induced free radical formation in skin.

Cutaneous Defense

The skin has evolved several natural protective mechanisms to defend against insult from visible and UV radiation exposure, high oxygen concentrations, and other environmental insults. For example, physical blockers of UV radiation absorption in the skin are the compact horny layer of the stratum corneum, which absorbs and scatters UV radiation, and melanin, which acts as a UV-absorbing optical filter and also a free radical scavenger. Although a correlation exists between free radical defenses of the epidermis and skin pigmentation, melanogenesis occurs in

the supra-basal and basal cells of the epidermis [Schallreuter and Wood, 1989.]. Only an assessment of free radical scavenging mechanisms on the outermost living and dead portions of the epidermis are the subject of this work because these free radical reactions occur before the interventions of melanin.

Antioxidants

In addition to physical UV radiation blockers, both enzymatic and non-enzymatic antioxidant defenses form a protective network against reactive forms of oxygen produced by UV radiation in the skin. Antioxidants are found to inhibit UV-induced lipid peroxidation both *in vitro* and *in vivo* and reduce chronic cutaneous damage by scavenging reactive oxygen species [Black and Chan, 1975].

The two main dietary antioxidants in skin are ascorbate and tocopherol. Ascorbate, vitamin C, is the major water-soluble chain breaking antioxidant [Frei *et al.*, 1989]. Ascorbate is found in large quantities in the skin and may be the key antioxidant in skin based on its ability to reduce nitroxide free radicals [Fuchs *et al.*, 1989]. The amount of ascorbate present in human and mouse skin is given in Table 1. Ascorbate may also protect the skin by recycling the antioxidant tocopherol.

Tocopherol (TOH), vitamin E, is the major lipophilic antioxidant found in mammalian tissues [Burton and Ingold, 1986]. Levels of tocopherols in human and mouse skin are given in Table 1. Tocopherol has a weak UV filter effect; furthermore, it is proposed to inhibit UVB radiation-induced erythema irrespective of whether it is applied to skin before or after irradiation

[Potapenko *et al.*, 1984]. Tocopherol's protective effects against UV-induced free radical damage may be due to its ability to out compete the lipid propagation reaction (Equation I- 4) [Patterson, 1981].

Table 1. Ascorbate and tocopherol levels in skin.

Antioxidant	Species	Tissue	Concentration	Reference
Ascorbate	Human	Total Skin	0.23 μmol/gram dry wt	Stuttgen and Schaefer, 1974
		Epidermis	0.06 μmol/gram wet wt	Priestley and Foster, 1959
		Epidermis	3.8 μmol/gram wet wt	Shindo *et al.*, 1994
		Dermis	0.7 μmol/gram wet wt	Fuchs *et al.*, 1989a
	Mouse	Total Skin	0.007 μmol/gram protein	Fuchs *et al.*, 1989a
α-Tocopherol	Human	Epidermis	180-675 ng/mg protein	DeSimone *et al.*, 1987
			31 nmol/gram wet wt	Fuchs *et al.*, 1989a
		Dermis	16.2 nmol/gram wet wt	Fuchs *et al.*, 1989a
γ-Tocopherol	Human	Epidermis	3.26 nmol/gram wet wt	Fuchs *et al.*, 1989a
		Dermis	1.78 nmol/gram wet wt	Shindo *et al.*, 1994
Tocopherol	Mouse	Whole Skin	200 pmol/mg protein	Fuchs *et al.*, 1989b
			5 nmol/gram wet weight	Packer *et al.*, 1991

$$LOO^{\bullet} + TOH \longrightarrow LOOH + TO^{\bullet} \qquad k = 8 \times 10^{4}\ M^{-1}s^{-1} \qquad \text{(I-9)}$$

Because of tocopherol's ability to scavenge lipid peroxyl radicals, tocopherol is studied in Chapter VI as a protectant against UV radiation-induced free radical formation and photodamage.

Another dietary antioxidant is the carotenoid precursor to vitamin A, β-carotene. β-carotene is a lipophilic antioxidant that prevents lipid peroxidation in model membranes; it directly quenches singlet oxygen [Burton and Ingold, 1984] and lipid peroxyl radicals [Cabrini *et al.*, 1986]. Topical application of β-carotene to skin significantly reduced UVB radiation-induced lipid peroxidation in hairless mice [Pugliesi and Lampley, 1985], possibly by scavenging singlet oxygen and free radicals [Foote and Denny, 1968; Pollitt, 1975; Krinsky and Deneke, 1982]. Typical levels of β-carotene in human skin are ≈ 222 ng/gram protein in the epidermis [Vahlquist *et al.*, 1982] and ≈ 230 ng/gram protein in total skin [Newcomb *et al.*, 1990].

The skin also contains antioxidant enzymes that although not directly examined in this thesis, may contribute significantly to the skin defense. Superoxide dismutase (SOD) is a metal-protein complex that catalyzes the dismutation of superoxide anion radicals into hydrogen peroxide and oxygen [Niwa, 1987]. Human skin SOD consists mainly of CuZn-SOD (1.6 - 1.8 U/mg protein[2]) located in the lower layers of the epidermis [Kobayashi *et al.*, 1991]. Although skin is continuously exposed to an oxidizing environment, the content of total SOD in

[2] Assay by Floche [Floche, 1984], where one unit is defined as the amount of SOD inhibiting the cytochrome c reduction rate by 50% under given assay conditions.

the epidermis is much lower when compared with other tissues such as heart and kidney [Oberley *et al.*, 1990]. Pretreatment of the epidermal surface of guinea pigs with liposomal CuZn-SOD prior to UVB exposure prevents the increase in lipid peroxide formation [Miyachi *et al.*, 1987].

Catalase (CAT) is a heme enzyme that catalytically decomposes two molecules of hydrogen peroxide to water and oxygen and may also oxidize a substrate using a hydroperoxide as a hydrogen donor. Catalase can decompose hydrogen peroxide produced by near-UV radiation and may possibly act as a photosensitizer [Eisenstark and Perrot, 1987].

The selenoenzyme glutathione peroxidase (GPx) can reduce and detoxify H_2O_2 as well as various organic hydroperoxides at the expense of glutathione (GSH) to form oxidized glutathione (GSSG). GSH is naturally regenerated from GSSG by the catalyst glutathione reductase (GR). Depletion of GSH in skin of UVB exposed mice by buthionine S,R-sulfoximine, an irreversible inhibitor of γ-glutamylcysteine synthase, results in an increased number of sunburn cells formed [Hanada *et al.*, 1991]; individual keratinocyte cell death appearing in the epidermis that is hypothesized to result from UV-induced reactive oxygen species.

Although glutathione is important in protection against oxidative stress, membrane-bound phospholipid hydroperoxides are not susceptible to direct reduction by GPx [Raes *et al.*, 1987]. Instead, the oxidized fatty acyl group must first be hydrolyzed by phospholipase A_2. Thus, GPx can only act on liberated fatty acid hydroperoxides. The selenium-dependent

peroxidase, phosopholipid hydroperoxide glutathione peroxidase (PHGPx) directly reduces hydroperoxides within phospholipid membranes [Thomas *et al.*, 1990]. Therefore, PHGPx may be more important in protecting membranes against UV radiation-induced lipid peroxidation. Unfortunately, there are no available data on the levels of PHGPx in skin.

Ubiquinones/ols are electron carriers that contain a lipophilic side chain and a redox active quinone/hydroquinone head group. Ubiquinone in the epidermis is bound to both mitochondrial and non-mitochondrial cytoplasmic components and is thought to play a metabolic role in the mitochondrion [Brody, 1968]. Ubiquinols can act as antioxidants by scavenging singlet oxygen or by inhibiting lipid peroxidation [Caprini *et al.*, 1986] Ubiquinone 10 is detectable in human skin at ≈ 7 U/gram [Shindo *et al.*, 1994], while ubiquinone 9 is found in mouse skin at concentrations on the order of 36 - 98 pmol/mg protein [Giovannini *et al.*, 1988].

In addition to these systems, there is also a membrane bound antioxidant in the skin called thioredoxin reductase [Rozell and Hansson, 1985]. It is proposed that thioredoxin reductase reduces nitroxides as well as superoxide anion radicals in the epidermis and constitutes a first line of defense against free radical damage at the epidermal surface [Schallreuter *et al.*, 1978]. However, its role in free radical defense is not well understood and criticism has been raised on interpretation of studies of thioredoxin reductase performed thus far [Fuchs, 1988].

Effects of Cell Type on Antioxidant Levels

Antioxidant enzyme defenses vary depending on skin cell type. Fibroblasts have more catalase, peroxidase, and SOD activity than either keratinocytes or melanocytes [Yohn *et al.*, 1991]. Melanocytes were found to have the smallest amounts of the antioxidants measured and may rely on the radical scavenging ability of melanin rather than other antioxidant enzymes. However, melanin is stored in membrane-bound cytoplasmic vesicles and may not be available to freely scavenge non-melanosomal toxic oxygen species. Therefore, melanin would not be protective against cell membrane or cytoplasmic insults, which would be a disadvantage during acute UV exposure.

When working with cells in culture the preferred culture media of each different cell type may affect antioxidant status; however, altering the media did not affect the antioxidant hierarchy among the three skin cell types examined. In addition, there is no difference in antioxidant enzyme activity in cells taken from Black versus Caucasian people [Yohn *et al.*,1991].

In this thesis project, whole skin, epidermis and dermis intact, from albino mice was used so there were no melanocytes present and no discrepancies due to tissue culture media. The human skin samples used in Chapter VII were obtained from Caucasian biopsies.

Effects of Age on Antioxidant Levels

Chronic UV radiation exposure accelerates photoaging of the skin [Richard *et al.*, 1994]. The free radical hypothesis of aging has been the predominant theory. A recent paper by W. Orr and R. Sohol was the first to show a direct relationship between free radicals,

antioxidants, and aging [Orr and Sohol, 1994]. Many reports dealing with the free-radical theory of aging have focused on the possibility that tissue antioxidant capacity decreases as a function of age. However, when studying the antioxidant profile of the skin of young and old hairless mice, catalase, superoxide dismutase, and glutathione peroxidase activity were unchanged. Only glutathione peroxidase from the epidermis showed a decrease in activity due to age. Both the absolute level of oxidized glutathione and the ratio of oxidized to reduced glutathione were higher in the dermis from old mice. Hydrophilic and lipophilic antioxidants did not change as a function of age, nor did the lipid hydroperoxide levels. These results suggest that skin aging is not accelerated in old age due to a decrease in the antioxidant capacity of the tissue. The data are compatible, however, with the idea that continuous damage to skin tissue accumulates throughout an organism's lifetime because radical scavenging cannot be 100% efficient [Lopez-Torres *et al.*, 1994]. In this research project, mice used in experiments were between 4 weeks and 18 months old. In this time frame there should not be any significant alterations in the skin's antioxidant capacity.

Ultraviolet Radiation Effects on Antioxidants

Antioxidant enzymes may be depleted or inactivated during UV radiation exposure resulting in lowered defense capabilities. Depending upon what oxidative products are produced, antioxidants may be affected to varying degrees. For example, although glutathione peroxidase is quite resistant to oxidative damage by hydrogen peroxide, it is quite vulnerable to depletion by hydroperoxides [Vessey and Lee, 1993], which are known to be produced by UV

radiation-induced lipid peroxidation in skin [Punnonen *et al.*, 1991]. Table 2 summarizes some of the studies of the effects of UV radiation on skin antioxidant levels. Several of the studies report changes in the levels of SOD in UV exposed skin [Punnonen *et al.*, 1991, Maisuradze *et al.*, 1987; Pence and Naylo, 1990]. The conflicting reports of changes in antioxidant levels may be due to the inconsistencies in methodology, such as measuring total SOD versus CuZn and MnSOD separately, cell type examined, and UV dose used in the different studies.

Dose Response of Ultraviolet Radiation on Antioxidants

Different doses of UV radiation may directly produce varying levels of free radical formation and also deplete or inhibit levels of antioxidants to different degrees [Shindo *et al.*, 1994]. A dose response study of the effects of acute ultraviolet irradiation on non-enzymatic skin antioxidants found that ascorbate was rapidly depleted at doses between 0 and 5 J/cm^2 but was less affected by doses greater than 5 J/cm^2. In contrast, glutathione, ubiquinol, and α-tocopherol remained relatively unchanged at doses between 0 and 5 J/cm^2, but decreased to varying degrees with doses from 5 to 25 J/cm^2; ubiquinol was completely depleted, whereas α-tocopherol dropped by 30%. The concentration of lipid hydroperoxides increased as dose increased. Even at the lowest dose, 80% of the mouse minimal erythemal dose (MED), lipid hydroperoxide formation was observed [Shindo *et al.*, 1994]. In the acute UV radiation exposure experiments presented in this

Table 2. Acute UV radiation-exposure decreases skin antioxidant levels.

Sample type	Wavelength	Time post-UV	Results	Reference
Keratinocyte	UVB	30 min	↓ CAT , ↓ SOD	Punnonen *et al.*, 1991
Mouse	>280 nm	immediate	↓ GR, ↓ CAT, = GPx, = SOD	Fuchs *et al.*, 1989
Rat	UVB	immediate	↓ SOD, ↓ GR, ↓ GPx	Maisuradze *et al.*, 1987
Mouse	UVB	12 - 72 hr	↓ CAT , ↓ SOD	Pence *et al.*, 1990
Mouse	UVB	3 hr	= SOD	Eisenstark *et al.*, 1987
Guinea pig	UVB	immediate	= SOD	Fuchs *et al.*, 1989
Mouse	>280 nm	immediate	↓ GSH, ↑ GSSG, = $AscH^-$	Fuchs *et al.*, 1989
Mouse	UVB	10 min	↓ GSH, ↑ GSSG	Connor and Wheeler, 1987
Mouse	>280 nm	immediate	↓α-tocopherol, ↓ ubiquinol 9	Suttgen and Schaefer, 1974

Note: = refers to no change reported;

↓ indicates significant reduction;

↑ indicates significant increase.

thesis, the same UV radiation source and dose was used to prevent inconsistencies in free radical flux.

Antioxidant Supplementation

Supplementation of skin with various antioxidants may compensate for UV radiation-induced depletion thereby preventing free radical damage. Topical application and dietary supplementation of certain antioxidants were found to decrease erythema following acute UV exposure and delay the onset of tumor formation in chronically exposed animals [Pauling, 1991]. Topical application of ascorbate or α-tocopherol was found to be most effective against short-term UV radiation-induced lipid peroxidation products in the skin, whereas application of glutathione, superoxide dismutase, and catalase were found to have minimal to no protective effect in the system examined [Bissett *et al.*, 1990]. Dietary supplementation of antioxidants, though found to be less effective than topical application due to the length of time required to reach optimal concentrations in the skin, are also found to protect against UV radiation-induced damage [Record *et al.*, 1991]. These antioxidant studies provide strong circumstantial evidence of a significant role for antioxidants in protecting skin against UV radiation-induced damage. Chapter VI presents a detailed study of the effects of three different forms of tocopherol on reducing UV radiation-induced free radical formation and signs of photoaging.

Current Protection

Sunscreens have been reported to prevent squamous cell carcinomas in animals [Klingman *et al.*, 1980] and protect against some premalignant changes in humans [Thompson *et al.*, 1993]. However, sunscreen protection against UV radiation-induced inflammation may encourage prolonged exposure to UV radiation and thus may actually increase the risk of photoaging and skin cancer development [Wolf *et al.*, 1994]. Sunscreens (*para*-aminobenzoic acid (PABA), ethyl hexyl p-methoxy cinnimate, and benzophenones) are effective in protecting against UV radiation-induced epidermal erythema and hyperplasia; however, they failed to protect against enhancement of melanoma growth [Wolf *et al.*, 1994]. Prolonged exposure to wavelengths in the UVA region, are proposed to be partially responsible for the increased incidence of cutaneous melanoma [Klepp and Magnus, 1979]. Thus, other forms of photoprotection must be developed to protect universally against premalignant changes that may result in melanoma or non-melanoma skin cancer.

Significance

This work explores the production of free radicals by UV radiation in skin. Specifically, this project examines the use of the ascorbate free radical as a marker of oxidative stress in chemical and biochemical system (Chapter III) and applies this marker to the study of UV radiation-induced free radical formation in skin (Chapter IV). It also investigates the potential role of iron, and determines whether topical application of metal chelator Desferal® can influence this process (Chapter V). The potential use of topically applied tocopherols, in the

reduction of free radical formation and photodamage is examined in Chapter VI. Finally, the Skh-1 mouse model is compared to the use of human skin biopsies in the study of UV radiation-induced free radical formation in Chapter VII.

This work provides a better understanding of the mechanisms involved in UV radiation-induced damage to skin. It also allows the development of a novel approach for protection against photoaging and the prevention of skin cancer. Instead of only blocking the UV radiation from being absorbed as is done now with UV absorbers, such as PABA and cinnamate, common ingredients found in over-the-counter sunscreens, skin can be protected by intercepting UV radiation-induced free radicals with metal chelators and antioxidants before the propagation of deleterious oxidative reactions can occur. The development of this innovative photoprotective concept is of particular importance due to the unknown magnitude of repercussions that will result from depletion of our earth's natural sunscreen, the ozone layer.

CHAPTER II

ELECTRON PARAMAGNETIC RESONANCE METHODOLOGY

Principles and Instrumentation

Free radicals are, in general, short-lived paramagnetic species. Because of their high reactivity, absolute bimolecular rate constants for free radical reactions are most often in the 10^6-10^9 $M^{-1}s^{-1}$ range. Thus, radicals usually have short lifetimes, $t_{1/2} \approx$ 10^{-3}-10^{-9} s, making them difficult to detect in room temperature, aqueous conditions.

Electron paramagnetic resonance (EPR), also known as electron spin resonance (ESR), is an important spectroscopic technique for the study of free radicals [Carrington and McLachlan, 1967; Thornally, 1986; Campbell and Divek, 1984]. The basic techniques and instrumentation of EPR will be discussed in this chapter. For a more in depth explanation, there are a variety of helpful reviews and books on the topic of EPR techniques [Poole and Farach, 1994; Atherton, 1973; Symons, 1978; Wertz and Bolton, 1972].

A basic schematic of an EPR spectrometer is given in Figure 2. The technique involves placing a sample into an applied magnetic field (H_o). The sample is exposed to monochromatic microwave radiation generated by a klystron. The wavelength of radiation is a few centimeters. A waveguide directs this radiation into the sample cavity that lies between the poles of the electromagnet. With the microwave frequency held constant, the magnetic field H_o is swept gradually until resonance is achieved. At

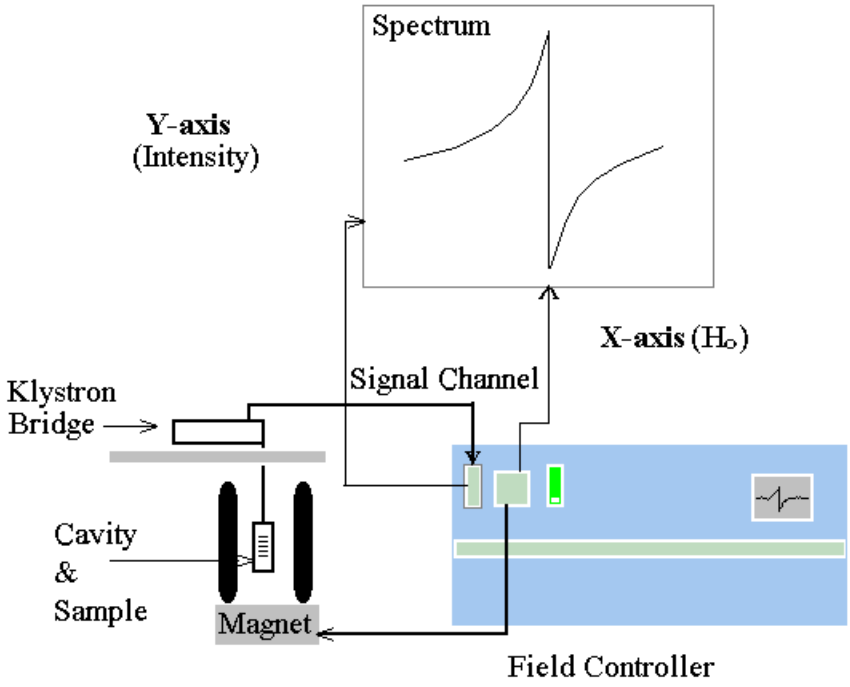

Figure 2. The general outlay of an EPR spectrometer.

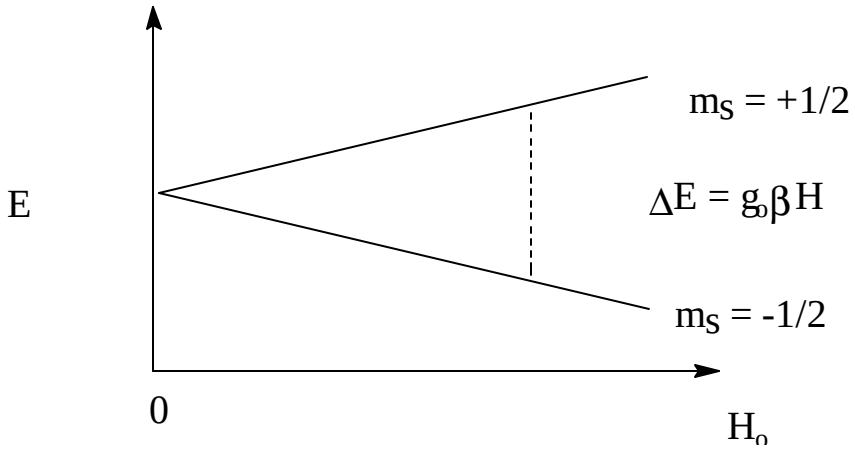

Figure 3. Variation of the spin state energy as a function of the applied magnetic field.

resonance, the amount of energy absorbed by the sample is maximized. Energy absorption is monitored by a crystal detector. A system employing modulation coils and a phase-sensitive detector aids in sensitivity and makes it most appropriate to present the spectrum as the first derivative of the absorption spectrum.

In the presence of a magnetic field, the electron can exist in one of two quantum states: a low energy state where the magnetic moment is aligned parallel with the applied magnetic field ($m_s = -½$), or a high energy state, where the magnetic moment is aligned anti-parallel to the applied magnetic field ($m_s = +½$). As the lower spin state is more populated, microwave energy absorption occurs during transitions to the higher energy state at resonance (Figure 3).

In the EPR experiment, free radical spin centers are promoted from the low energy to high energy state by absorption of microwave radiation. The spins return to the low energy state through relaxation effects. The absorption of microwave radiation occurs at resonance; when $\Delta E = h\nu = g_o\beta_e H_o$, where h is Plank's constant, ν is the operating microwave frequency of the spectrophotometer (fixed), β_e is the electron Bohr magneton (a constant), H_o is the applied magnetic field strength (varies), and g_o is a proportionality constant, the g factor.

For a free electron, $g_o = 2.00232$[3]. This is the free spin g value. For an unpaired electron in an atom or molecule, there will also be orbital angular momentum. The orbital and spin magnetic moments interact and deviations of the g_o factor from the free spin value are observed. There are small deviations in the g_o factor from one radical to another that can

[3] The g_o implies that g is isotropic; since g is a tensor (*i.e.*, $g = (g_{xx} + g_{yy} + g_{zz})/3$).

provide useful information. For example, in carbon-centered organic free radicals the g_o factor is always close to the free electron value. However, for metal compounds the g_o factor does vary substantially from species to species, and can be used to gain information about the electronic structure of the metal ion. In addition to the g_o factor, three other parameters can provide information; linewidth, intensity, and hyperfine coupling constants.

Linewidth is defined as the width at half-maximum of the observed spectral lines. Line shape describes the Gaussian-Lorentzian distributions of the free radical spectral species (Figure 4).

Another useful parameter is intensity. The intensity of a spectral line is proportional to the amount of radical present. By comparing signal intensity with known concentrations of free radicals in solution, it is possible to make quantitative determinations of radical species generated under various experimental conditions.

A fourth aspect of EPR spectra that is useful are the EPR hyperfine splitting patterns and coupling constants. Hyperfine constants describe the interaction of the electron with neighboring nuclei that have magnetic moments. Hyperfine splittings arise because the small changes in the effective magnetic field strength, produced by neighboring nuclei, are experienced by the unpaired electron. As an example, an unpaired electron localized around a nitrogen atom will actually be subject to one of three different effective magnetic fields corresponding to the three spin states of ^{14}N. Thus, there will be three energy absorptions giving rise to a triplet absorption spectrum. The hyperfine splitting patterns and coupling constants can be used to

identify radical species and can indicate the minimum number of species that comprise a spectrum. The hyperfine constant is given the symbol (a) and are usually reported in units of magnetic field strength (Gauss or Tesla).

EPR spectra are usually collected as the first derivative of the absorption spectra, because for EPR the absolute magnitude of ΔE is quite small and the excess population of electrons in the lower energy state is very small. Therefore, it is common to try to improve the signal to noise level of this small net absorption by recording the spectrum as a first derivative curve, as opposed to a direct absorption curve. Because spectra are usually displayed as first derivatives, line widths are conveniently measured as the distance (in Gauss or Tesla) between the maximum and minimum of a line, the peak-to-peak linewidth (ΔH_{pp}). Signal height intensities are measured as the total amplitude of each line.

Spin Trapping Techniques

EPR is the best method available to directly detect free radicals; however, when working with room-temperature aqueous solutions, EPR has limitations. Some radicals give such broad lines in the liquid phase that they are undetectable, while others may be so reactive that they never accumulate to give detectable concentrations. EPR spin- trapping techniques overcome these problems by extending the lifetime of free radicals. The chemistry involves the addition reaction of a highly reactive radical to a diamagnetic

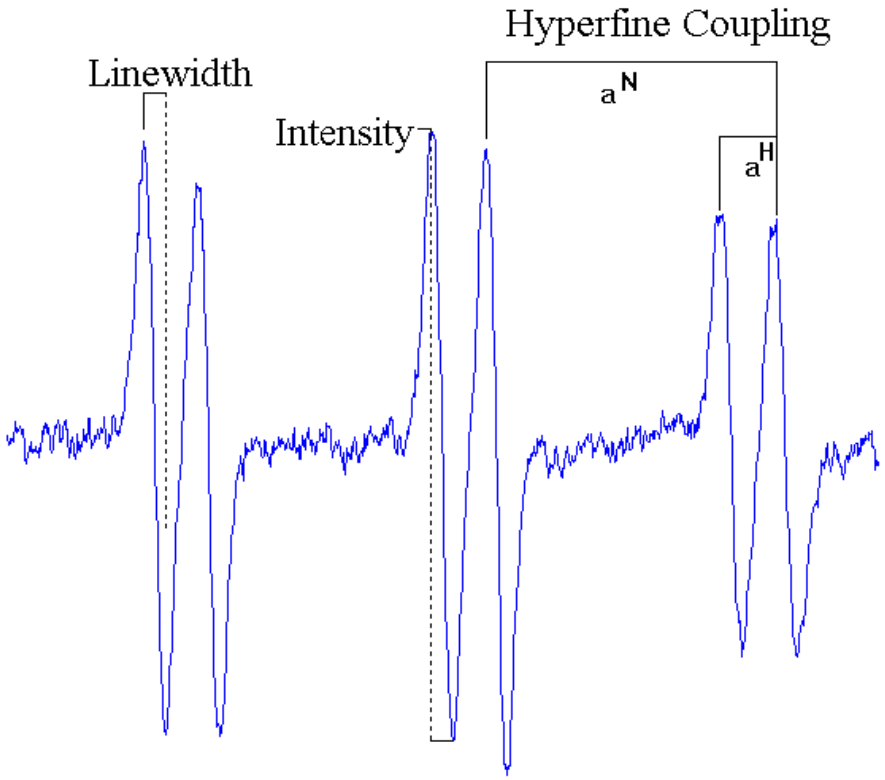

Figure 4. Electron paramagnetic resonance spectrum of a carbon-centered radical adduct of POBN with useful parameters labeled.

compound (spin trap), forming a long-lived free radical product (spin adduct), which is EPR detectable [Buettner, 1987; Janzen, 1971; Janzen, 1990; Mason and Mottley, 1987]. Spin adducts can be produced with a wide range of radicals, such as carbon-, nitrogen-, oxygen-, or sulfur-centered radicals. Spin traps do not react readily with resonance-stabilized radicals, such as ascorbate free radical; however, resonance stabilized radicals can usually be observed directly.

Most spin traps are converted to nitroxide (aminoxyl) radical spin adducts upon reaction with the transient radical. Because of the high stability of these species and their characteristic triplet spectra from the ^{14}N hyperfine coupling, spin traps are used to identify and examine the nature of short-lived radicals both *in vitro*, and *in vivo*. The second-order rate constant for the spin trapping reaction varies between 10^1 $M^{-1}s^{-1}$ to 10^9 $M^{-1}s^{-1}$, depending on the spin trap, solvent, and the radical species [Thornally, 1986]. For instance, the reaction of the nitrone spin trap, 5,5-dimethyl-1-pyrroline-*N*-oxide (DMPO) with the radical $R^{\bullet}$ is shown in Figure 5. The resulting radical adduct is EPR visible and provides a spectrum that can be used to identify the original reacting radical species.

Spin trapping allows detection of free radicals in real time. For example, the $HO^{\bullet}$ radical is not detectable by EPR in room temperature aqueous solution because of its broad linewidth and short lifetime, $t_{½} \approx$ ns - μs. However, the hydroxyl radical reacts with the spin trap DMPO to produce the spin adduct DMPO/$^{\bullet}$OH, which has a relatively narrow linewidth, $\Delta H_{pp} \approx$ 1G, and long lifetime, $t_{½} \approx$ seconds to hours, depending on

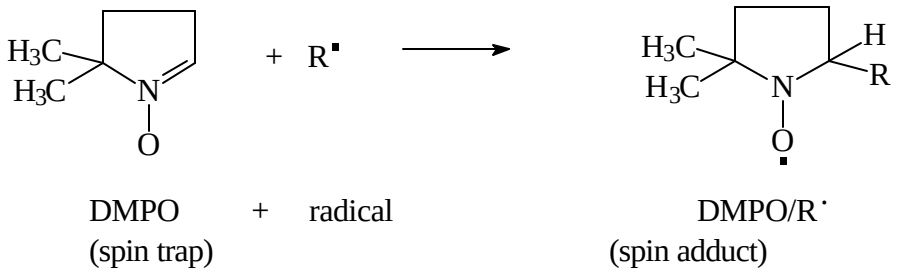

Figure 5. 5,5-dimethyl-1-pyrroline-*N*-oxide spin trapping of a radical.

experimental conditions. These characteristics allow easy EPR detection and quantitation of DMPO/•OH. DMPO is used in Chapter III in a paired comparison study with ascorbate to measure oxidative stress in three different chemical and biochemical systems.

The most commonly used spin traps DMPO, α-[4-pyridyl 1-oxide]-N-*tert*-butyl nitrone (POBN) shown in Figure 6, and N-*tert*-butyl-α-phenylnitrone (PBN) have a β-hydrogen that can provide considerable information about the radical trapped.

The nature of the spin trap and the radical trapped determines the appearance of the EPR spectrum, as reflected in the hyperfine splittings [Buettner, 1987]. The magnitude of the hyperfine splitting is affected by the magnetic moment of the nucleus where the unpaired electron is localized, the geometry of the spin adduct, and by the solvent [Mason and Mottley, 1987]. The integrative nature of spin trapping has provided a wealth of information on free radical processes in the chemical, biochemical, and biological sciences.

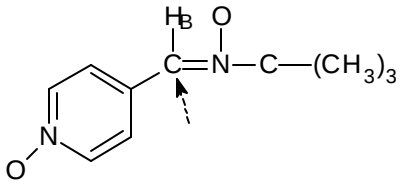

Figure 6. The structure of POBN is shown.
The arrow indicates where a free radical will add to form a spin adduct. Both the nitrogen and the beta hydrogen (H_β) provide hyperfine splitting information.

CHAPTER III

ASCORBATE RADICAL AS A MARKER OF OXIDATIVE STRESS[4]

Overview

The ascorbate anion is an endogenous water-soluble antioxidant that is present in biological systems. The one-electron oxidation of ascorbate produces the ascorbate free radical that is easily detectable by electron paramagnetic resonance (EPR), even in room temperature aqueous solution. The ascorbate radical has a relatively long lifetime compared to other free radicals, such as hydroxyl, peroxyl, and carbon-centered lipid radicals. This longer lifetime in conjunction with its relatively narrow EPR linewidth makes it easily detectable by EPR. This chapter describes the EPR detection of the ascorbate radical and its use as a marker of oxidative stress.

Ascorbate, The Terminal Small-Molecule Antioxidant

Introduction

Ascorbate (**I**) is ubiquitous, yet there is still much to be learned about its chemistry, biochemistry, and biology. Ascorbate is an excellent reducing agent [Lewin, 1976; Davies *et al.*, 1991; Buettner, 1993; Creutz, 1981]. It readily undergoes two consecutive, yet reversible,

---

[4] Portions of the work presented in this chapter have been published. GR Buettner and BA Jurkiewicz: Ascorbate radical as a marker of oxidative stress: An EPR study. *Free Radic Biol Med* 14:49-55, 1993; and GR Buettner and BA Jurkiewicz: Chemistry and biochemistry

one-electron oxidation processes to form the ascorbate radical (**II**) as an intermediate. Loss of a second electron yields dehydroascorbic (**III**) [Lewin, 1976], shown in equation III-1:

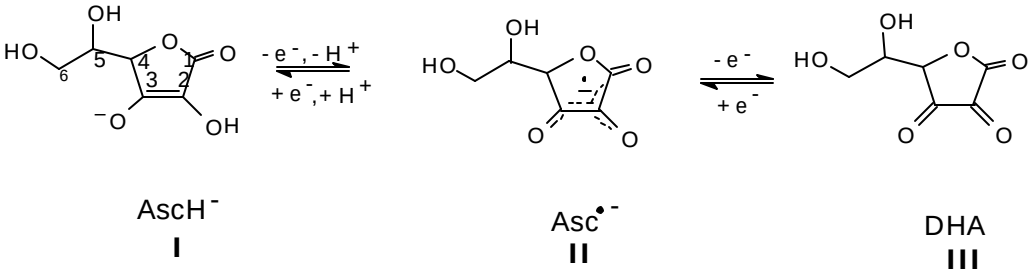

Because $Asc^{\bullet -}$ has its unpaired electron in a highly delocalized π-system, it is a relatively unreactive free radical. These properties make ascorbate a superior biological, donor antioxidant [Buettner, 1993; Creutz, 1981; Frei *et al.*, 1989; Halliwell, 1990; McCay, 1985; Rees and Slater, 1987; Niki, 1991; Krinsky, 1992; Koppenol and Butler, 1985; Kalyanaraman *et al.*, 1992; Navas *et al.*, 1994; Rose and Bode, 1993; Retsky, 1993; Sharma and Buettner, 1993].

The ascorbate free radical is a strong acid having a pK_a of -0.86 [Davis *et al.*, 1986]. Thus, it will exist as a monoanion, $Asc^{\bullet -}$, over the entire biological pH range. $Asc^{\bullet -}$, **II** is usually referred to in brief as the ascorbate free radical. The suffix "ate" being used because it is a charged species. The short name ascorbyl radical would be used for $AscH^{\bullet}$, the neutral protonated form of $Asc^{\bullet -}$; the ending "yl" being used for this neutral species.

---

of ascorbic acid. In: *Handbook of Antioxidants*, eds. L Packer and E Cadenas, Marcel Dekker Inc., New York, 91-115, 1995.

When biological fluids or tissues are examined by electron paramagnetic resonance spectroscopy, $Asc^{\bullet -}$ will most likely be observed, see Figure 1 below. This is consistent with ascorbate's role as the terminal small-molecule antioxidant [Buettner, 1993].

Ascorbate Thermodynamics and Kinetics

As can be seen in Table 3, ascorbate is thermodynamically at the bottom of the pecking order of oxidizing free radicals. That is, all oxidizing free radicals with greater reduction potentials, which includes $HO^{\bullet}$, $RO^{\bullet}$, $LOO^{\bullet}$, $GS^{\bullet}$, the urate radical, and even the tocopheroxyl radical ($TO^{\bullet}$), can be reduced by ascorbate. Therefore, we have:

$$AscH^{-} + X^{\bullet} \longrightarrow Asc^{\bullet -} + XH$$

where $X^{\bullet}$ can be any of the above oxidizing free radicals. This table is adapted from references [Buettner, 1993; Sharma and Buettner, 1993; Wardman, 1989]. From Table 4 we see that the kinetics of these electron (hydrogen atom) transfer reactions are rapid. Thus, both thermodynamically and kinetically, ascorbate can be considered to be an excellent antioxidant.

Although ascorbate itself forms a radical in this reaction, a potentially very dangerous oxidizing radical ($X^{\bullet}$) is replaced by the relatively innocuous $Asc^{\bullet -}$. $Asc^{\bullet -}$ does not react by an addition reaction with O_2 to form potentially dangerous peroxyl radicals. Ascorbate (probably Asc^{2-}, *vida infra*) and/or $Asc^{\bullet -}$ appear to produce very low levels of superoxide [Scarpa *et*

al., 1983; Williams and Yandell, 1982]. But by removing $O_2^{\bullet -}$, superoxide dismutase provides protection from this possibility [Winterbourn, 1993;

Table 3. One-electron reduction potentials at pH 7.0 for selected radical couples.

Redox Couple	$E^{o'}$/mV
$HO^{\bullet}$, H^{+}/H_2O	+ 2310
$RO^{\bullet}$, H^{+}/ROH (aliphatic alkoxyl radical)	+ 1600
$ROO^{\bullet}$, H^{+}/ROOH (alkyl peroxyl radical)	+ 1000
$GS^{\bullet}/GS^{-}$ (glutathione)	+ 920
$PUFA^{\bullet}$, H^{+}/PUFA-H (*bis*-allylic-H)	+ 600
$HU^{\bullet -}$, H^{+}/UH_2^{-} (Urate)	+ 590
$TO^{\bullet}$, H^{+}/TOH (Tocopherol)	+ 480
H_2O_2, H^{+}/H_2O, $HO^{\bullet}$	+ 320
$Asc^{\bullet -}$, H^{+}/Ascorbate monoanion	+ 282
Fe(III)EDTA/ Fe(II)EDTA	+ 120
$O_2/ O_2^{\bullet -}$	- 330
$Paraquat^{2+}$/ $Paraquat^{\bullet +}$	- 448
Fe(III)DFO/ Fe(II)DFO (Desferal)	- 450
RSSR/ $RSSR^{\bullet -}$ (GSH)	- 1500
H_2O/ e^{-}_{aq}	- 2870

Table 4. Rate constants for reactions of the equilibrium mixture of $AscH_2/AscH^-/Asc^{2-}$.

Radical	$k_{obs}/M^{-1}s^{-1}$	(pH 7.4)	Ref.[a]
$HO^\bullet$	1.1×10^{10}		[Buxton *et al.*, 1988]
$RO^\bullet$ (*tert*-Butyl alkoxyl radical)	1.6×10^{9}		[Erben *et al.*, 1987]
$ROO^{\bullet -}$ (Alkyl peroxyl radical)	$1\text{-}2 \times 10^{6}$		[Neta *et al.*, 1990]
$Cl_3COO^\bullet$	1.8×10^{8}		[Packer *et al.*, 1980]
$GS^\bullet$ (Glutathiyl radical)	6×10^{8}	(5.6)	[Tambe *et al.*, 1991; Forni *et al.*,1983]
$UH^{\bullet -}$ (Urate radical)	1×10^{6}		[Simic and Jovanovic, 1989]
$TO^\bullet$ (Tocopheroxyl radical)	2×10^{5} b		[Buettner, 1993]
$Asc^{\bullet -}$ (Dismutation)	2×10^{5} c		[Bielski, 1982]
$CPZ^{\bullet +}$ (Chlorpromazine radical)	1.4×10^{9}	(5.9)	[Pelizzetti *et al.*, 1979]
Fe(III)EDTA/Fe(II)EDTA	$\approx 10^{2}$ d		
$O_2^{\bullet -}/HO_2^\bullet$	1×10^{5} c		[Cabelli and Bielski, 1983]
	2.7×10^{5}		[Nishikimi, 1975]
Fe(III)Desferal/ Fe(II)Desferal	Very slow		[Buettner, 1986; Buettner, 1990]

a) A summary of free radical solution kinetics can be found in Ross, 1994.

b) Estimated k_{obs} for $TO^\bullet$ when in a biological membrane.

c) k is pH dependent, thus this is k_{obs} at pH 7.4.

d) Estimated from data in [Buettner, 1988; Kahn, 1967; Scarpa, 1983]

Koppenol, 1993]. Thus, the biological organism is protected from further free radical-mediated oxidations. In addition, $Asc^{\bullet -}$ as well as dehydroascorbic can be recycled back to ascorbate by enzyme systems. Ascorbate's ubiquitous presence in biological systems in conjunction with its role as an antioxidant strongly suggests that the ascorbate free radical would also be present *in vivo.*

Equilibrium

The ascorbate free radical will be present in solutions due to both autoxidation and metal catalyzed oxidation of ascorbate. Foerster *et al.* observed that $Asc^{\bullet -}$ can also arise from comproportionation of $AscH^-$ and DHA [Foerster *et al.*, 1965],

$$AscH^- + DHA \rightleftharpoons 2\,Asc^{\bullet -} + H^+ \qquad \text{(III-2)}$$

$$K = \frac{[Asc^{\bullet -}]^2}{[AscH^-]\,[DHA]} \qquad \text{(III-3)}$$

Using EPR they determined the equilibrium constant for this process and noted that it was pH dependent. The equilibrium constant K was found to vary from 5.6×10^{-12} at pH 4.0 to 5.1×10^{-9} at pH 6.4. Later, after the acid-base properties of ascorbic acid and ascorbate free radical were understood, it was possible to develop an expression for K at any pH value [Bielski *et al.*, 1985].

$$K = \frac{[Asc^{\bullet -}]^2 [H^+] + \{1+[H^+]/10^{-pK}\}}{[DHA] [AscH_2]_{total}} = 2.0 \times 10^{-15}\ M^{-2} \quad \text{(III-4)}$$

where pK_1 is the first ionization constant of ascorbic acid and $[AscH_2]_{total}$ is the analytical concentration of $AscH_2$, *i.e.*, $[AscH_2]_{total} = [AscH_2] + [AscH^-] + [Asc^{2-}]$.

Detection of the Ascorbate Free Radical

Absorption Spectra

Pure ascorbic acid solutions are colorless as neither the diacid nor the monoanion have significant absorbances in the visible region of the spectrum. However, each has an absorbance in the ultraviolet region.

1. Ascorbic Acid: The diacid has an approximately symmetrical Gaussian absorption spectrum with $\varepsilon_{244} = 10{,}800\ M^{-1} \bullet cm^{-1}$ in aqueous solution [Lewin, 1976].

2. Ascorbate monoanion: Compared to the diacid, the peak of the absorption curve for the monoanion is red-shifted to 265 nm. A wide range of molar extinction coefficients have been reported, ranging from 7,500 -

20,400 $M^{-1} \cdot cm^{-1}$ [Lewin, 1976]. We find that ε_{265} = 14,500 $M^{-1} \cdot cm^{-1}$ best reflects our experimental observations when doing experiments in near-neutral buffered aqueous solutions [Buettner, 1988].

3. Ascorbate Radical: The ascorbate free radical has an approximately symmetrical Gaussian shaped absorption curve with ε_{360} = 3,300 $M^{-1} \cdot cm^{-1}$ and a half-width at half-maximum of about 50 nm [Bielski *et al.*, 1985]. With this small extinction coefficient, $Asc^{\bullet -}$ will not be observable by standard UV-visible spectroscopy in steady state experiments.

4. Dehydroascorbic: Dehydroascorbic (acid) has a weak absorption at 300 nm, ε_{300} = 720 $M^{-1} \cdot cm^{-1}$ [Lewin, 1976].

EPR Detection of the Ascorbate Free Radical

The ascorbate free radical is usually detected by EPR as a doublet signal with a^H = 1.8 G, $\Delta H_{pp} \approx$ 0.6 G and g = 2.0052, Figure 7. However, each line of the ascorbate doublet is actually a triplet of doublets, a^{H4} = 1.76 G, $a^{H6}(2)$ = 0.19 G, and a^{H5} = 0.07 G [Laroff *et al.*, 1972]. In most biological experiments where the $Asc^{\bullet -}$ EPR signal will be weak, a compromise is made in the choice of modulation amplitude. The usual choice is to sacrifice resolution of the hyperfine structure for improved sensitivity. A modulation amplitude of ≈ 0.65 G maximizes the ascorbate free radical doublet peak-to-peak signal amplitude [Buettner, 1992].

The EPR power saturation curve of $Asc^{\bullet -}$ in room temperature aqueous solutions shows that saturation effects begin at ≈ 16 milliwatts and maximum signal height is achieved at 40 milliwatts nominal power when using an aqueous flat cell and a TM_{110} cavity, see Figure 8. Thus, if quantitation of the $Asc^{\bullet -}$ levels is desired, appropriate

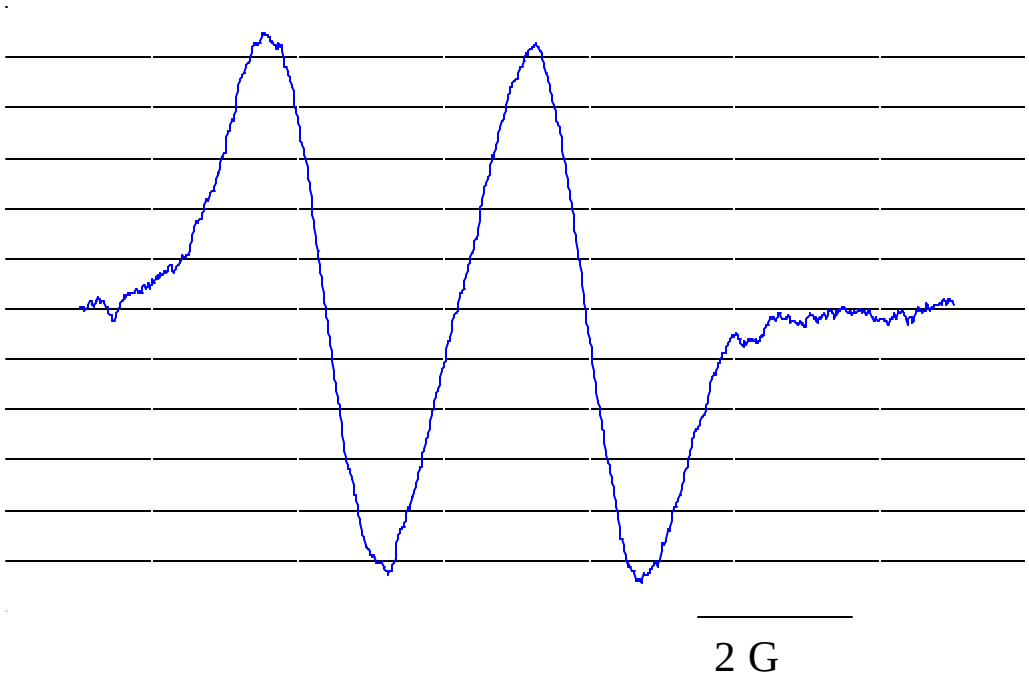

Figure 7. An example of the ascorbate radical EPR doublet signal in buffer. Each line of the ascorbate radical doublet is actually a triplet of doublets; in aqueous solution the EPR spectral parameters of $Asc^{\bullet -}$ are g value = 2.00518; a^{H4} = 1.76; a^{H6} (2) = 0.19 G; a^{H5} = 0.07 G. However, instrument settings were chosen for maximum sensitivity; thus, the hyperfine splittings for H5 and H6 are within the linewidth, and only a doublet with $a^{H4} \approx 1.8$ G is observed.

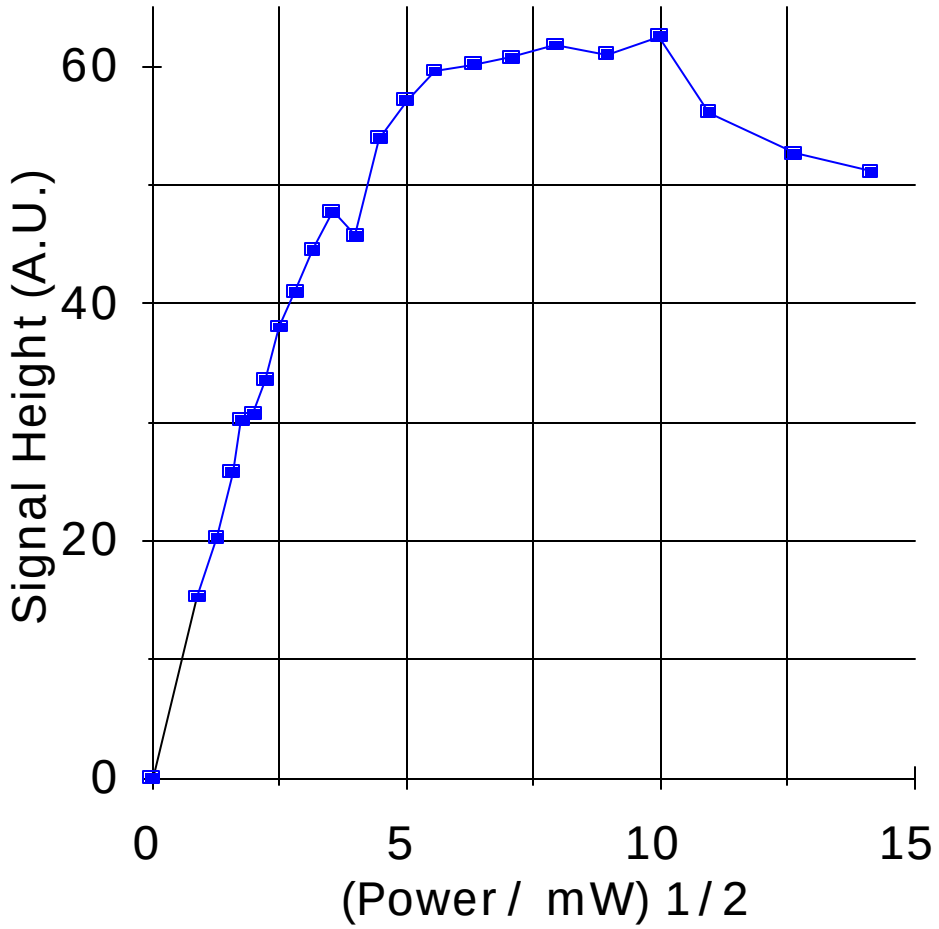

Figure 8. EPR power saturation curve for the ascorbate free radical.
Signal heights are arbitrary units. $Asc^{\bullet -}$ was observed in a demetalled 50 mM pH 7.8 phosphate buffer containing 10 mM ascorbate. EPR spectrometer instrument settings were: 0.65 modulation amplitude; 10 G/167 s scan rate; 0.167 s time constant [Buettner and Kiminyo, 1992].

corrections for saturation effects must be included in the calculations.

Ascorbate Free Radical as a Marker of Oxidative Stress

It is proposed that ascorbate, *i.e*., the ascorbate free radical, which is naturally present in biological systems, can be used as a noninvasive indicator of oxidative stress. The ascorbate radical is a relatively stable, non-toxic radical species, that is easily detectable by EPR. As oxidative stress increases in a system, the steady state $Asc^{\bullet -}$ concentration increases. Based on these observations, those parameters that would need to be considered to accurately use the ascorbate radical as a marker, such as pH and concentration were examined.

Materials and Methods

Hypoxanthine, xanthine oxidase (XO), ascorbic acid, 5,5-dimethyl-pyrroline-1-oxide (DMPO), deferrioxamine mesylate, chelating resin, and riboflavin were obtained from Sigma Chemical Co., St. Louis, MO. The DMPO was purified with charcoal and stored as a 1.0 M aqueous solution. 2,2′-Azo *bis*(2-amidinopropane) dihydrochloride (AAPH) was obtained from PolySciences Company, Warrington, PA. All buffers were treated with chelating resin using the batch method [Buettner, 1988]; absence of adventitious catalytic metals was verified with ascorbate [Buettner, 1988].

The concentration of $Asc^{\bullet -}$ and DMPO/$^{\bullet}$OOH were determined by double integration of the EPR spectra using 3-carboxy proxyl (Aldrich Chem. Co., Milwaukee, WI) as a standard. The standard spectra were obtained with the same instrument settings as used in

collecting the experimental spectra, except for receiver gain. Saturation effects were accounted for as necessary [Buettner and Kiminyo, 1992]. EPR spectra were collected with a Bruker ESP 300 ESR spectrometer (Bruker Instruments, Karlsruhe, Germany), using a TM_{110} cavity and aqueous flat cell.

Ascorbate Radical Background Signals

In the experiments where the concentration of $Asc^{\bullet -}$ was determined with varying amounts of ascorbate, the solutions contained: 50 mM phosphate buffer pH 7.4, 50 µM deferoxamine mesylate, and various concentrations of ascorbate. The deferrioxamine mesylate was present in the buffer overnight to ensure complete chelation of adventitious iron [Buettner, 1990]. In the experiments where the $Asc^{\bullet -}$ concentration was determined at various pH values, the solutions contained 50 mM phosphate buffer, 50 µM deferrioxamine mesylate (overnight), and 500 µM ascorbate.

For the detection of the ascorbate free radical, EPR instrument settings were modulation amplitude, 0.71 G; scan rate, 6.0 G/84 s; time constant, 1.3 s; power, 40 milliwatts; and receiver gain, $5x10^5$.

Xanthine Oxidase

In the experiments where XO was used as a source of oxyradicals, the solutions contained 500 µM ascorbate or 50 mM DMPO; 500 µM hypoxanthine; 50 µM or 250 µM

DETAPAC; and 0 - 100 U/mL[5] of XO in 50 mM phosphate buffer, pH 7.8 for DMPO or pH 7.4 for $Asc^{\bullet -}$.

EPR spectral scans were initiated approximately one minute after addition of XO. For the DMPO spin trapping experiments, instrument settings were modulation amplitude, 0.96 G; scan rate, 80 G/168 s; time constant, 0.33 s; power, 40 milliwatts; and receiver gain, 5×10^5. For the detection of the ascorbate free radical, instrument settings were: modulation amplitude, 0.71 G; scan rate, 6.0 G/84 s; time constant, 1.3 s; power, 20 milliwatts; and receiver gain, 5×10^5.

Riboflavin

In the experiments where riboflavin and light were used as a source of oxygen centered radicals, the solution contained 500 µM ascorbate or 50 mM DMPO; 1 mM diethylenetriaminepentaacetic acid (DETAPAC); various concentrations of riboflavin in 50 mM phosphate buffer pH 7.8 for DMPO or pH 7.4 for $Asc^{\bullet -}$.

EPR spectra were collected at the same instrument settings as the XO experiment except for receiver gain. The light source was a Bausch & Lomb 100 W tungsten microscope light focused on the TM_{110} cavity grid. The light fluence rate at the sample, as measured using a Yellow Springs Instrument (Yellow Springs, OH) model 65A radiometer with a 6551 probe,

[5] 1 unit converts 1.0 µM xanthine to uric acid per minute at pH 7.5, 25°C

was ≈ 150 Wm^{-2}, assuming the cavity grid transmits 75% of the incident light. Infrared radiation from the light was removed by a 3 cm water filter.

Azo Initiator, AAPH

In the chemical system where AAPH was used as a source of water soluble peroxyl radicals, the solution contained 500 µM ascorbate or 50 mM DMPO, 50 µM DETAPAC, and various concentrations of AAPH in 50 mM phosphate buffer pH 7.4. In the experiment using human plasma, the concentration of ascorbate was 58 µM.

EPR spectra were collected at the same settings as the XO and riboflavin experiments except for receiver gain. EPR spectra were collected 10 minutes after the introduction of AAPH in the chemical system and six minutes after in the plasma system.

Results

Autoxidation[6]

Ascorbate is readily oxidized in solution. However, the rate of this oxidation is dependent upon pH and the presence of catalytic metal ions [Buettner, 1986; Buettner, 1990; Buettner, 1988; Kahn and Martell, 1967a; Kahn and Martell, 1967b; Guzman *et al.*, 1936; Borsook *et al.*, 1937; Weissberger *et al.*, 1943; Halliwell and Foyer, 1976.]. The diacid is very slow to oxidize. Consequently, at low pH, *i.e.*, less than 2 or 3, ascorbic acid solutions are

[6] In this thesis the term autoxidation means oxidation in the absence of metal catalysts [Miller *et al.*, 1990]. The term oxidation is used more broadly and includes all oxidations, with or without catalysts.

quite stable, assuming catalytic transition metal ions are not introduced into the solutions. However, as the pH is raised above pK_1 (4.2), $AscH^-$ becomes dominant and the stability of the ascorbate solution decreases. This loss of stability is usually the result of the presence of adventitious catalytic metals (on the order of 1 μM) in the buffers and salts that are typically employed in studies at near neutral pH [Buettner, 1988]. For example, in room temperature aerated, aqueous solutions at pH 7.0 (50 mM phosphate buffer) 10 - 30% of 125 μM ascorbate is lost in just 15 minutes. This large variation is the result of different sources and grades of phosphate used in the buffer preparation. However, if extreme care is taken to remove these trace levels of transition metals, this rate of loss can be lowered to as little as 0.05% in 15 minutes [Buettner, 1988], thus demonstrating the extreme importance of metals in controlling ascorbate stability. At pH 7.0 an upper limit for the observed rate constant for the oxidation of ascorbate is 6×10^{-7} s^{-1} under the given experimental conditions [Buettner, 1988]. However, even in carefully demetalled solutions as the pH is increased the rate of oxidation will also increase. Figure 9 shows the increase in ascorbate radical concentration as a function of pH. This can be attributed to the increasing concentrations of the ascorbate dianion present. Williams and Yandell have made an estimate based on the Marcus theory of electron transfer that the ascorbate dianion would undergo true autoxidation, reaction III-5 [Williams and Yandell, 1982].

$$Asc^{2-} + O_2 \longrightarrow Asc^{\bullet -} + O_2^{\bullet -} \qquad k \approx 10^2\ M^{-1}s^{-1} \qquad \text{(III-5)}$$

These experimental results are consistent with those estimates [Buettner, 1990; Buettner, 1988]. Marcus theory would predict that the true autoxidation of $AscH^-$ would be much slower. Thus, at pH ≈ 7.4 the rate of autoxidation of an ascorbate solution is determined by the presence of Asc^{2-}.

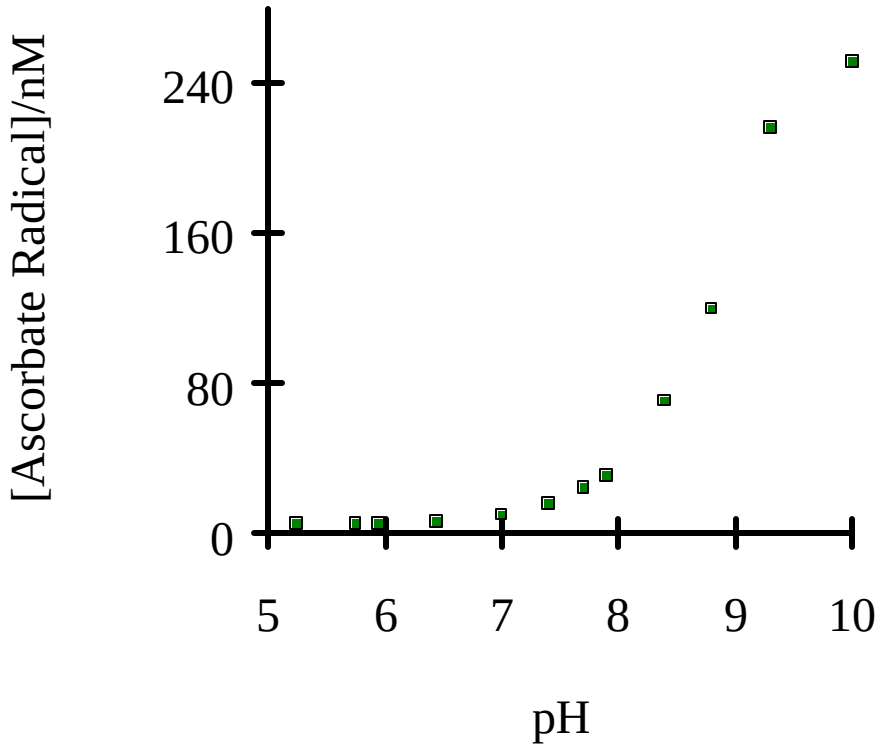

Figure 9. Background ascorbate radical concentration versus pH.
Each solution was made with 50 mM demetalled phosphate buffer that contained 50 μM desferoxamine mesylate, for at least 12 hours. To these solutions 500 μM ascorbate was added and the EPR spectra were collected. The points represent the $Asc^{\bullet-}$ concentration observed in the second of three EPR scans, where the values had a standard deviation of less than 1 nanomolar. Ascorbate radical was determined using 3-carboxy proxyl as a standard.

Typical buffers employed in biochemical and biological research have approximately 1 μM iron and < 0.1 μM copper [Buettner, 1988]. But because copper is ≈ 80 times more efficient as a catalyst for ascorbate oxidation than iron, it is the adventitious copper that is the major catalyst of ascorbate oxidation [Buettner, 1988].

The DMPO nitrone spin-trapping system is EPR silent in the absence of impurities or a free radical generating system. However, background levels of the ascorbate radical are observable in an ascorbate solution in metal free pH 7.4 buffer. This background $Asc^{\bullet -}$, produced by the one-electron oxidation of ascorbate, is thought to arise from the auto-oxidation of the ascorbate dianion; thus, the $Asc^{\bullet -}$ concentration will vary as a function of ascorbate concentration (Figure 10).

Figure 9 demonstrates the importance of pH control. At pH values greater than ≈ 8, there is significant background ascorbate oxidation, which may limit the use of $Asc^{\bullet -}$ steady state concentration as a measure of oxidation stress. However, at near neutral pH, the background steady state concentration of $Asc^{\bullet -}$ is minor, but if the pH is held constant, then changes in $Asc^{\bullet -}$ concentration can be used as a measure of oxidative stress.

At pH 7.4, the concentration of $Asc^{\bullet -}$ increases as the concentration of ascorbate is increased (Figure 4). At low concentrations of ascorbate, *i.e.*, less than ≈100 μM, the steady-state concentration of $Asc^{\bullet -}$ varies ≈ exponentially, whereas above 100 μM, the $Asc^{\bullet -}$ steady-state concentration varies ≈ linearly, within the noise of the experiment.

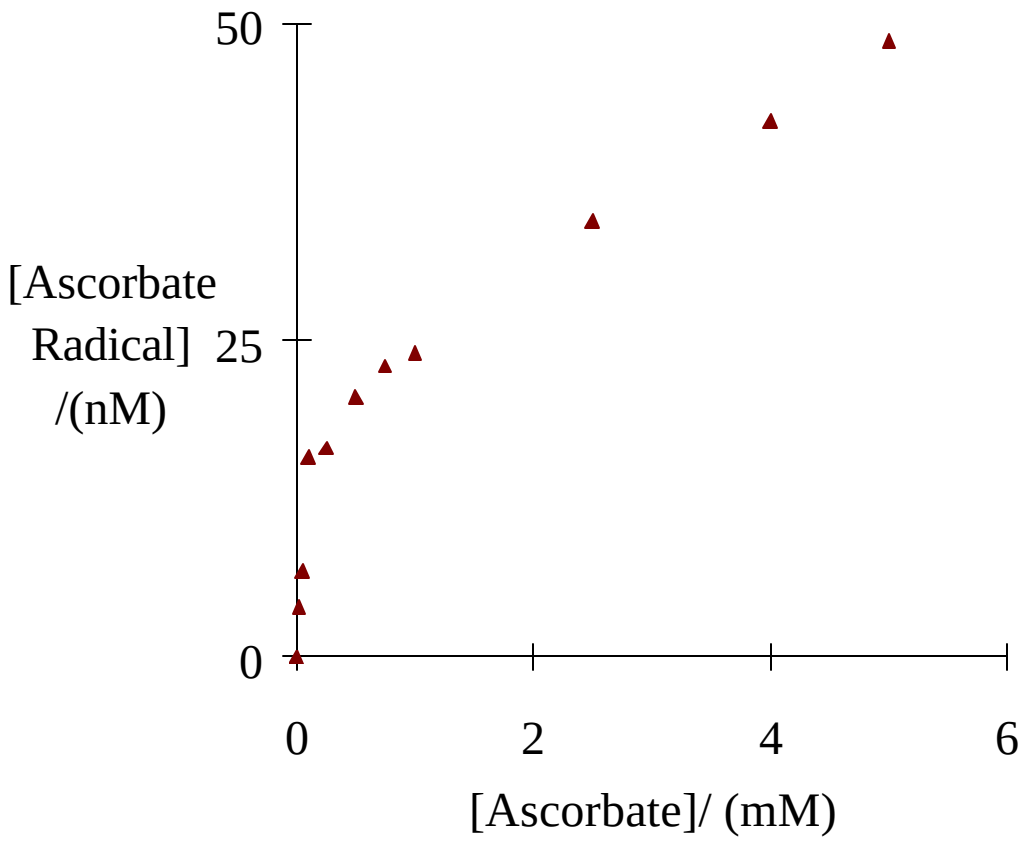

Figure 10. Background [$Asc^{\bullet -}$] versus [Ascorbate].
The solutions contained various concentrations of ascorbate in phosphate buffer pH 7.4.

Xanthine Oxidase

Xanthine oxidase catalyzes the oxidation of hypoxanthine or xanthine to uric acid producing hydrogen peroxide and superoxide, $O_2^{\bullet -}$.

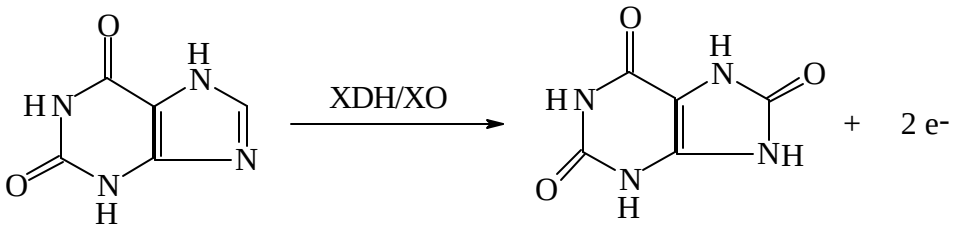

Xanthine Uric Acid

hypoxanthine (xanthine) + O_2 $\longrightarrow$ xanthine (urate) + $O_2^{\bullet -}$ + H_2O_2 (III-6)

The flux of superoxide in this system can be varied by changing the concentration of xanthine oxidase while holding the other variables constant. Figure 11 shows the effect of increasing XO concentrations on ascorbate radical and DMPO/$^{\bullet}$OOH EPR signal intensity. As the concentration of xanthine oxidase is increased, producing more superoxide, there are nearly parallel increases in both the ascorbate free radical and DMPO/$^{\bullet}$OOH EPR signals. The ascorbate free radical and the DMPO/$^{\bullet}$OOH EPR spectra are shown in Figure 12. Both the ascorbate free radical and DMPO/$^{\bullet}$OOH EPR signal intensities vary with time (Figure 13). Naturally, the form of these curves will change as a function of the XO concentration (data not shown).

Riboflavin

Riboflavin (Rib) is a photosensitizer that produces a strongly oxidizing triplet, ^{3}Rib*.

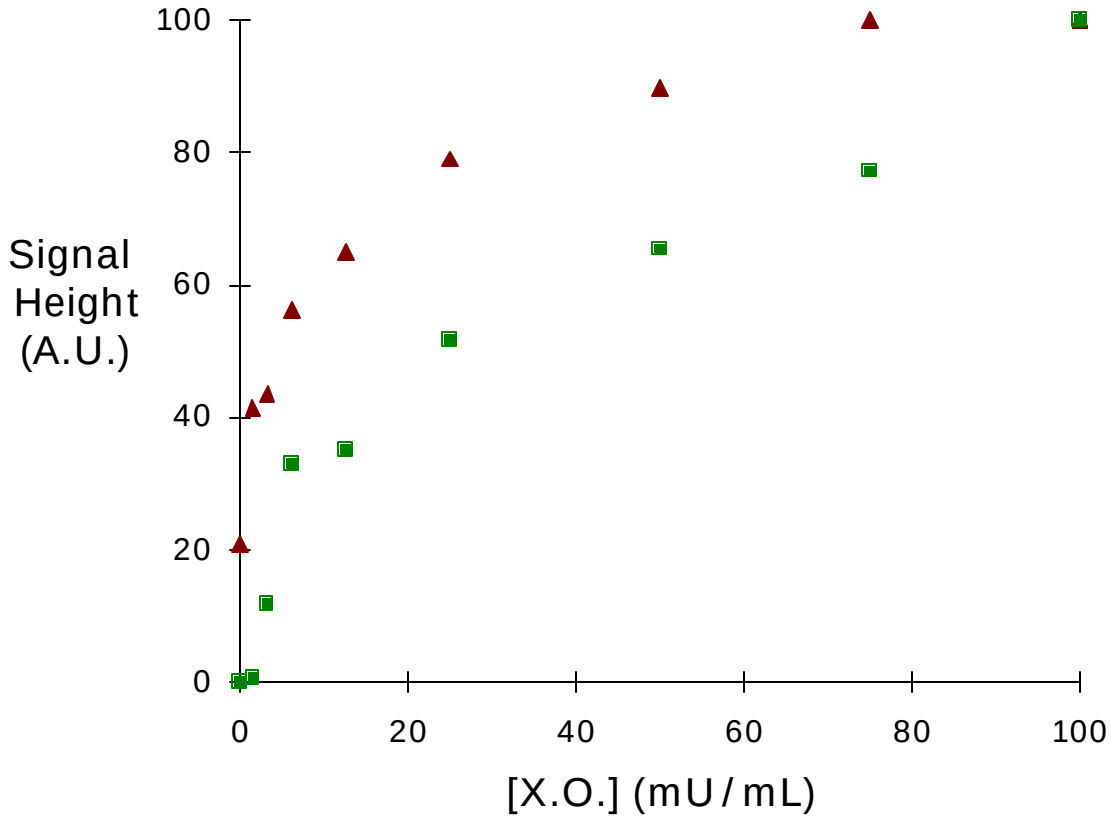

Figure 11. Xanthine oxidase-produces radicals.
$Asc^{\bullet -}$, ♦, and DMPO/$^{\bullet}$OOH, ■, EPR signal height (arbitrary units) versus XO concentration. The solutions contained: 500 µM ascorbate or 50 mM DMPO; 500 µM hypoxanthine; 50 µM or 250 µM DETAPAC; and various concentrations of XO in 50 mM phosphate buffer, pH 7.8 for DMPO or pH 7.4 for $Asc^{\bullet -}$. The results have been normalized to the highest value of each curve ([$Asc^{\bullet -}$] = 53 nM at 100 A.U.; [DMPO/$^{\bullet}$OOH] = 2.0 µM at 100 A.U.).

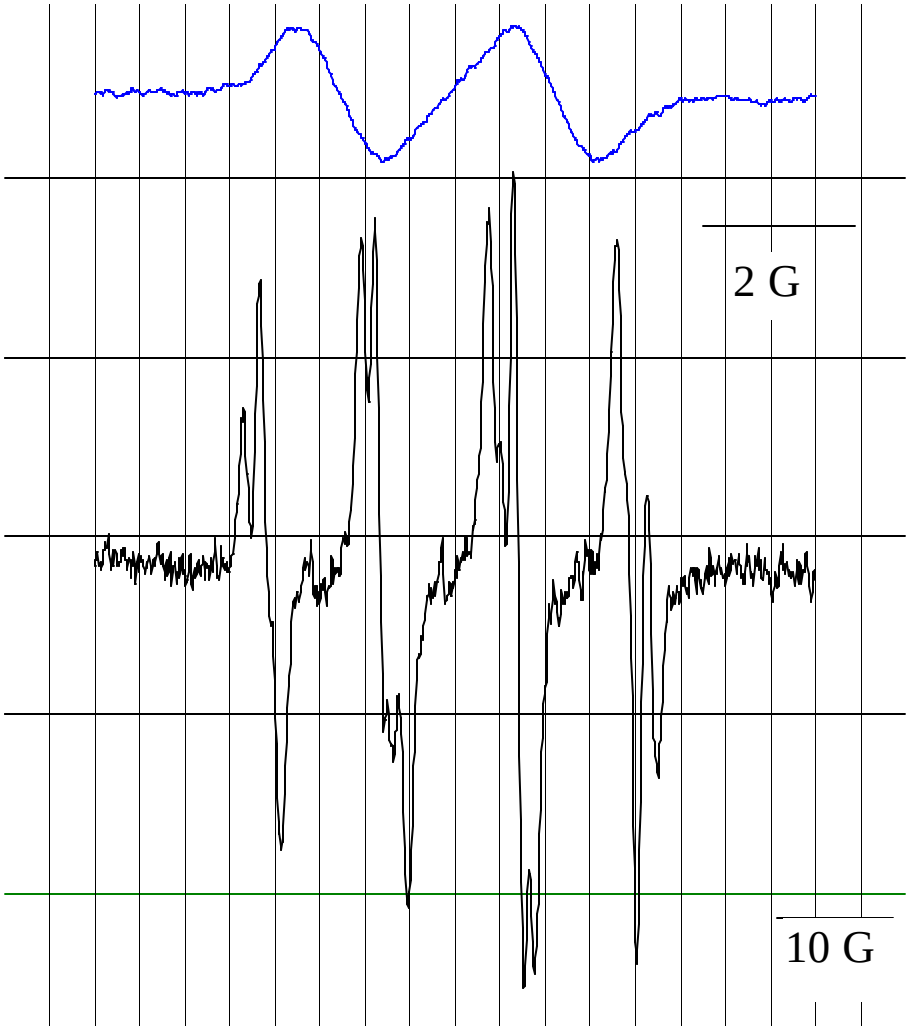

Figure 12. EPR spectra of ascorbate free radical and DMPO/$\dot{O}$OH produced by xanthine oxidase.
The upper EPR spectrum is of the ascorbate free radical signal produced in a xanthine oxidase solution. Solutions contained: 500 µM ascorbate, 50 µM DETAPAC; 3.1 mU/mL xanthine oxidase; 0.5 mM hypoxanthine in 50 mM phosphate buffer, pH 7.4.
The lower EPR spectrum is of DMPO/$\dot{O}$OH produced by xanthine oxidase. Solutions contained: 50 mM DMPO; 50 µM DETAPAC; 100 mU/mL xanthine oxidase; 0.5 mM hypoxanthine in 50 mM phosphate buffer, pH 7.8.

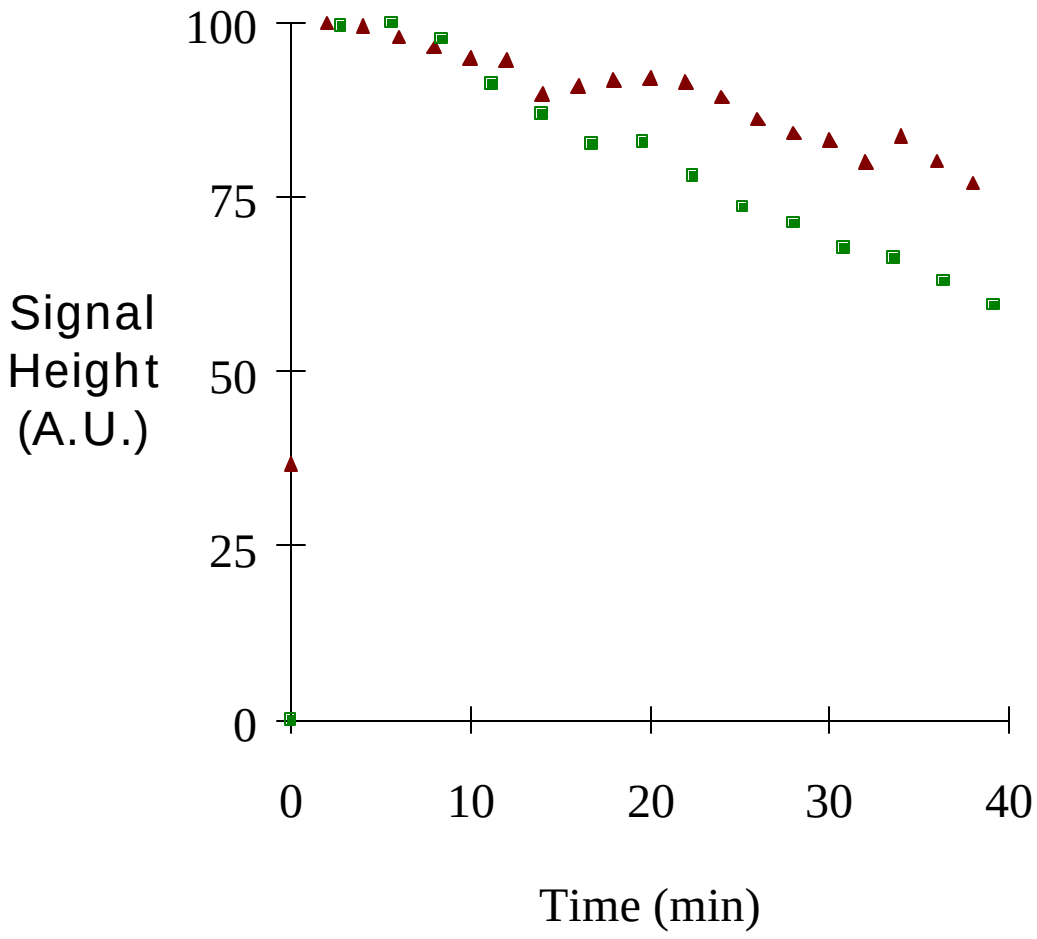

Figure 13. Time course of ascorbate and DMPO/$^{\bullet}$OOH EPR signal intensities. $Asc^{\bullet -}$, ♦, and DMPO/$^{\bullet}$OOH, ■, EPR signal height (arbitrary units) versus time in minutes. The solutions contained: 500 µM ascorbate or 50 mM DMPO; 500 µM hypoxanthine; 50 µM or 250 µM DETAPAC; and 25 mU/mL of XO in 50 mM phosphate buffer, pH 7.8 for DMPO or pH 7.4 for $Asc^{\bullet -}$. Each curve shows the temporal EPR signal intensity of the radical signal after the introduction of XO.

$$Rib + h\nu \longrightarrow {}^3Rib^* \qquad \text{(III-7)}$$

$${}^3Rib^* + D\text{-}H \longrightarrow Rib^{\bullet -} + D^{\bullet} + H^+ \qquad \text{(III-8)}$$

$$Rib^{\bullet -} + O_2 \longrightarrow O_2^{\bullet -} + Rib \qquad \text{(III-9)}$$

This triplet is reduced by electron donors (D-H); both EDTA and DETAPAC can be oxidized by the triplet state of riboflavin. The reduced riboflavin ($Rib^{\bullet -}$) can in turn reduce dioxygen to superoxide. Thus, riboflavin can serve as a source of superoxide, but will only generate superoxide in the presence of light. The flux of superoxide can be varied in a riboflavin system by changing the riboflavin concentration while holding the other variables and light fluence rate constant. The spin trap DMPO will form an adduct with superoxide, shown in Figure 14. Using riboflavin in the presence of light as a source of superoxide, nearly parallel increases in both $Asc^{\bullet -}$ and DMPO/$^{\bullet}$OOH EPR signal intensity are observable as the amount of riboflavin was increased (Figure 15). DMPO itself, has no significant absorbance in the UV-visible range (Figure 16) and thus will not participate in this photochemistry.

Azo Initiator, AAPH

The free radical initiator AAPH undergoes thermal decomposition at a constant rate (at a fixed temperature) producing carbon-centered sigma radicals ($R^{\bullet}$). These sigma radicals will react with oxygen at nearly diffusion-controlled rates yielding peroxyl radicals ($ROO^{\bullet}$), reaction III-10 [Niki, 1990].

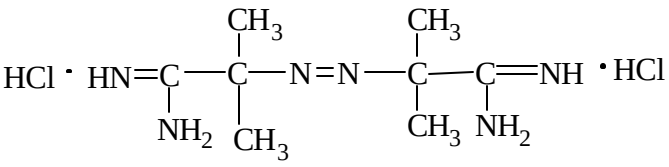

AAPH = 2,2'-azo-*bis* (2-amidinopropane) dihydrochloride

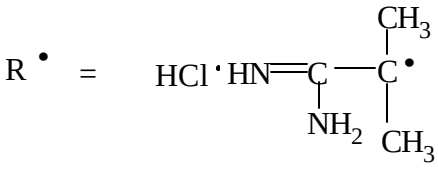

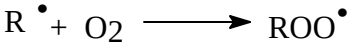

(III-10)

Thus, AAPH, in an oxygen-containing system, produces a constant flux of oxidizing free radicals that can oxidize ascorbate or produce spin adducts with DMPO as shown in Figure 17. When using AAPH as a source of oxidizing radicals in simple buffer solution, nearly linear increases in both the DMPO/$^{\bullet}$OH adduct, $a^N = a^H = 14.8$ G, and ascorbate free radical EPR signal intensities are observable as the concentration of AAPH was increased (Figure 18). In the experiment using plasma containing 58 µM ascorbate, a value typical of physiological conditions, the $Asc^{\bullet -}$ EPR signal intensity was also found to increase as the concentration of AAPH increases (Figure 19).

Discussion

The ascorbate free radical is naturally detectable by EPR at low steady-state levels in biological samples, such as leaves from crops [Stegmann *et al.*, 1993], plasma [Sharma and Buettner, 1993; Minetti *et al.*, 1992; Miller and Aust, 1989], synovial fluid [Buettner

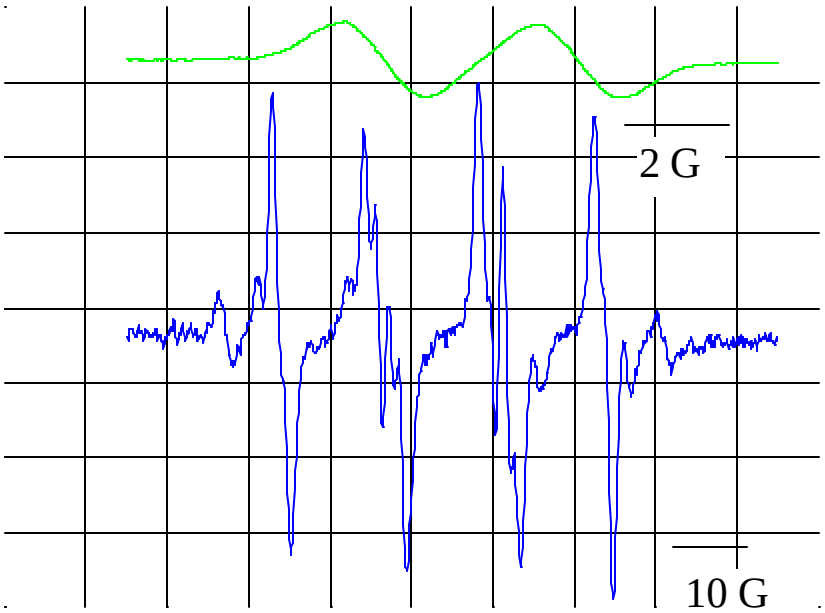

Figure 14. EPR spectra of the ascorbate free radical and DMPO/$\dot{O}$OH signals produced by riboflavin.
The upper EPR spectrum is of the ascorbate free radical signal in a riboflavin containing system in the presence of visible light. Solutions contained: 500 µM ascorbate, 25 µM riboflavin in phosphate buffer, pH 7.4. The lower EPR spectrum is of DMPO/$\dot{O}$OH produced by riboflavin. Solutions contained: 50 mM DMPO, 1 mM DETAPAC; 12.5 µM riboflavin in 50 mM phosphate buffer, pH 7.8.

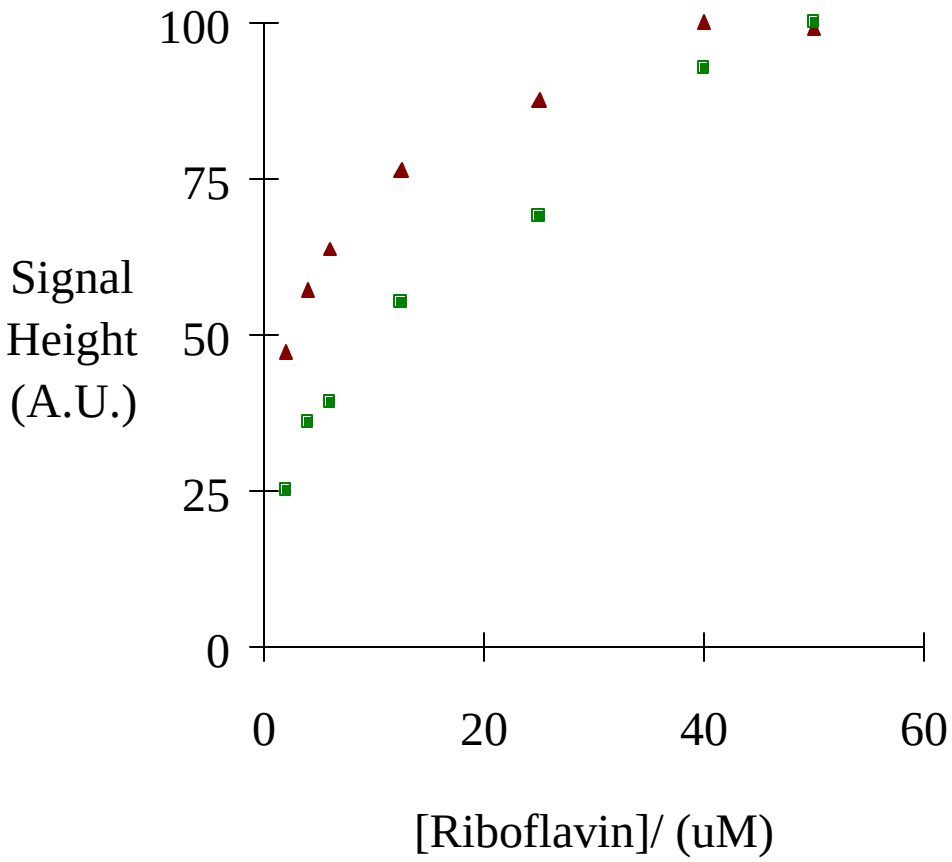

Figure 15. Riboflavin-produced radicals.
$Asc^{\bullet -}$, ♦, and $DMPO/^{\bullet}OOH$, ■, EPR signal height (arbitrary units) versus riboflavin concentration. The solution contained: 500 µM ascorbate or 50 mM DMPO; 1 mM DETAPAC; various concentrations of riboflavin in 50 mM phosphate buffer, pH 7.8 for DMPO or pH 7.4 for $Asc^{\bullet -}$. The results were normalized to the highest value of each curve ($[Asc^{\bullet -}]$ = 30 nM at 100;
$[DMPO/^{\bullet}OOH]$ = 1.8 µM at 100).

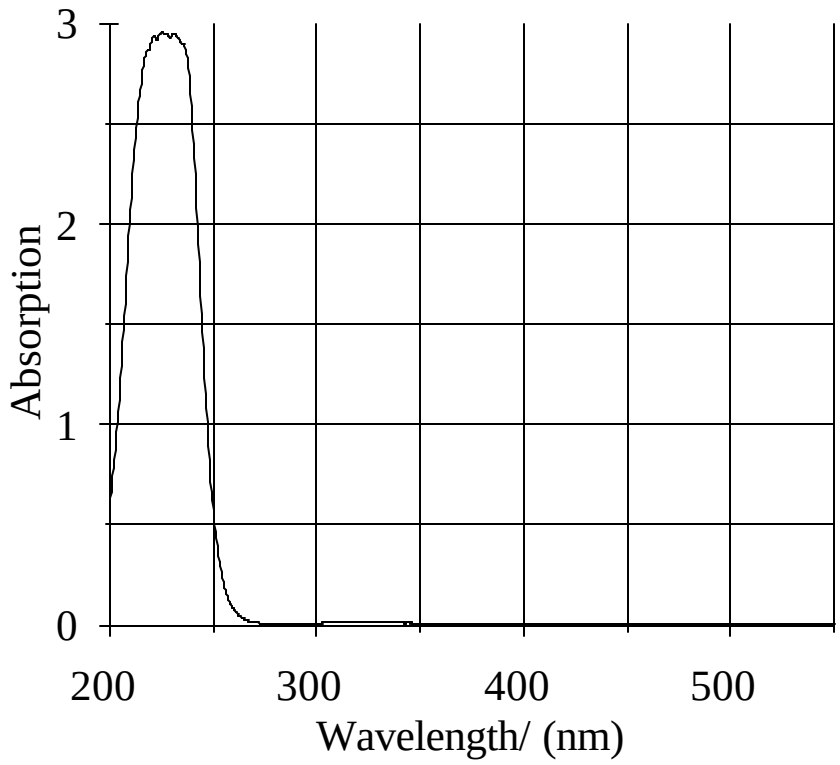

Figure 16. DMPO does not absorb significantly in the visible range.
The absorption spectrum of 50 mM DMPO in water was obtained with a Milton Roy Spectronic 3000® Array spectrometer. There is no significant absorption in the visible region. Note, the maximum absorbance at ≈ 232 nm would be much higher with this concentration of DMPO. This spectrum is not a true absorption spectrum of DMPO, but does demonstrate that there is no absorption at wavelengths greater than 300 nm.

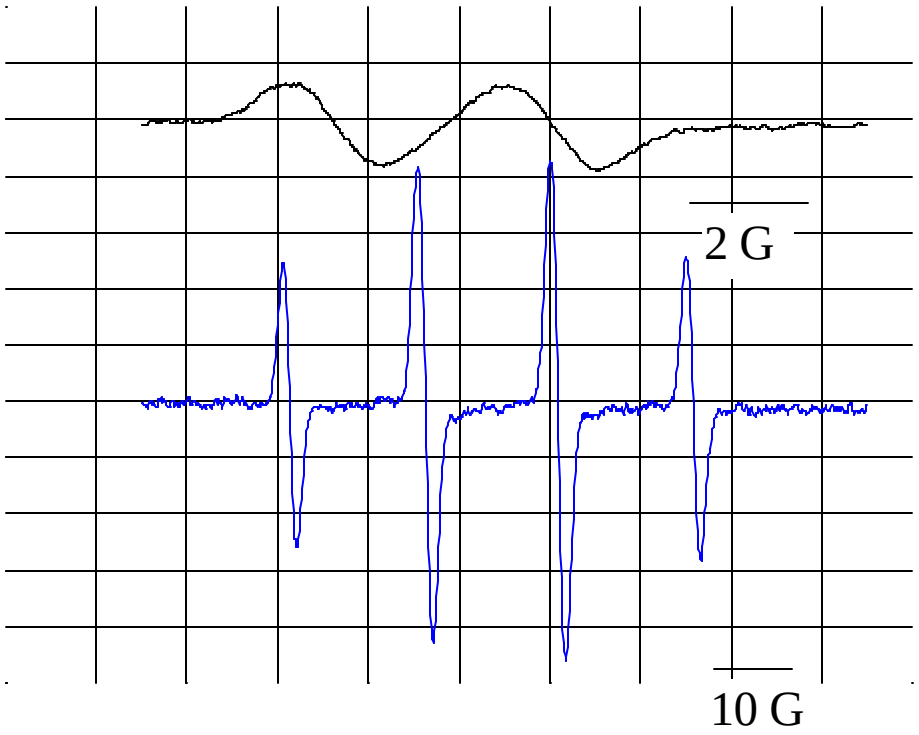

Figure 17. EPR spectra of ascorbate and DMPO/$^{\bullet}$OR produced by AAPH. The upper EPR spectrum is of the ascorbate free radical in an azo-initiating system. Solutions contained: 500 µM ascorbate, 10 mM AAPH, 50 µM DETAPAC in pH 7.4 phosphate buffer. The lower EPR spectrum is of DMPO/$^{\bullet}$OH produced by AAPH ($a^N = a^H = 14.8$ G). Solutions contained: 50 mM DMPO; 50 µM DETAPAC; 8 mM AAPH in phosphate buffer, pH 7.4.

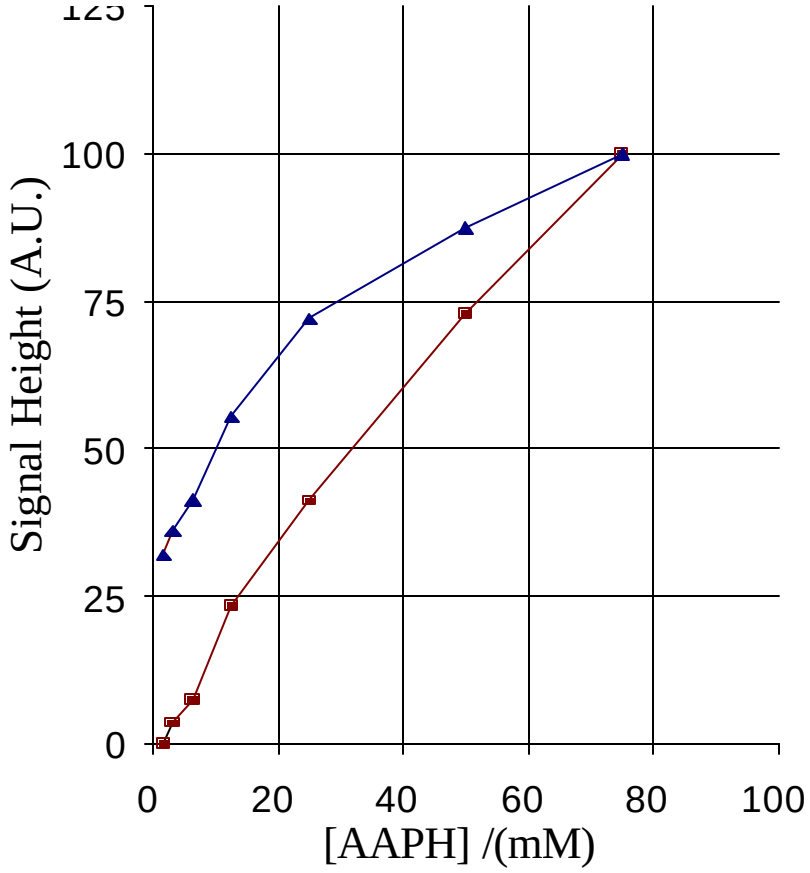

Figure 18. Azo initiator-produced radicals in buffer.
$Asc^{\bullet -}$, ♦, and DMPO/$^{\bullet}$OH, ■, EPR signal height (arbitrary units) versus AAPH concentration. The solutions contained: 500 µM ascorbate or 50 mM DMPO; 50 µM DETAPAC, and various concentrations of AAPH in 50 mM buffer pH 7.4. The results have been normalized to the highest value of each curve
([$Asc^{\bullet -}$] = 36 nM at 100; [DMPO/$^{\bullet}$OH] =2.3 µM at 100).

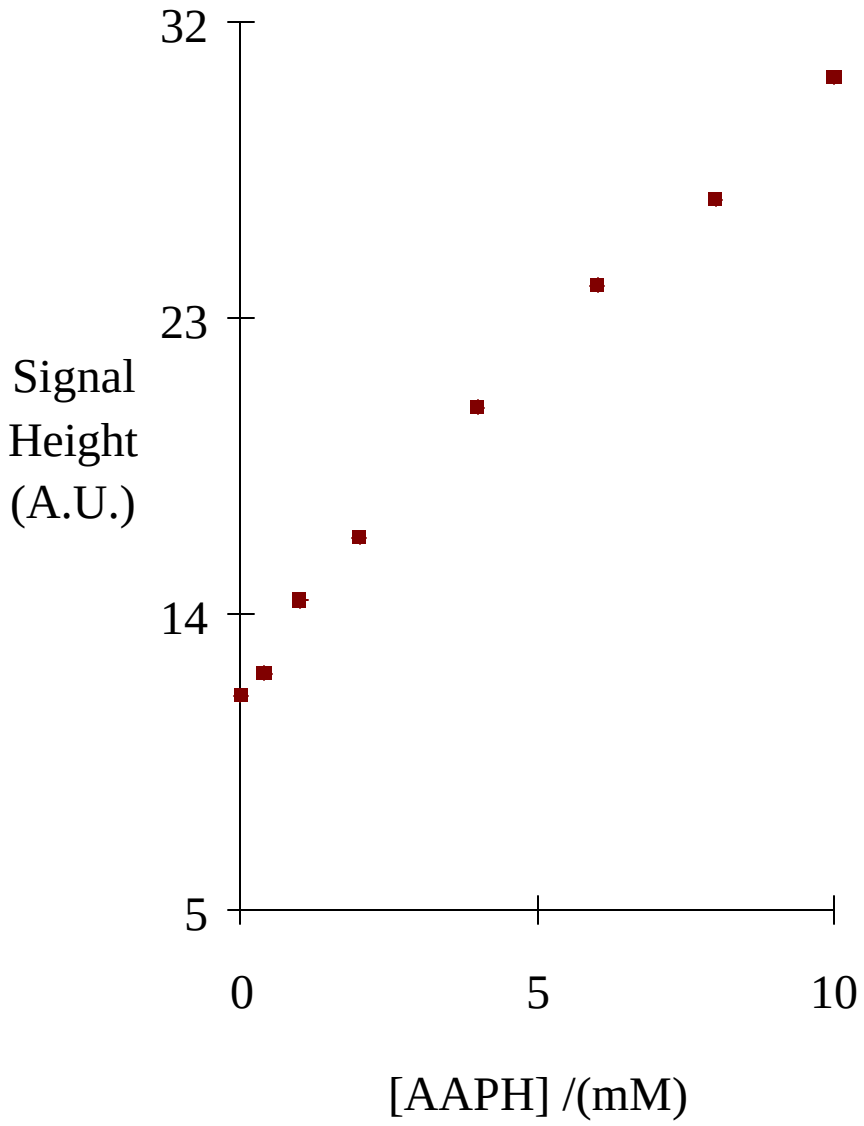

Figure 19. Azo initiator-produced $Asc^{\bullet -}$ radicals in plasma.
$Asc^{\bullet -}$ EPR signal height (arbitrary units) versus AAPH concentration. The plasma contained 58 μM ascorbate and varying concentrations of AAPH.

and Chamulitrat, 1990], skin [Buettner *et al.*, 1987; Jurkiewicz and Buettner, 1994], and lens of the eye (Chapter VIII). As oxidative stress increases in a system, the steady state $Asc^{\bullet -}$ concentration increases. These findings are consistent with the role of ascorbate as the terminal small-molecule antioxidant (See Table 3). Thus we propose that ascorbate, *i.e.*, the ascorbate free radical, can be used as a noninvasive indicator of oxidative stress [Buettner and Jurkiewicz, 1993; Roginsky and Stegmann, 1994].

The ascorbate radical as a marker of oxidative flux has been shown to be useful in the study of free radical oxidations in many biological systems including mouse skin [Buettner *et al.*, 1987; Jurkiewicz and Buettner, 1994; Timmins and Davies, 1993], hepatocytes [Tomasi *et al.*, 1989], and ischemia reperfusion of hearts [Arroyo *et al.*, 1987; Nohl *et al.*, 1991; Sharma *et al.*, 1994][7]. Human serum and rat plasma intoxicated with paraquat and diquat, known superoxide generators, have increased ascorbate radical levels [Minakata *et al.*, 1993]. In animal experiments, sepsis has also been shown to increase $Asc^{\bullet -}$, indicating the involvement of oxidative stress with this health problem [Stark *et al.*, 1988]. Sasaki *et al.* have investigated the use of $Asc^{\bullet -}$ signal intensity in combination with measurements of $AscH^{-}$ and DHA in human serum as an indicator of oxidative stress in human health problems that range from aging to xenobiotic metabolism [Sasaki *et al.*, 1982; Sasaki *et al.*, 1983; Sasaki *et al.*, 1984; Ohara

[7] In a quite different approach Pietri *et al.* [Pietri *et al.*, 1990; Pietri *et al.*, 1994] have used $Asc^{\bullet -}$ as a probe for plasma ascorbate concentrations. In their approach, a 1:1 mixture of plasma and dimethylsulfoxide is examined for $Asc^{\bullet -}$ by EPR. They claim that the $Asc^{\bullet -}$ is an

et al., 1992]. Taken together, these studies demonstrate that the ascorbate radical level in biological systems may be useful for monitoring free radical oxidations *in vivo*, particularly when free radical production is low and other methods are insensitive.

In general, quantitative aspects of $Asc^{\bullet -}$ generation and decay have been limited principally to fast kinetic studies [Bielski, 1982; Burkitt and Gilbert, 1990]. These studies have demonstrated that $Asc^{\bullet -}$ decays by a pH-dependent second-order dismutation process, k^{obs} (pH 7) = 2 x 10^5 M^{-1} s^{-1}. A recent study has demonstrated that the steady-state level of $Asc^{\bullet -}$, as observed by EPR, can be used as a marker for the rate of metal-catalyzed oxidation of ascorbate [Buettner, 1990].

Ascorbate has many functions in living systems, but a key feature is its ability to serve as a water-soluble antioxidant. In fact, ascorbate is the most effective water-soluble antioxidant in human blood plasma [Frei *et al.*, 1989; Frei *et al.*, 1988]. These observations are consistent with the thermodynamic properties of the ascorbate radical/ascorbate couple (Table 3). Because of the low reduction potential of the $Asc^{\bullet -}/AscH^-$ couple, $E^{o'}$ = + 282 mV, ascorbate will react with nearly every oxidizing radical that can arise in a biological system. This one-electron oxidation of $AscH^-$ results in the production of $Asc^{\bullet -}$, a resonance-stabilized tricarbonyl species that is readily observable by EPR.

---

index of the transient changes in plasma ascorbate status during ischemia/reperfusion. Whereas, in this study the $Asc^{\bullet -}$ levels reflect the ongoing free radical flux in the system being examined.

In the above experiments, using three different free radical-generating systems, the EPR signal height of $Asc^{\bullet -}$ was found to correlate with the flux of initiating free radicals as measured by DMPO spin trapping. However, it must be kept in mind that there is always a background oxidation of ascorbate yielding a low level of $Asc^{\bullet -}$ [Buettner, 1990]. This background $Asc^{\bullet -}$ signal intensity is a function of pH, catalytic metal concentration, oxygen concentration, and ascorbate concentration. As demonstrated here, when these variables are controlled, the steady state $Asc^{\bullet -}$ EPR signal intensity serves as a marker for the degree of free radical oxidative stress in the system.

In a biological system, it may be difficult to control all the variables that influence the $Asc^{\bullet -}$ EPR signal intensity. Thus, it is important that control experiments be carefully planned; a paired comparison design would be ideal. Therefore, in this work the spin trap DMPO was used in a paired comparison with ascorbate.

EPR spin trapping is a widely used technique that has provided both structural and quantitative information about reactive free radical formation, whereas the ascorbate free radical does not provide structural information of the precursor radicals. However, spin traps must be added to the system being measured and may be toxic to living species at the required concentrations for typical biochemical investigations. In addition, they are relatively expensive, whereas ascorbate is a natural, nontoxic endogenous biological compound. Consequently, the ascorbate radical level in biological systems may be useful for monitoring free radical reactions *in vivo*, particularly when free radical production is low and other methods are insensitive.

Because of the limitations of spin trapping, there is a need for complementary methods to detect oxidative radical production.

It is proposed that ascorbate (*i.e.*, the ascorbate free radical), which is naturally present in biological systems, can be used as a noninvasive indicator of oxidative stress. The ascorbate radical is a relatively stable, nontoxic radical species that is easily detectable. As oxidative stress increases in a system, the steady-state $Asc^{\bullet -}$ concentration increases. Thus, the EPR intensity of this radical can serve as an indicator of the degree of free radical oxidative processes taking place in chemical, biochemical, or biological systems.

Based on these results, it is proposed that the ascorbate radical signal height of mouse skin can serve as an indicator of the amount of oxidative damage occurring when the skin is irradiated with UV radiation.

CHAPTER IV

FREE RADICALS IN UV RADIATION-IRRADIATED SKIN[8]

Introduction

The ascorbate free radical is detectable by EPR at low steady-state levels in most biological samples, such as plant leaves [Stegmann *et al.*, 1993], plasma [Rose and Bode, 1993; Minetti *et al.*, 1992; Miller and Aust, 1989], synovial fluid [Buettner and Chaulitrat, 1990], skin [Buettner *et al.*, 1987], and lens of the eye. In Chapter III, the steady state $Asc^{\bullet-}$ concentration was positively correlated with an increase in oxidative stress. It was proposed that ascorbate, *i.e.*, the ascorbate free radical, which is naturally present in biological systems, can be used as a noninvasive indicator of oxidative stress [Buettner and Jurkiewicz, 1993; Roginsky and Stegmann, 1994].

The ascorbate radical as a marker of oxidative flux has been shown to be useful in the study of free radical oxidations in many biological systems including mouse skin [Buettner *et al.*, 1987; Timmins and Davies, 1993], hepatocytes [Tomasi *et al.*, 1989], ischemia reperfusion of hearts [Arroyo *et al.*, 1987; Nohl *et al.*, 1991; Sharma *et al.*, 1994], and in Chapters IV - VII as a marker of UV radiation-induced free radical formation in skin.

---

[8] A version of this chapter has been published as a Rapid Communication. BA Jurkiewicz and GR Buettner: Ultraviolet light-induced free radical formation in skin: An electron paramagnetic resonance study. *Photochem Photobiol* 59:1-4, 1994.

UV radiation elicits different effects in skin depending on its wavelength. The depth to which a photon penetrates *in vivo* is dependent upon its wavelength. Up to 99% of UVB wavelengths (290 - 320 nm) are absorbed by the non-viable upper epidermis, yet these wavelengths are known to form thymidine dimers and other photoproducts that are directly associated with erythema and induction of non-melanoma skin cancer. However, the specific mechanisms involved in the production of this photodamage remain unknown.

While UVB exerts its effects primarily in the epidermis, UVA radiation (320 - 400 nm) penetrates more deeply and has been shown to induce polymorphonuclear cell infiltration, as well as endothelial cell damage in the microvasculature [Rosario *et al.*, 1979; Zheng and Klingman, 1993]. UVA radiation itself has been associated with photoaging [Bissett *et al.*, 1989; Moan, 1994], carcinogenesis, inflammation, and pigment darkening in skin [Klingman *et al.*, 1985]. UVA is approximately 1000 times less erythemogenic to skin than UVB, but sunlight contains on the order of 100 times more UVA than UVB. Human exposure to UVA is also increasing due to prolonged sun exposure resulting from use of UVB sunscreens that prevent sunburn formation, as well as the popular use of sun-tanning beds (330 - 400 nm) [Moan, 1994]. Hence, the objective of this study was to investigate by EPR the effects of both UVA and UVB radiation on ascorbate free radical production in skin.

The resonance-stabilized ascorbate free radical is detectable directly by EPR. However, the non-resonance stabilized free radicals initially produced in the skin by UV

radiation would have very short lifetimes at room temperature; thus EPR spin trapping techniques have been applied to detect these radicals.

Because spin traps themselves may be photochemically active, a photochemical system containing spin traps and a linoleic acid emulsion was also examined. The application of a liposome model to the study of UV radiation-induced lipid peroxidation is useful because it avoids the complications of possible interference from cellular components other than the membrane lipids [Yin *et al.*, 1992; Chatterjee and Agarwal, 1988].

Materials and Methods

The typical approach for studying free radicals produced in skin during UV radiation exposure has been to use homogenized skin samples. But, homogenizing the sample will produce confounding artifacts [Kozlov *et al.*, 1992; Draper *et al.*, 1993]; thus, in this study sections of skin are used, epidermis and dermis intact.

Vertebrate Animals

Skh-1 hairless mice were obtained from Charles River Laboratory, Portage, MI and were given a standard diet and water *ad libitum*. Skh-1 mice were selected for these photobiology experiments because they do not spontaneously develop carcinomas of the skin and are an excellent model of photoaging [Bissett *et al.*, 1989]. Other benign skin tumors, like papillomas, are very rare but sometimes develop in old animals [De Gruijl *et al.*, 1983]. In all studies only the dorsal skin of the mouse was used. The University of Iowa approved protocol number was #9406221 (expiration 7/22/95).

Direct Detection of Ascorbate Radicals in Skin

Whole dorsal skin was harvested from mice and cut into EPR usable pieces (approximately 1 cm^2). Samples were examined when either fresh (within one hour of sacrifice) or kept at dry ice or liquid nitrogen temperatures until EPR examination. The skin samples were placed in a Wilmad Glass Co. (Buena, NJ) tissue cell that had the lower positioning rod removed. This modified cell is easier to tune when using a tissue sample due to its increased rotational capabilities. A coverslide was held in place over the sample with Parafilm® ties. The epidermal surface of the skin was exposed to UV radiation while in the EPR cavity (Figure 20). In the experiments in the following chapters EPR spectra were obtained at room temperature using a Bruker ESP 300 spectrometer (Bruker Instruments; Karlsruhe, Germany) equipped with an ER035 Gaussmeter and an E1P-625A microwave frequency counter, operating at 9.73 GHz with 100-kHz modulation frequency. In the ascorbate experiments the EPR spectrometer settings were: microwave power, 40 milliwatts; modulation amplitude, 0.66 G; time constant, 0.3 s; scan rate, 8 G/41.9 s; receiver gain, 2 x 10^6.

For all experiments, the light source was a model 60100, 150 W Photomax® xenon arc lamp (Oriel Corporation; Stratford, CT). In those experiments examining the effects of solar radiation, UVB and UVA combined, on skin, wavelengths below ≈ 300 nm were filtered out using a Schott WG 305 filter, Duryea, PA, (14 $\mu W/cm^2$ UVB; 3.5 mW/cm^2 UVA). For the UVA experiments, irradiation was done using the same light setup, with the exception of using a Schott WG 335 nm filter (0.3 $\mu W/cm^2$ UVB; 3.3 mW/cm^2 UVA). For visible light experiments

wavelengths below 400 nm were filtered out using an Oriel 59472 filter in combination with an IR filter (0.23 mW/cm^2 UVA). Infrared radiation from the light was removed by a 5.0 cm quartz water filter. The filtered light fluence rate, assuming the cavity grid transmits 75% of the incident light, was measured using either a Yellow Springs Instrument (Yellow Spring, OH) model 65A radiometer with a 6551 probe or a Model IL 1400A International Light Inc. radiometer (Newburyport, MA) with UVA detector model SEL 0333; UVB detector model SEL 240. The percent UV transmittance for the different cutoff filters (Figure 21) was obtained with a Milton Roy Spectronic® 3000 Array UV spectrophotometer.

Indirect Detection - EPR Spin Trapping

For the spin trapping experiments, a 250 mM aqueous stock solution of α-[4-pyridyl 1-oxide]-N-*tert*-butyl nitrone (POBN) (Sigma Chemical Co., St. Louis, MO) was prepared immediately prior to use. No increase in background EPR signal occurred when POBN alone was exposed to UV radiation. Skin sections were placed on ice in weigh boats and 50 μL of 250 mM POBN was topically applied to the epidermis for ten minutes. The skin samples were lightly blotted with a Kimwipe® after incubation with spin trap and placed in a Wilmad Glass Co. tissue cell. Only the epidermal surface was exposed to UV radiation while in the cavity, using the same radiation source set up as in the ascorbate experiments (See Figure 1). EPR instrument settings for the spin trapping experiments were: microwave power, 40 milliwatts; modulation amplitude, 0.76 G; time constant 0.3 s; scan rate 60 G/41.9 s; receiver gain, 1 x 10^6.

For the liposome experiments, a 3 mM linoleic acid emulsion was made immediately prior to use in a metal-free phosphate buffer purged with nitrogen to prevent autoxidation, and covered with aluminum foil to prevent possible photooxidation [Yin *et al.*, 1992]. The pH of the emulsion was adjusted to 6.5 with strong HCl. The spin traps POBN, 10 mM, or DMPO, 50 mM, were added to the linoleate mixture prior to examination by EPR. The EPR instrument settings were: microwave power, 40 milliwatts; modulation amplitude, 0.66 G; time constant, 0.3 s; scan rate, 60 G/84 s; receiver gain, 1×10^6.

Statistics

Throughout this research project all experimental samples were compared to untreated, aged-matched control animals. For each experiment the number of skin samples was three or greater and taken from at least three different animals. Statistical significance of associations between cases and control was determined with Microsoft Excel (Microsoft Corporation, Seattle, WA) or Quattro Pro (Borland, Scotts Valley, CA) analysis tools running ANOVA and student t-test, wherever applicable. The resulting two sided p-values were determined significant at the 0.05 level.

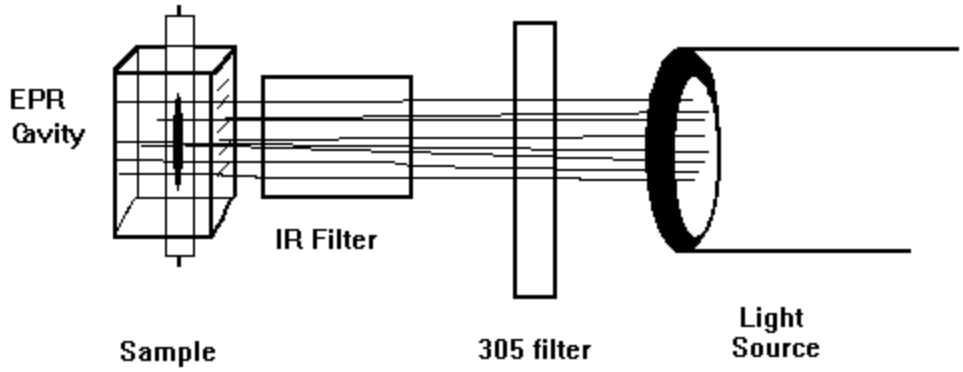

Figure 20. EPR and UV radiation source setup for EPR tissue cell experiments. The 305 filter cuts off all wavelengths below ≈ 300 nm. The IR filter is a water-filled large diameter (45 mm) cylindrical, quartz UV-visible cell having a 50 mm path length. The radiation source is an Oriel Photomax® system with a 150 W Xenon lamp. This system requires no special air handling due to ozone production. For the combined UVA and UVB irradiation skin experiments the lamp was operating at ≈ 3 mW/cm^2.

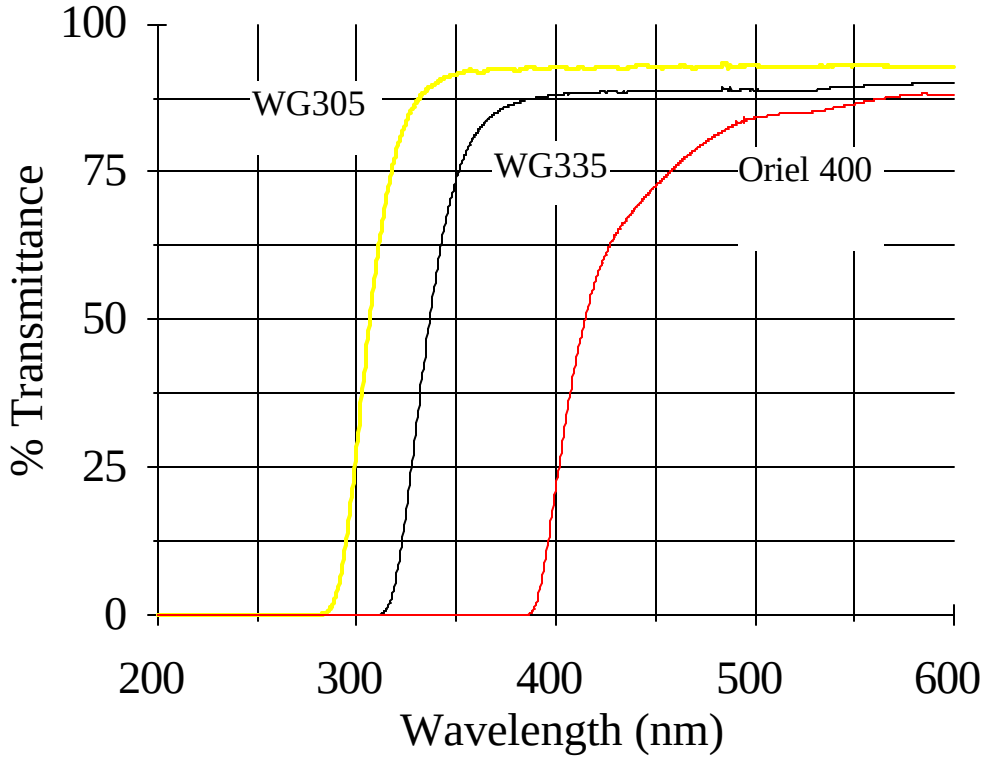

Figure 21. Spectra of the percent ultraviolet radiation transmittance of the WG 305, WG 335, and Oriel 400 filters.

Results and Discussion

Direct Detection of the Ascorbate Radical in Skin

The Role of UVA/UVB (300 - 400 nm)

The percent UV transmittance of the WG 305 filter is shown in Figure 2. Only those wavelengths greater than 300 nm were transmitted. Using room temperature EPR, the endogenous resonance-stabilized ascorbate free radical was observable by EPR, g = 2.0053, at a very low steady-state level in mouse skin [Buettner *et al.*, 1987], Figure 22. Each line of the ascorbate radical doublet is actually a triplet of doublets: a^{H4} = 1.76 G, a^{H6} (2) = 0.19 G, and a^{H5} = 0.07 G [Laroff *et al.*, 1972]. However, these EPR instrument settings were selected for maximum sensitivity; thus, only a doublet with $a^{H4} \cong$ 1.8 G is observed.

The direct detection of the ascorbate free radical by EPR is consistent with ascorbate's role as the terminal small-molecule antioxidant [Buettner, 1993]. Due to ascorbate radical's low reduction potential, + 282 E°′ mV [Williams and Yandell, 1985], nearly every oxidizing radical that can arise in a biological system will react with ascorbate forming the semi-dehydroascorbate radical, a resonance-stabilized, tricarbonyl free radical species. In Chapter III it was demonstrated that the ascorbate radical EPR signal can serve as an indicator of the flux of oxidative events occurring in a biochemical system [Buettner and Jurkiewicz, 1993]. Exposure of mouse skin to combined UVA and UVB radiation, while in the EPR cavity, results in an increase in the ascorbate radical

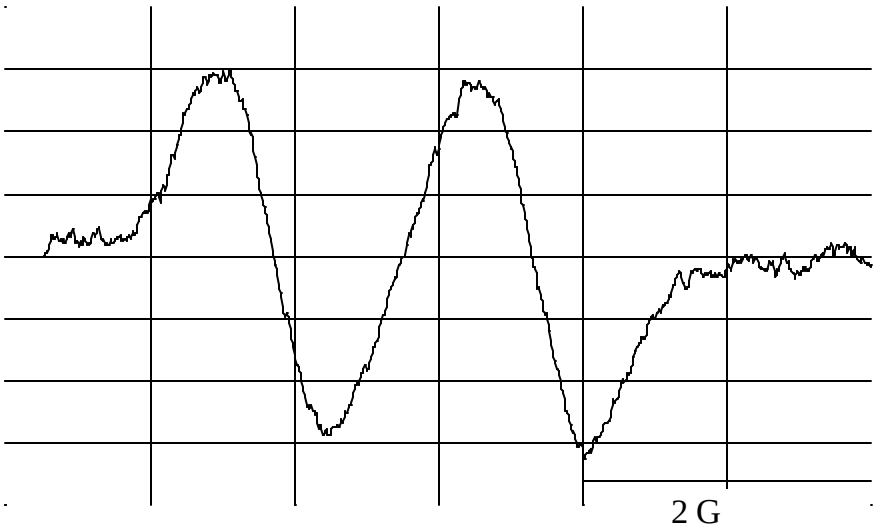

Figure 22. EPR spectrum of the ascorbate radical signal doublet in mouse skin during UV radiation exposure.

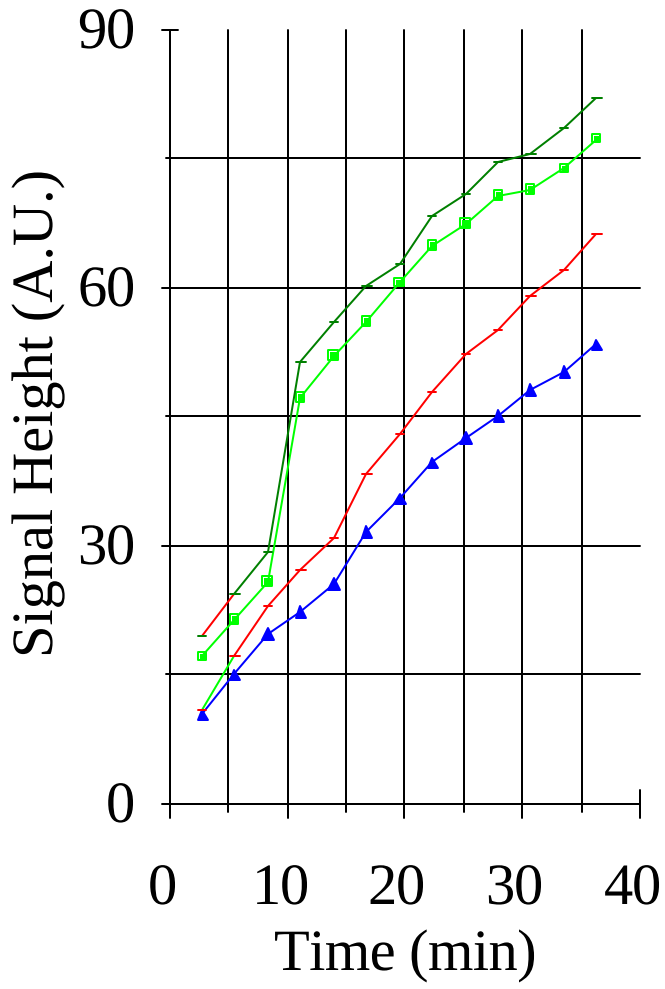

Figure 23. UV radiation increases the ascorbate radical signal in mouse skin. ♦, Ascorbate free radical EPR signal height in skin exposed to room light only. ■, Ascorbate free radical EPR signal height in skin during UV exposure. The light source was turned on after collection of the third data point. Each data point represents the mean of three or more different skin samples. The error bars represent the SEM. After UV radiation exposure, a Student's t-test showed differences between the points to be statistically significant, $p < 0.05$.

signal height indicating that during UV radiation exposure the skin is undergoing free radical oxidative stress (Figure 23). With continuous UV radiation exposure the ascorbate radical signal height remains elevated for up to 4 hours (not shown).

In these skin experiments both fresh and frozen samples were used. The ascorbate radical signal appears to be stable in skin samples that have undergone freezing and storage in liquid nitrogen. The endogenous ascorbate free radical baseline signal height was higher in the samples that were frozen in liquid nitrogen as compared to fresh samples, but the actual measured change in signal due to radiation exposure was nearly identical, ≈ 77.8 % ± 12.1% increase in fresh and ≈ 94.4% ± 4.2% increase in frozen skin (data represents mean percent increase ± SEM).

The Role of UVA (320 - 400 nm)

The effects of UVA radiation (320 - 400 nm) alone on free radical production in skin were also examined. In these experiments only those wavelengths above ≈ 320 nm were examined (Figure 21).

The UV radiation-induced ascorbate free radical signal increase was found to be almost identical in the > 320 nm radiation exposed samples as the > 305 nm radiation exposed samples (Figure 24). Thus, UVA wavelengths alone induce free radical formation in mouse skin. These data indicate that the chromophore in skin for UV radiation-induced ascorbate radical production absorbs UV wavelengths among 305 - 400 nm.

Formation of these free radicals can occur from the absorption of UVA or UVB wavelengths by many cellular components. As examples, UV irradiation of NADH or NADPH can produce superoxide anion radical or hydrogen peroxide. In addition, photochemical degradation of tryptophan can also produce hydrogen peroxide. Iron complexes may then react with hydrogen peroxide to generate hydroxyl radicals in a superoxide-driven Fenton reaction. In addition, flavins, quinones, and porphyrins may absorb UV wavelengths and undergo photochemistry to produce singlet oxygen.

Up to 20% of solar UVB radiation absorbed by the mouse skin reaches the viable cells of the epidermis, and about 10% penetrates to the dermis. However, a considerably higher proportion of UVA and visible light can reach the dermis [Bruls *et al.*, 1984]. Because UVA can penetrate into the dermis, the free radicals produced by these wavelengths may be more deleterious by interacting with and damaging the underlying cutaneous vasculature and supporting tissues. Until recently, the effects of UVA were thought to be innocuous, however, the carcinogenic risk of UVA and UVB radiation has been reported to be nearly equal in magnitude (though higher doses of UVA are required) [van Welden *et al.*, 1988]. Thus, sunscreens that block UVB wavelengths but allow the transmittance of UVA are not protective against free radical formation, photoaging, or skin cancer [van Welden *et al.*, 1988].

The Role of Visible Light (400 - 760 nm)

Visible light photons have generally been considered innocuous because of their low energies and biological targets in mammalian cells such as DNA, lipids, and proteins have

relatively weak extinctions at these wavelengths [Bruls *et al.*, 1984]. However, in skin, naturally occurring photosensitizing agents, such as riboflavin, can produce free radicals in the presence of visible light. Thus, the potential involvement of visible light in free radical production was examined.

The percent UV transmittance spectrum of the visible light filter is shown in Figure 21. Only those wavelengths above approximately 400 nm were transmitted. In Figure 25, it can be seen that exposure to visible light does not increase the ascorbate free radical EPR signal in mouse skin above ambient room light levels. Turning the overhead room lights off had no affect on ascorbate radical levels. This indicates that visible light has no detectable effect on free radical formation in mouse skin.

Indirect Detection - EPR Spin Trapping

Spin Trapping in Skin

Previously, the only spin trap that had been used in studying radicals formed in mouse skin by UV radiation is DMPO [Ogura *et al.*, 1991; Ogura *et al.*, 1987; Taira *et al.*, 1992]. Timmins, *et al.* used DMPO to trap tumor promoting organic peroxidase-induced radicals in pieces of mouse skin [Timmins and Davies, 1993]. In this peroxidase system, they were able to spin trap radicals characteristic of peroxyl, alkoxyl, and alkyl radicals. Thus, the use of DMPO was examined in this skin model to try to further identify the possible oxygen radicals involved in UV radiation-induced free radical

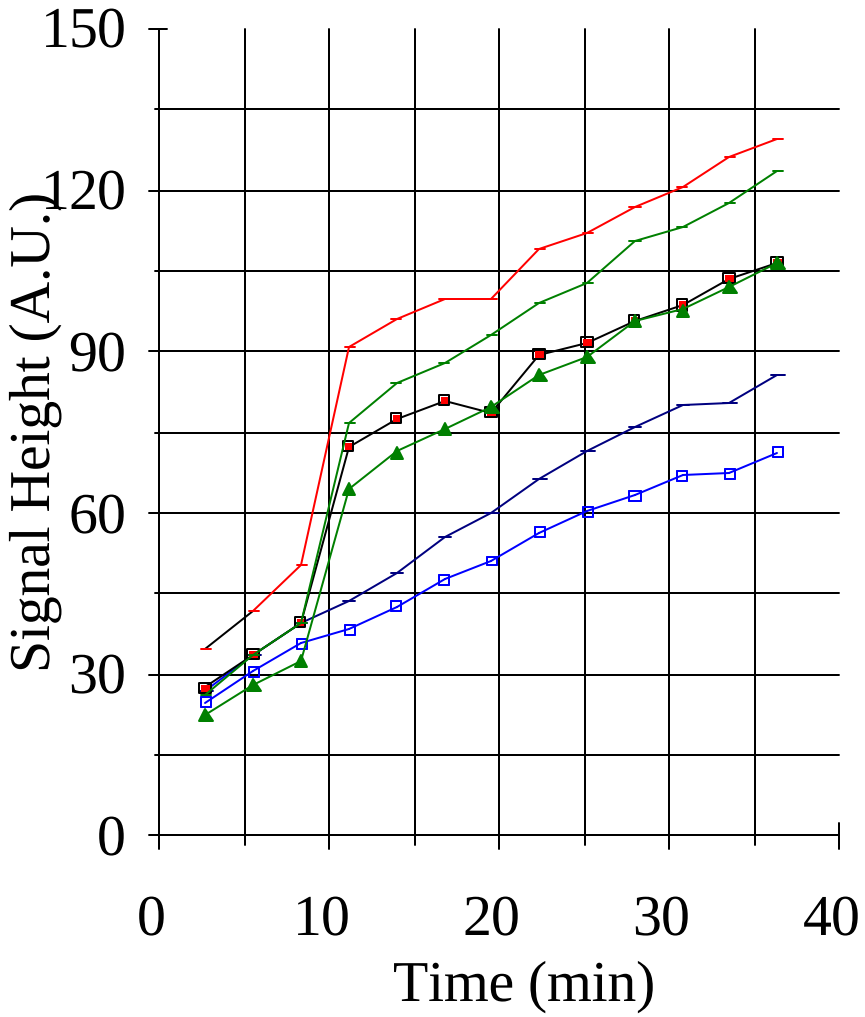

Figure 24. UVA increases the ascorbate radical signal height in mouse skin. ■, Ascorbate radical signal in skin exposed to combined UVB and UVA (305 nm filter) radiation; ♦, Ascorbate radical signal in skin exposed to UVA radiation (335 nm filter); □, Ascorbate radical signal in skin exposed to room light only. Each data point represents the mean of five different experiments. The epidermal surface of the skin was exposed to UV radiation while in the EPR after collection of the third data point. After radiation exposure a paired comparison of each curve found the UVA and combined UVA/UVB exposed samples to not be statistically different from one another.

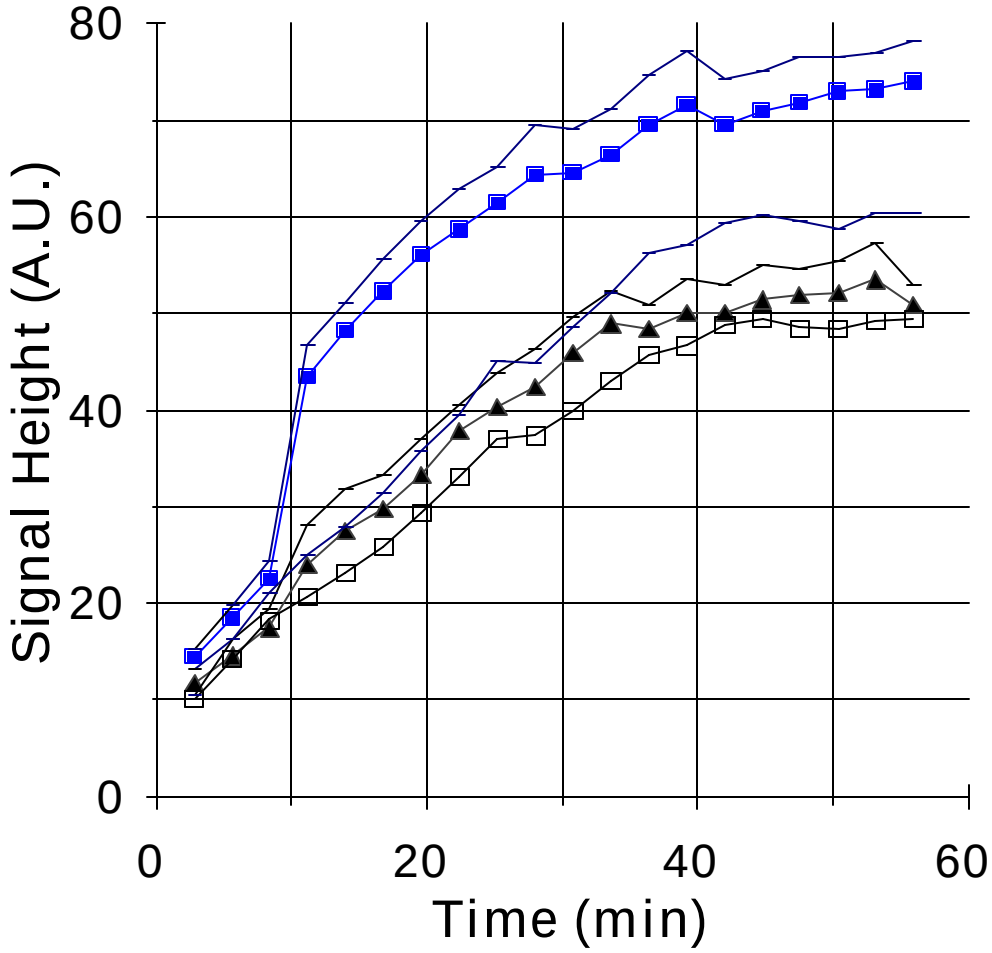

Figure 25. Ascorbate in skin exposed to UV versus visible light.
■, Ascorbate signal intensity from skin that was exposed to UV and visible light (305 nm filter); ♦, Ascorbate signal intensity from skin exposed to visible light only (400 nm filter); □, Ascorbate signal intensity from skin that was exposed to room light only. The data represent the mean of four separate experiments. The light was turned on after the third data point. After UV radiation exposure, a paired comparison of each curve showed the visible light exposed samples to not be statistically different than those samples exposed to room light.

formation. DMPO, 50 μL of a 1 mM charcoal purified stock, was topically applied to this UV radiation system in the same manner as the POBN; however, no spin trapped adduct was observable in the absence or presence of UV radiation. Only the ascorbate doublet was observed, Figure 26.

Other spin traps have also been examined for usefulness in trapping free radicals in skin. Because there was evidence that UV radiation-induces lipid peroxidation products in skin, spin traps for carbon-centered radicals were applied. Although DMPO is efficient at trapping hydroxyl and superoxide anion radicals, the water soluble nitrone spin trap α-4-(pyridyl-1-oxide)-*N-tert*-butylnitrone (POBN) may be better suited for skin studies due to its greater efficiency for trapping carbon-centered radicals, such as alkyl radicals, at physiologic pH (Figure 27).

With POBN, when skin was exposed to UV radiation a carbon-centered POBN spin adduct (*) as well as the ascorbate radical (^) was observed (Figure 28). For the POBN radical adduct, the EPR spectrum consists of three groups of lines due to nitrogen a^N and a doublet splitting due to β-hydrogen, a^H. The spectra exhibited hyperfine splittings characteristic of POBN/alkyl radicals, a^N = 15.56 G and a^H = 2.70 G, possibly generated from membrane lipids as a result of β-scission of lipid alkoxyl radicals to generate alkyl radicals, such as ethyl and pentyl radicals [Chamulitrat *et al.*, 1992]. Spin adducts were identified by evaluation of hyperfine splitting constants and compared with published data [Buettner, 1987].

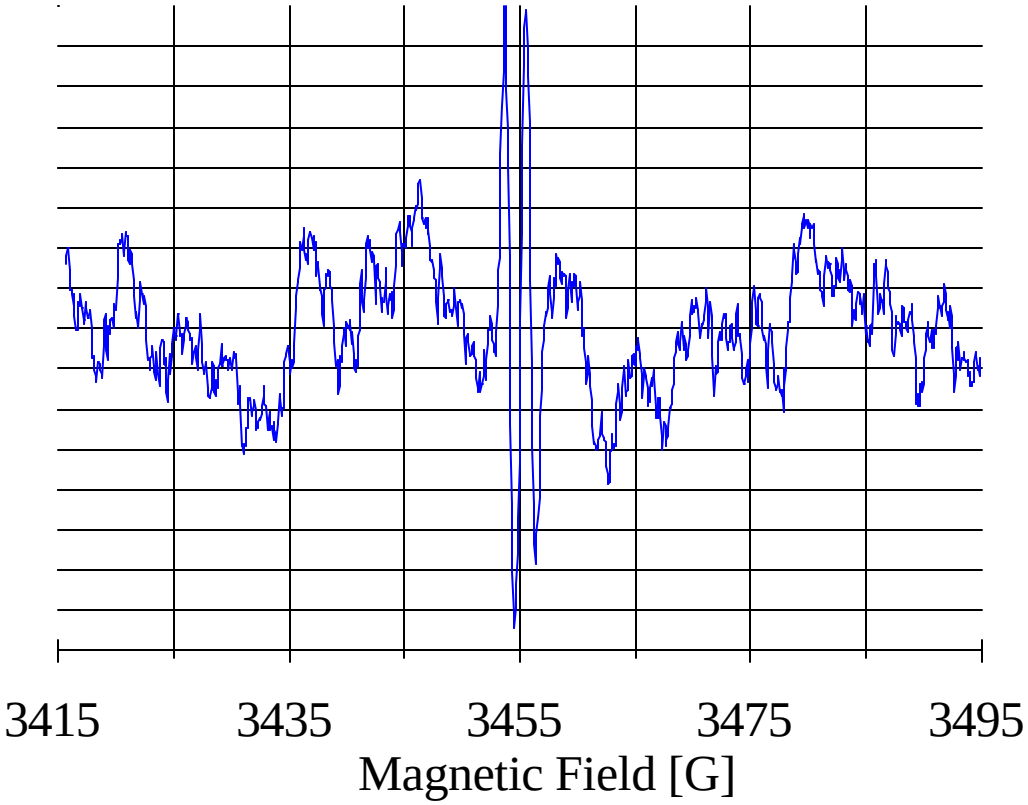

Figure 26. An EPR spectra of mouse skin treated with the spin trap DMPO. The only observable signal is of the ascorbate free radical doublet. This spectrum represents 10 signal-averaged scans during continuous UV irradiation. EPR instrument settings for the spin trapping experiments were: microwave power, 40 milliwatts; modulation amplitude, 1.06 G; time constant 0.3 s; scan rate 80 G/84 s; receiver gain, 1 x 10^6.

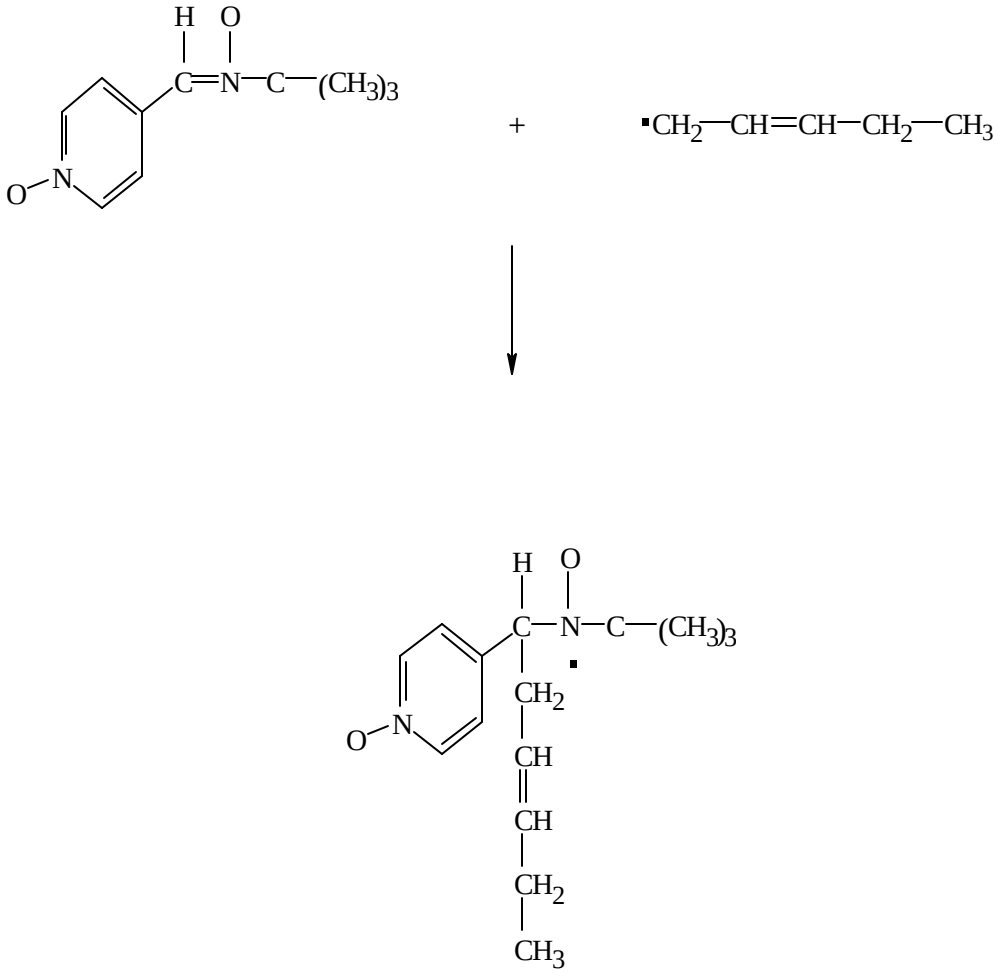

Figure 27. The reaction of the spin trap α-4-(pyridyl-1-oxide)-*N-tert*-butylnitrone with an alkyl radical to form an EPR visible adduct.

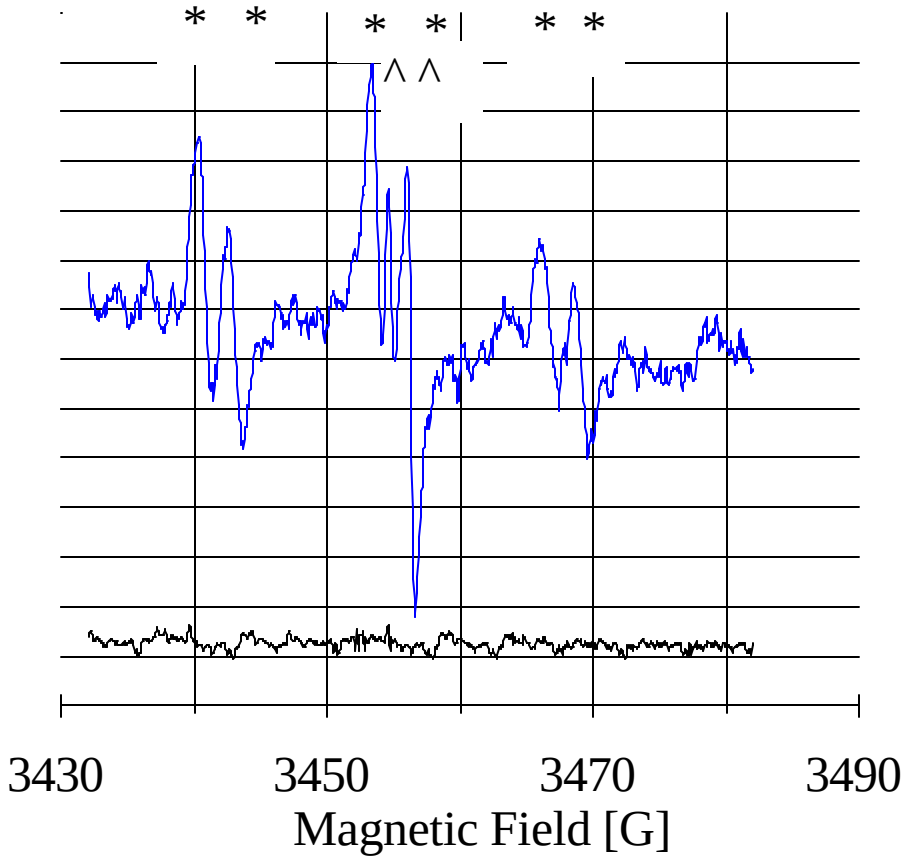

Figure 28. POBN spin trapping of UV radiation-induced radicals in skin.
The lower spectrum is from skin exposed to room light. The upper spectrum is from skin exposed to the combined UVA and UVB radiation source (Schott WG 305 filter). When skin was exposed to UV radiation a carbon-centered POBN spin adduct (*) as well as the ascorbate radical (^) was observed.

The exact location of these UV radiation-induced free radical formation in skin is unknown. The spin trap may be penetrating through the membranes or only trapping lipid radicals present on the superficial dead layer of skin, the stratum corneum. Thus, the stratum corneum of the skin was removed by tape stripping or by gentle scraping with a razor blade to examine whether having the viable layers of the epidermis exposed to UV radiation will change free radical production. There was no difference found in either the type or amount of free radical in this 'exposed' skin (data not shown), indicating that free radical formation must be occurring in the viable layers of the skin. Thus, this EPR spin trapping method provides a unique tool to study UV radiation-induced lipid peroxidation in intact skin.

Linoleic Acid

Because spin traps themselves may be photoreactive, POBN was also examined in a lipid emulsion system. The lipid composition of skin is predominantly in the linoleate (18:2) form [Bowser *et al.*, 1985]; therefore this form was examined. The exposure of a linoleic acid emulsion to UV radiation while in the EPR cavity did not result in any baseline level of lipid peroxidation due to autoxidation, as measured by POBN[9]. The possible role of iron was also examined in this system. Either ferric iron (10 μM) or ferrous iron (10 μM) was incubated for 10 minutes with 3 mM of the linoleic acid emulsion prior to addition of either spin trap. The iron containing emulsion system was exposed to UV radiation while in the EPR cavity. A small

[9] These experiments were also repeated using 50 mM of the spin trap DMPO. No signal was detected in the presence or absence of UV radiation.

signal consistent with the breakdown of POBN spin trap was observable when the ferrous iron containing emulsion was exposed to light, indicating that in this system iron may be a weak chromophore. These results indicate that our results in skin are not simply due to POBN photochemistry.

Photooxidation of lipids may be one of the initial steps involved in UV radiation-induced skin damage [Shibamoto, 1994]. The presence of lipid peroxidation products in our mouse skin model is not surprising considering it has been reported that in normal human skin the content of lipid peroxides are higher in sun-exposed sites than in non sun-exposed sites [Bissett and McBride, 1992], and in chronically exposed areas of human skin lipid peroxidation products are increased following UV exposure [Meffert *et al.*, 1976].

Lipid peroxidation products themselves, such as 4-hydroxynonenol and malondialdehyde, can be directly genotoxic and mutagenic [Basu and Marnett, 1983; Goldschmidt, 1984]. In addition, lipid peroxidation products and peroxides formed at the membrane can cause membrane fluidity changes, increase ion permeability, inactivate membrane enzymes and receptors, diffuse to the nucleus and create damage there, or be released outside the cell, where they may induce damage to surrounding cells [Emerit *et al.*, 1991]. Peroxidized lipids can covalently bind to proteins [Nielsen, 1981] and DNA [Ames *et al.*, 1982], and may also induce apoptosis [Ramakrishnan *et al.*, 1993; Ramakrishnan *et al.*, 1995a; Ramakrishnan *et al.*, 1995b].

This work provides the first direct evidence for UV radiation-induced free radical formation in intact skin. Using spin trapping techniques we were able to detect carbon-centered radicals with hyperfine splittings typical for lipid alkyl radicals. Lipid peroxidation is a complex free radical chain reaction initiated by the abstraction of a *bis*-allylic hydrogen atom from a polyunsaturated fatty acid. Initiation of this process requires the presence of iron or other catalytic metals, and thus iron was examined as a possible chromophore and catalyst in this UV radiation-induced lipid peroxidation in Chapter V.

CHAPTER V

THE ROLE OF IRON IN UV RADIATION-INDUCED FREE RADICAL FORMATION IN SKIN[10]

Iron is a requirement for significant free radical-induced lipid peroxidation [Miller *et al.*, 1990]. It has been shown that the amount of non-heme iron in skin increases with chronic UV exposure [Bissett *et al.*, 1991]; the presence of this iron may promote lipid peroxidation. In addition, iron may act as a chromophore for UV radiation. Although Fe(III) cations do not absorb significantly in the UV range [Yin *et al.*, 1992], complexation by ligands can increase their absorption in the UV region. Photolysis of Fe(III) ligand-complexes, such as ferritin, can result in formation of Fe(II) as well as hydroxyl radicals [Larson *et al.*, 1992; Aubailly *et al.*, 1994], both of which can be involved in lipid peroxidation. Free radicals, hydrogen peroxide, and iron contribute to skin inflammatory disorders, including psoriasis and sunburn formation [Trenam *et al.*, 1992]. Thus, the role of iron, both as catalyst and chromophore, in UV radiation-induced radical formation was examined.

In this study the first objective was to localize and quantitate iron in chronic UV radiation-exposed mouse skin by histological staining, x-ray microanalysis techniques, and by measuring the amount of chelatable iron in skin using low temperature EPR techniques. It was

---

[10] A version of this chapter has been published as a Rapid Communication. BA Jurkiewicz and GR Buettner: Ultraviolet light-induced free radical formation in skin: An electron paramagnetic resonance study. *Photochem Photobiol* 59:1-4, 1994.

then hypothesized that if iron is involved in lipid peroxidation, then topical application of iron should increase free radical formation in skin. Finally, the use of metal chelators to reduce the UV radiation-induced increase in free radical signal was examined.

Localization and Quantitation of Iron in Skin

Chronic exposure, more than 12 weeks, to UV radiation is found to significantly increase the basal amounts of non-heme iron in Skh-1 mouse skin [Bissett *et al.*, 1991]. The specific aim of this first section of the chapter was to examine the location of iron in UV radiation-exposed and unexposed mouse skin samples by histological staining followed by analysis with light microscopy and by scanning electron microscopy (SEM) x-ray microanalysis of freeze dried skin. The chelatable skin iron was quantitated in these chronically exposed samples using low temperature EPR spectroscopy techniques.

Materials and Methods

Histological Localization- Light Microscopy

Skin biopsies were taken from mice that were exposed to UV light (315 nm peak emission) for 12 weeks with 30 mJ/cm^2, 50% of the mouse minimum erythemal dose (MED), as well as unexposed age matched controls. Skin samples were kindly provided by Procter and Gamble, Cincinnati, OH. The iron content of UV radiation exposed skin was examined histologically. Skin was dehydrated in ethanol (70-100%) followed by xylene and embedded in paraffin under vacuum conditions. Samples were sectioned at 6 to 10 μm and stained for

ferrous iron using a modified Lillies method [Sheehan and Harpchak, 1987]. The method follows:

1. Hydrate slides
2. Immerse slides for 1 hour in a solution containing 2.2 mg of potassium ferrocyanide in 200 mL 0.06N HCl
3. Wash with 0.01N HCl
4. Counter stain with 6% eosin for 3 minutes
5. Dehydrate in xylene and coverslip

Both UV and unexposed skin samples were stained simultaneously using identical parameters. Slides were kept in an acidic solution during staining to keep the iron in the ferrous form. After staining, slides were examined with a Leitz Diaplan® light microscope.

X-ray Microanalysis

UV irradiated and non-exposed dorsal skin samples were also examined by SEM x-ray microanalysis. Briefly, this technique involves high energy beam electrons interacting with shell electrons of the specimen atom so that an inner shell electron is ejected. The removal of the electron temporarily ionizes the atom until an outer shell electron drops into the vacancy, releasing energy as a characteristic x-ray. Different elements fill vacancies in shells in unique ways, generating a spectrum that can be used to identify the element.

Freeze drying of the skin was necessary in this study because conventional SEM fixative techniques dissolve and redistribute diffusible substances and elements. Also osmium and other

commonly used fixatives can interfere with elements of interest when examining biological samples by x-ray microanalysis. Samples were freeze-dried using dry ice and ethanol to achieve temperatures of ≅ -90 C in a vacuum system for 24 hours. The samples were examined using a Hitachi S-2700 SEM operating at 15 kV, following Delta I instructions.

EPR Measurement of Fe(III)Desferal®

Skin, in 50 mM demetalled phosphate buffer pH 7.4, was homogenized on ice using a motor driven Teflon® pestle homogenizer, followed by sonication. The homogenate was incubated with the metal chelator Desferal® and frozen in liquid nitrogen prior to EPR examination.

EPR spectra were obtained using a Bruker ESP 300 spectrometer operated at 9.43 GHz with 100 kHz modulation frequency. All EPR measurements were made at 100 K using an ER4111VT variable temperature apparatus. Signal averaging (multiple scans of the same sample) was used to improve the signal to noise ratio. The EPR spectrometer settings for the Fe(III)Desferal® complex were: optimal microwave power, 80 milliwatts; modulation amplitude, 16 G; time constant 1.6 s; scan rate 500 G/84 s; receiver gain, 2.5×10^5.

Results

Histological Localization- Light Microscopy

Using light microscopy, a substantial increase in the amount of iron deposition in the basal layers of the UV radiation exposed skin was found as compared to the unexposed skin

Figure 29. The heaviest deposition of staining was found in the lower regions of the epidermis, the stratum germinativum where the viable cells are located, and also in the dermis (arrows). Staining was not associated with any specific cellular structures. Quantitation of iron using a black and white imaging system was difficult due to lack of contrast. The UV radiation exposed skin samples showed signs of dermal thickening as well as an increased number of cysts formed in the dermal layer indicating collagen degradation [Bissett *et al.*, 1987].

X-ray Microanalysis

In the x-ray microanalysis experiments, results are presented as an average of three measurements taken at the top (epidermis), middle (basement membrane), and lower portions (dermis) of a cross section of skin (Figure 30). No iron was detectable in either UV radiation exposed or unexposed skin samples by this technique. Previous x-ray microanalysis studies of iron in skin have used samples from guinea pigs and humans with detectable levels of iron in the range of 50 - 400 μg/g tissue [Forslind *et al.*, 1985], which is well above the estimated concentration of iron in mouse skin samples. In the

Figure 29. Iron staining is increased in chronically exposed skin samples.

Light microscope pictures of epidermal and dermal layers of UV radiation exposed (upper) and unexposed mouse skin (lower). The arrows indicate areas of intense staining. The pictures were magnified 277 times, and the micron bars equal 100 μm.

UV radiation exposed mouse skin, calcium, phosphorus, potassium, and sulfur were found to be increased compared to controls. The significance of this change in distribution is unknown. The presence of calcium in the UV radiation exposed skin may be due to radiation-induced damage to membrane transport proteins affecting ionic homeostasis leading to increased calcium. Increases in the permeability of the phospholipid bilayer can also cause an increase in cellular calcium concentrations.

When comparing the elemental distribution of the mouse skin versus reported literature on human skin [Noble, 1991], there are similarities between the elemental profile of the chronically exposed mouse skin and the human skin. This could possibly indicate that the human skin in this referenced study was obtained from a sun exposed region; unfortunately, the sample source was not indicated.

EPR Measurement of Fe(III)Desferal®

The amount of catalytically active iron present in skin is not known; thus EPR techniques have been applied to measure the amount of chelatable iron in skin. Many complexes of Fe(III) are paramagnetic and often exhibit an EPR signal at g = 4.3. Fe(III)Desferal® is paramagnetic and thus, the measurement of the EPR signal of Desferal®-iron complexes after treatment with Desferal® may be used as a method for estimating the concentration of chelatable Fe(III) in a sample (the structure of Desferal® is shown in Figure 31). Because Desferal® may penetrate into cells [Laub *et al.*, 1983], it has been used in this study to examine concentrations of Fe(III) in skin.

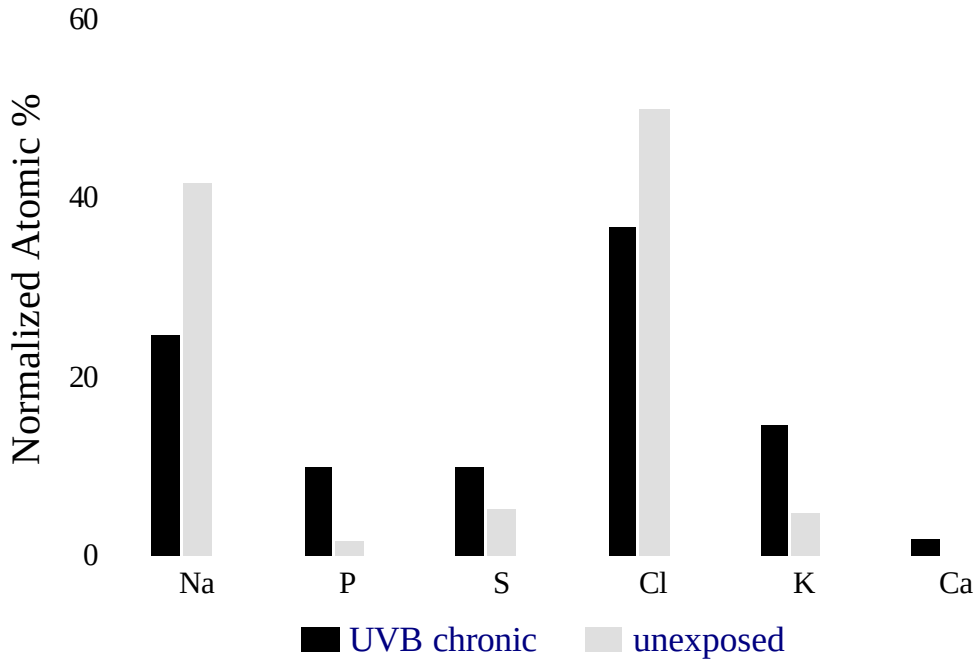

Figure 30. X-ray microanalysis element profile of unexposed and chronic UV radiation exposed skin samples.
In each group, the bar value represents a normalized average of two different skin samples measured at three separate locations of skin. The results are normalized to 100% of the total elemental concentration.

Fe(III) forms a complex with the iron chelator Desferal® that gives an EPR detectable signal at g = 4.3 (Figure 32) [Kozlov *et al.*, 1992]. This signal was examined using the variable temperature accessory set at 100 K to control the level of background noise and enhance signal. Signal intensity is known to increase with the square root of the microwave power until saturation begins to occur, thus, the optimal microwave power to maximize the Fe(III)Desferal® signal was determined (Figure 33) [Buettner and Kiminyo, 1992]. The EPR signal intensity was found to correlate with the Fe(III)Desferal® concentration (Figure 34). This approach can determine levels of Desferal® chelatable metals as low as 0.5 μM. In the absence of Desferal® a very weak signal was observable at g = 4.3, indicating the presence of endogenous paramagnetic iron complexes in skin.

In a chemical system, the signal intensity of the Fe(III)Desferal® complex correlates with the amount of free iron, thus in the skin homogenates we can obtain an estimate of the amount of chelatable iron (*i.e.*, non-heme iron) in skin. By using the standard curve (Figure 34), the amount of Desferal® chelatable iron in a skin homogenate was estimated (Table 5).

These data show that mouse skin contains between 5.2 - 10.0 μM chelatable iron, depending on UV radiation exposure. These values are consistent with those found in the literature. In biological fluids, the iron concentration using the bleomycin assay was found to be between 3-5 μM [Halliwell and Gutteridge, 1985]. In synovial fluid, an iron-dependent ascorbate oxidation assay found 10 μM of free iron [Buettner and Chamulitrat,

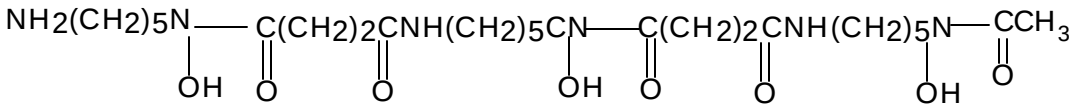

Figure 31. The structure of Desferal® (desferrioxamine B).
This is a natural product isolated from *Streptomyces pilosus* that forms iron complexes.

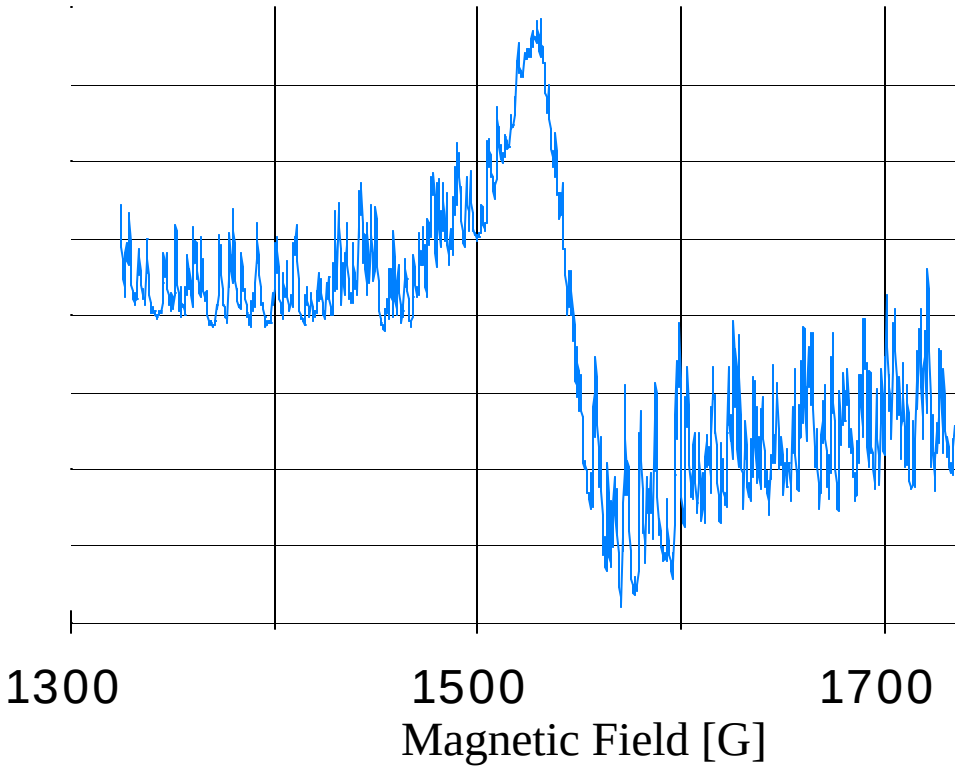

Figure 32. Fe(III)Desferal® signal (g-value = 4.3) at 100 K.
The [Fe(III) Desferal] was 4 μM.

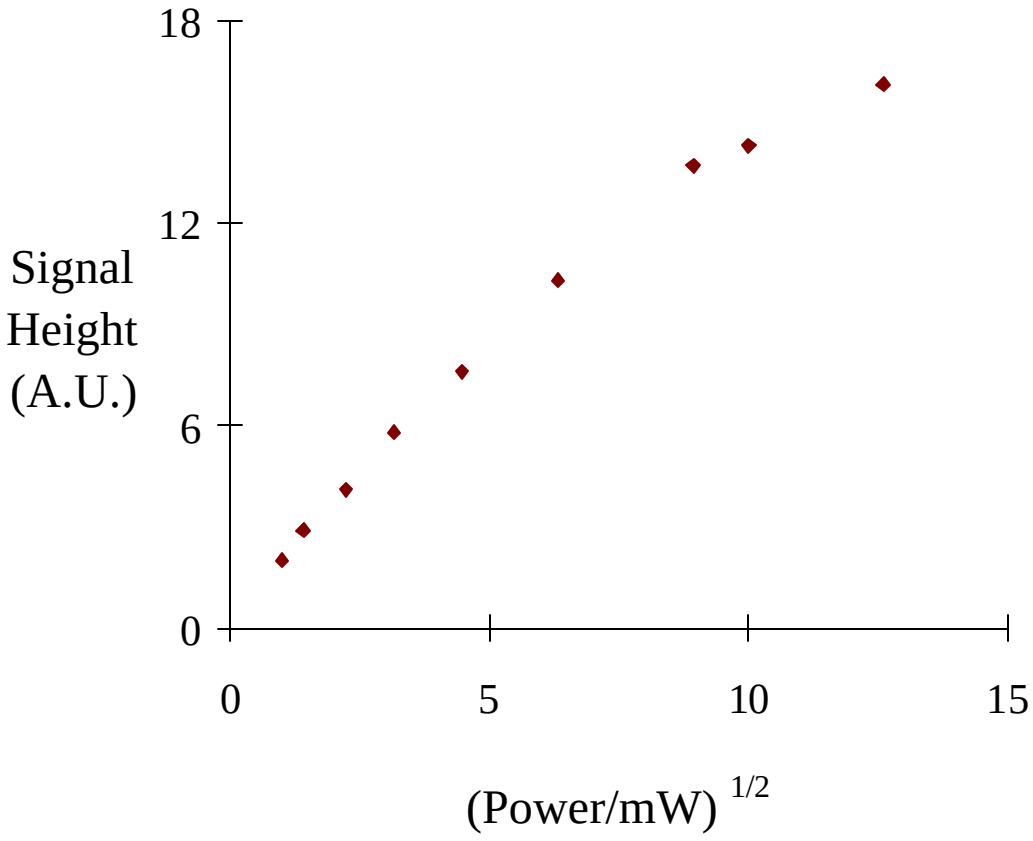

Figure 33. Power saturation curve of Fe(III)Desferal® signal.
Solution contained 10 μM Fe(III), 1 mM Desferal®, and metal-free phosphate buffer pH 7.4.

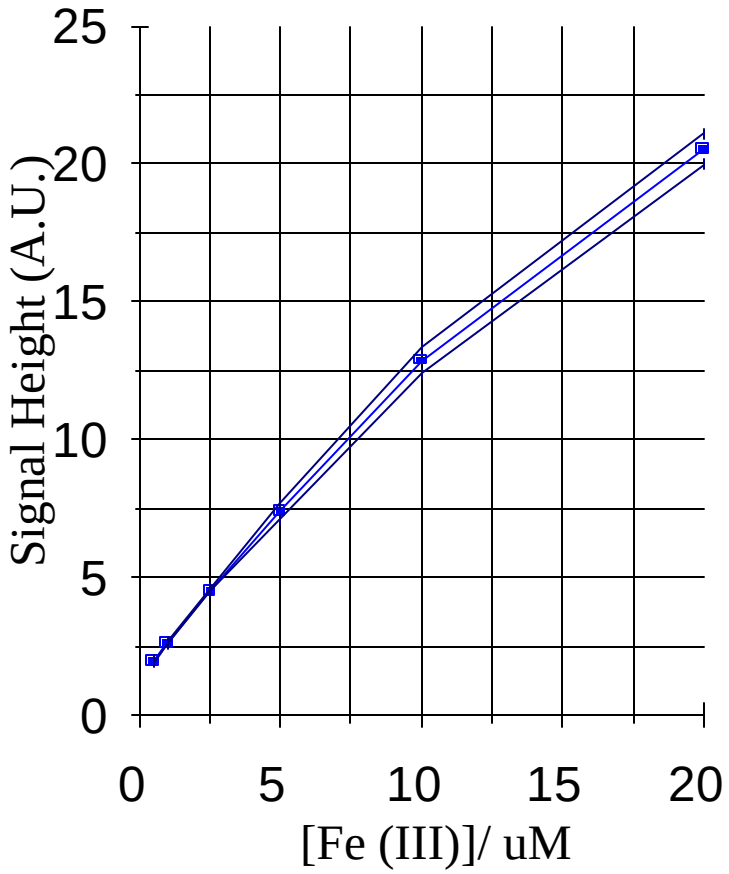

Figure 34. EPR calibration curve of Fe(III)Desferal® complex.
Solutions contained 1 mM Desferal® and varying amounts of Fe(III) in metal-free phosphate buffer pH 7.4. Data represents the mean of three experiments ± SEM.

Table 5. Fe(III)Desferal® EPR signal height.

Sample	Signal Height (A.U.)	[Fe(III)Desferal] /μM
No UV exposure	4.4 ± 0.4	5.2 ± 0.5
UV exposed (16 weeks)	7.4 ± 1.7	10.0 ± 2.3

Note: Samples were standardized by wet weight and area prior to homogenization. Signal height data represents the mean of three experiments ± SEM. Signal heights of the UV exposed skin samples were found not be statistically different ($p > 0.15$) than non-exposed skin samples.

1990]. From these reports and our results, it can be concluded that free iron is present in tissues at notable concentrations. In the mouse skin model an increase in chelatable iron is detectable in UVB exposed mouse skin. Thus, UV radiation increases the levels of iron in skin and some of this iron is present in a 'loose' chelatable form.

Topical Application of Iron or Iron Chelators

Skin is a significant site of iron excretion [Green *et al.*, 1968; Weintraub *et al.*, 1965]. Although iron is naturally present in unexposed mouse skin (≅ 100 ppm) [Bissett *et al.*, 1991], the application of iron to skin should simulate similar conditions present during chronic UV radiation exposure. Topical application of catalytic levels of solutions of iron, $FeSO_4$, $FeCl_3$, or Fe-Desferal®, to mouse skin prior to UV radiation exposure could lead to an increase in free radical formation and lipid peroxidation. Using these forms of iron it can be determined what species of iron is most effective in catalyzing lipid peroxidation in skin.

If iron is involved in UV radiation-induced radical formation, then chelation of this iron will reduce this radical flux. Chelators protect, in general, by altering the rate of reaction of the bound metal or by removing metals from solution or target sites so that they can not participate in oxidation-reduction reactions. Topical application of iron chelators to skin is photoprotective against skin wrinkling and tumor formation in a chronic UV radiation exposure model [Bissett *et al.*, 1991].

Topical application of the iron chelator Desferal® or di-2-furanylethanedione dioxime (FDO), a proposed iron chelator [Bissett *et al.*, 1994], should chelate free iron in the skin and

prevent the involvement of this iron in free radical reactions. In mouse skin, both Desferal® and FDO were examined as protectants against free radical formation in acute UV radiation-exposure in skin. FDO was also examined in a chronic UV radiation-exposed model. Chelation of iron in UV radiation exposed skin should reduce oxidative reactions occurring in skin and subsequently delay or prevent dermatopathology associated with UV radiation exposure.

Materials and Methods

For the iron addition experiments, 40 μL of a stock solution of 250 mM POBN spin trap was topically applied to skin for 8 minutes. Spin trap was blotted from skin and 15 μL of 1 mM Fe(III), 10 mM Fe(II), or Fe-Desferal® (1:30) was applied to skin prior to EPR analysis. Skin was positioned in the EPR cavity and examined using the same radiation source setup as previous spin trapping experiments, Chapter IV. The EPR instrument parameters were: microwave power, 40 milliwatts; modulation amplitude, 1.06 G; time constant, 0.66 s; scan rate, 10 G/41.9 s; receiver gain, 1×10^6. The first low field doublet of POBN was used for all measurements.

For the topical chelator experiments, 50 μL of a 10 mM stock solution of Desferal® were topically applied to the dorsal skin of Skh-1 mice for approximately 10 minutes prior to treatment with the spin trap POBN, 50 μL of a 250 mM stock solution. Skin samples were blotted and placed in the EPR cavity. The epidermal surface was exposed to UV radiation while in the EPR cavity. The first low field doublet of the POBN radical adduct was measured.

The EPR parameters were: microwave power, 40 milliwatts; modulation amplitude, 0.75 G; time constant, 0.3 s; scan rate, 60 G/41.9 s; receiver gain, 1 x 10^6.

For the chemical chelation experiments 50 μM of FDO, EDTA, or Desferal® were added to a solution containing 1 μM Fe(III) and 250 μM ascorbate in a demetalled phosphate buffer, pH 7.4. FDO was obtained from Eastman Kodak Co., Rochester NY. The EPR spectrometer settings for the ascorbate radical were: microwave power, 40 milliwatts; modulation amplitude, 0.7 G; time constant, 1.3 s; scan rate, 6 G/84 s; receiver gain, 5 x 10^5.

For the nitric oxide spin trapping experiments, MGD was synthesized as follows: First dissolve 2.0 g NaOH in 20 mL of DI water. Add 9.76 g of N-methyl-D-glucamine (Sigma F.W. = 195.2) and stir. The solution should be kept cold on ice at about 5°C. In a fume hood make a solution of 5 mL CS_2 (Fischer CS_2; F.W. = 76.14) in 15 mL ethanol (95%). This should be added dropwise to the glucamine solution while the temperature is less than 10°C. Add 50 mL of methanol and stir at room temperature for 16 hours. Filter the solid, dry in air, and finally over P_2O_5 in a desiccater. The product should be a white solid. The yield should be 12.1 g, which is approximately 80%.

Then, to make Fe(II)$(MGD)_2$: Bubble buffer (water) with Argon. Add the desired amount of MGD (5 equivalents). Add 1 equivalent of Fe(II)SO_4. Note, the solution must be used immediately as it will oxidize. A yellow solution that will turn black. The MGD spin trapping EPR spectrometer settings were: microwave power, 40 milliwatts; modulation amplitude, 1.06 G; time constant, 0.8 s; scan rate, 80 G/84 s; receiver gain, 1 x 10^4.

For the FDO acute UV radiation exposure study, Skh-1 mice were topically treated with 0.1 mL of vehicle (55:25:20; EtOH: propylene glycol: water) or 5% FDO in vehicle three times a week for 3 weeks. Free radical formation was examined by EPR where 50 µL of 250 mM POBN were topically applied to the epidermis for ten minutes, blotted, and samples examined by EPR. The POBN spin trapping EPR spectrometer settings were: microwave power, 40 milliwatts; modulation amplitude, 1.06 G; time constant, 0.6 s; scan rate, 10 G/41.9 s; receiver gain, 1×10^6. The UV radiation source set up was a Photomax® 150 W xenon arc lamp; wavelengths below 300 nm were filtered out using a Schott WG 305 filter and infrared radiation from the light was removed by a 5 cm water filter (same as in Chapter IV, Figure 20).

For the chronic exposure study, animals were either treated with vehicle and not exposed to UV radiation, or topically treated with 100 µl of 2% FDO in vehicle or vehicle alone and exposed to UVB radiation (315 nm peak emission) three times a week (Monday, Wednesday, Friday) for 21 weeks. The ascorbate free radical signal was measured. The EPR spectrometer settings were: microwave power, 40 milliwatts; modulation amplitude, 0.6 G; time constant, 1.3 s; scan rate, 6 G/167.7 s; receiver gain, 2×10^6.

Results

Topical Application of Iron

Using the spin trap POBN, the typical carbon-centered lipid-derived radical adduct spectra were obtained (a^N = 15.56 G, a^H = 2.70 G), characteristic of spin trapped alkyl radicals generated from membrane lipids. In the experiments involving topical Fe(III) there was no

increase in either baseline ambient radical levels, nor an increase in the UV radiation-induced radical flux. These results suggest that ferric iron does not act as a photosensitizer for free radical production (Figure 35).

When Fe(II) was applied to skin there was no significant increase in ambient radical levels, however, there was an approximately three-fold increase in signal upon UV radiation exposure (Figure 36). These results indicate that the ferrous form of iron could be acting as a UV radiation chromophore.

Topically applied chelated iron did not act as a pro-oxidant, but actually reduced the ambient as well as UV radiation-induced free radical formation (Figure 37). This reduction in signal was probably due to the chelate binding endogenous metals in skin. Thus, the role of chelators in protecting against UV radiation-induced free radical formation was examined.

Topical Application of Desferal®

Topical treatment with the metal chelator Desferal® resulted in a significant reduction of the POBN adduct signal increase (Figure 38), suggesting a role for iron in

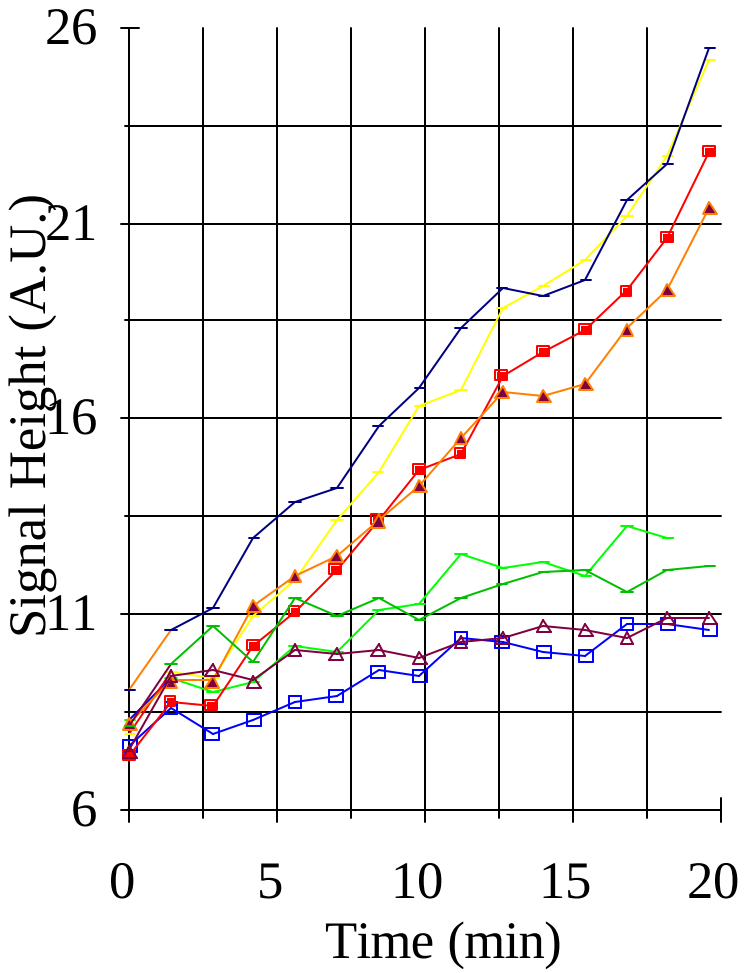

Figure 35. Fe(III) does not increase free radical formation in skin.
♦, POBN signal in skin treated with Fe(III) and exposed to UV radiation; ■, skin treated with POBN alone and exposed to UV radiation; Δ, POBN signal in skin treated with Fe(III) and exposed to room light; □, skin treated with POBN and exposed to room light. Error bars represent the SEM.

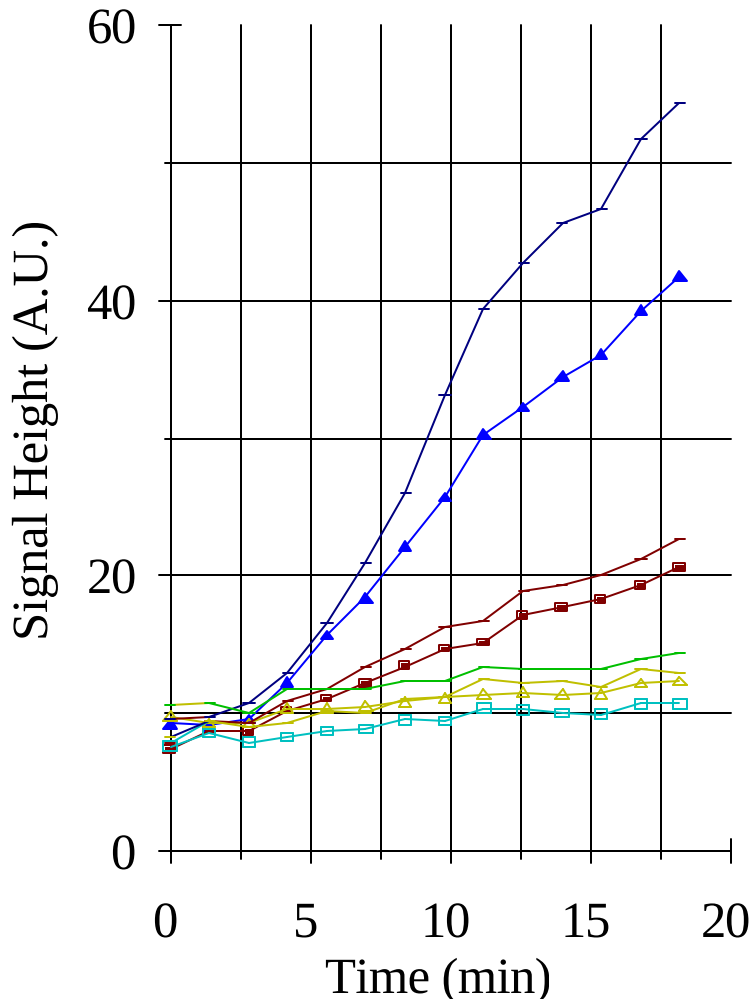

Figure 36. Fe(II) may act as a photosensitizer for free radical production. σ, POBN adduct signal height in skin treated with Fe(II) and exposed to UV radiation; ■, skin treated with POBN alone and exposed to UV radiation; Δ, POBN signal in skin treated with Fe(II) and exposed to room light; □, skin treated with POBN and exposed to room light. Error bars represent the SEM.

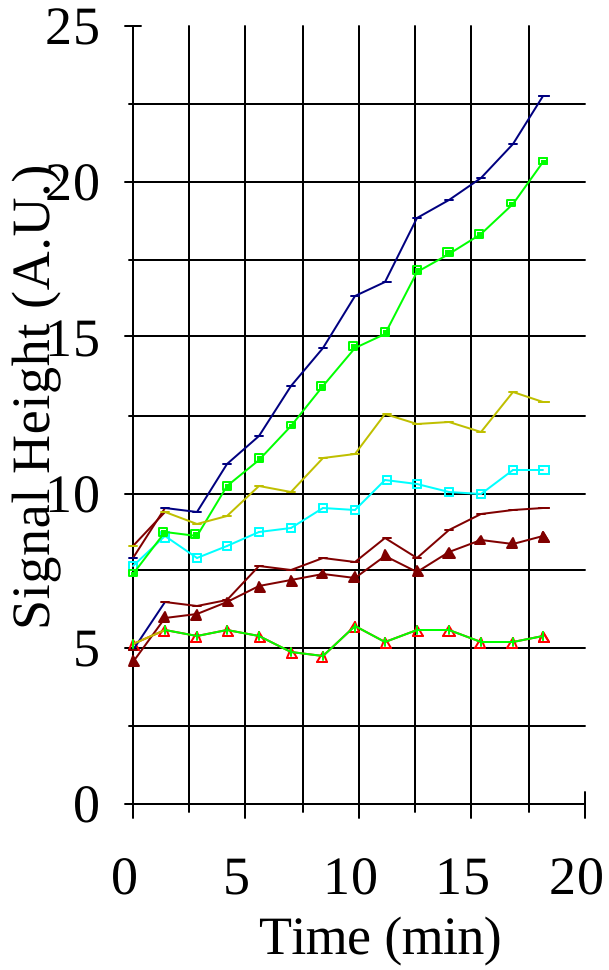

Figure 37. Chelated iron is not a pro-oxidant in skin.
♦, POBN signal height in skin treated with Fe(III)Desferal® and exposed to UV radiation; ■, skin treated with POBN alone and exposed to UV radiation; Δ, POBN signal in skin treated with Fe(III)Desferal® and exposed to room light; □, skin treated with POBN and exposed to room light. Error bars represent the SEM.

catalysis of UV radiation-induced free radical formation. Desferal® has no significant UV radiation absorption at wavelengths greater than 280 nm (Figure 39, UV absorbance). Therefore, its mechanism for photoprotection cannot be simply due to physically blocking the UV radiation. These results indicate that iron is involved in UV radiation-induced free radical formation in skin and chelators protect against this iron-induced free radical formation.

It is assumed that Desferal® is protecting only by acting to chelate iron. The chelating group in Desferal®, the hydroxamate moiety, can be oxidized to form a nitroxide radical; thus, Desferal® can also serve as a donor antioxidant. In our experiments no Desferal® nitroxide radical signal was detectable, indicating that it may be acting solely as a chelator. However, in these experiments the nitroxide radical flux may be too low to be detectable.

Iron Catalysis

Di-2-furanylethanedione dioxime (FDO) is a proposed iron chelator and a skin photoprotectant [Bissett *et al.*, 1994]. The structure of FDO is as follows:

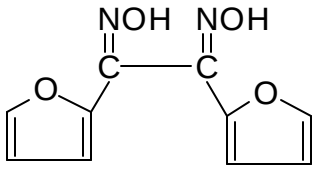

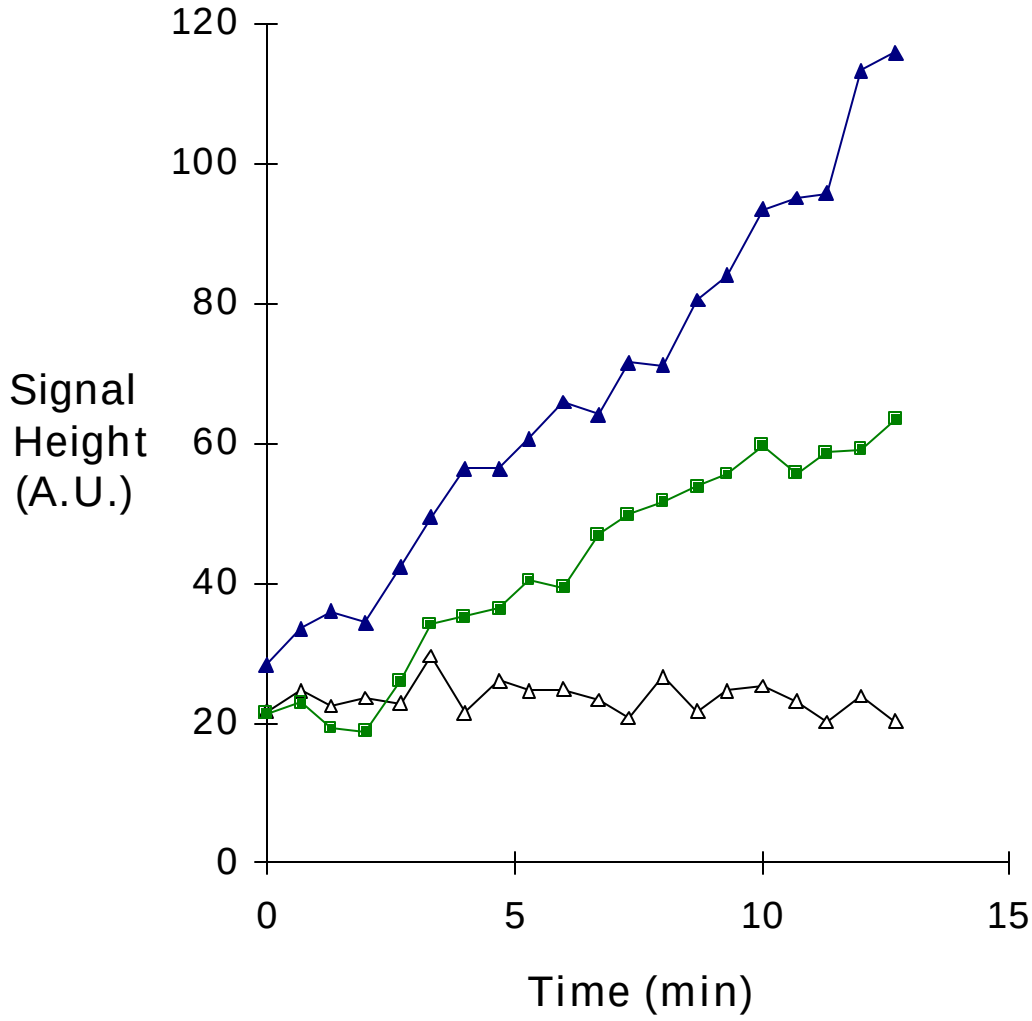

Figure 38. Skin treated with Desferal® prior to UV radiation exposure has decreased POBN adduct signal.
Δ, POBN spin adduct signal intensity from untreated skin that was exposed to room light only; ♦ POBN spin adduct signal intensity from untreated skin that was exposed to UV radiation; ■, POBN spin adduct signal intensity from skin treated with Desferal® and exposed to UV radiation. The data represent the mean signal height in at least three separate experiments. After UV radiation exposure, a paired comparison of each curve showed them to be statistically different, $p < 0.05$.

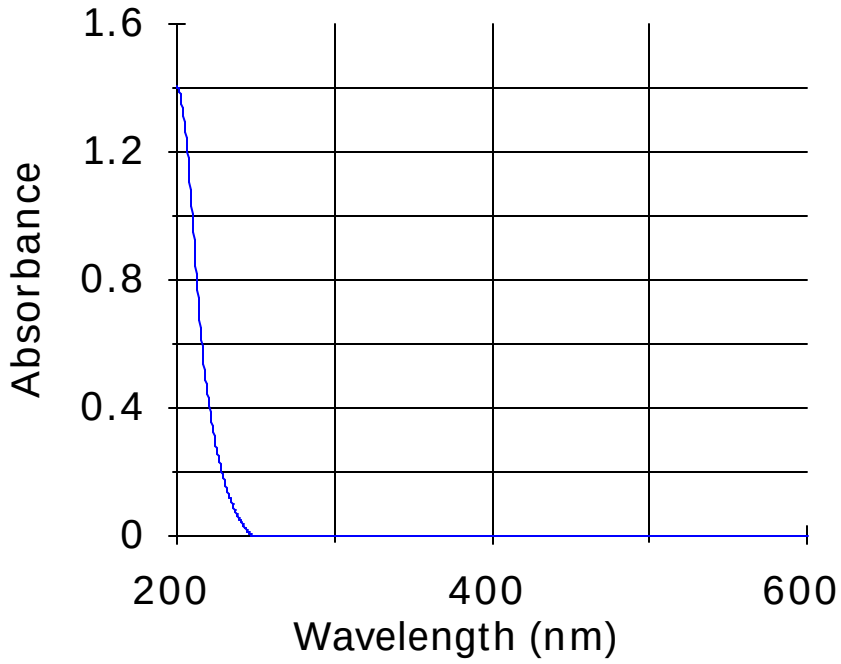

Figure 39. Desferal® does not absorb UV radiation.
The absorbance spectrum of 50 μM Desferal® is shown.

It is hypothesized that FDO protects by inhibiting UV radiation-induced iron catalysis of oxygen radical production. To test this hypothesis FDO was examined in a chemical system as an iron chelator using the ascorbate free radical EPR signal as an indicator of oxidative catalytic efficiency of metals.

In the experiments where the ascorbate free radical was used as a measure of metal catalysis, 50 μM of chelate was added to the phosphate buffer containing 1 μM iron. This converts the iron to a standard catalytic form. Ascorbate, 250 μM, was then introduced and the steady-state EPR concentration (signal height) of the ascorbate free radical was measured. Rather than being an inhibitor of catalysis, Fe-EDTA was found to be an excellent catalyst of ascorbate oxidation. FDO was found to only be a modest inhibitor and Desferal® provided significant protection against ascorbate oxidation, as measured by EPR (Table 6).

With increasing time and exposure to room light, the FDO alone in a water:ethanol solution (50:50) yielded a three-line EPR spectrum that had hyperfine splittings (a^N = 16.2 G) consistent with nitroxide radicals (Figure 40). These results indicate that FDO may be acting as an antioxidant through formation of a stable nitroxide radical. This signal was usually not observable in a 'fresh' solution of FDO, indicating that the solution itself or a contaminant may undergo a decomposition process to form a nitroxide. Nitroxide radicals may have SOD activities [Samuni *et al.*, 1991].

Table 6. The ascorbate radical signal height as a measure of iron catalysis.

	$Asc^{\bullet -}$ Signal Height (A.U.)
Baseline (ascorbate + buffer)	39.7 ± 3.9
FDO	42.6 ± 3.8
EDTA	47.8 ± 1.3
Desferal®	32.5 ± 1.3
Fe(III) alone	83.2 ± 0.9
Fe(III) + FDO	68.5 ± 5.5
Fe(III) + EDTA	171.8 ± 6.9
Fe(III) + Desferal®	41.7 ± 2.2

Note: The data represent the mean ± SEM of at least four different experiments.

Because FDO has -NOH groups, we proposed that FDO may break down or somehow react to form nitric oxide [Andronik-Lion *et al.*, 1992]. Nitric oxide acts an endothelium-derived relaxing factor [Palmer *et al.*, 1987]. Arteries taken from rabbit were used to measure the effect of FDO on contraction or relaxation of smooth muscle. FDO was diluted in a solution of ethanol:water (10^{-4} - 10^{-7} M) and examined using rabbit aorta mounted for isometric recording of tension in a setup similar to that designed by Furchgott and Zawadzki [Furchgott and Zawadzki, 1980]. Briefly, aortic strips were mounted for isometric recording of tension. The strips were recontracted with noradrenalin. Using this isometric system, in the absence of UV radiation FDO was found to have no vasodilatory or contracting actions at the concentrations used in our experimental system. These results indicate that FDO may not have any endothelial relaxing activities.

FDO was further examined for production of nitric oxide by using the nitric oxide spin trap MGD. Using a nitric oxide-containing solution as a standard, a three line EPR signal was observable with a_N = 12.5 G and g_0 = 2.04, consistent with trapping of nitric oxide [Komarov *et al.*, 1993], Figure 41. When FDO was added to the MGD spin trap FDO was found to release nitric oxide in the presence of UV radiation, and the three line signal was observable for up to 48 hours after irradiation, Figure 42.

FDO Protection in Acute UV Radiation Exposure of Skin

Topical application of FDO to mouse skin for three weeks decreased the ambient

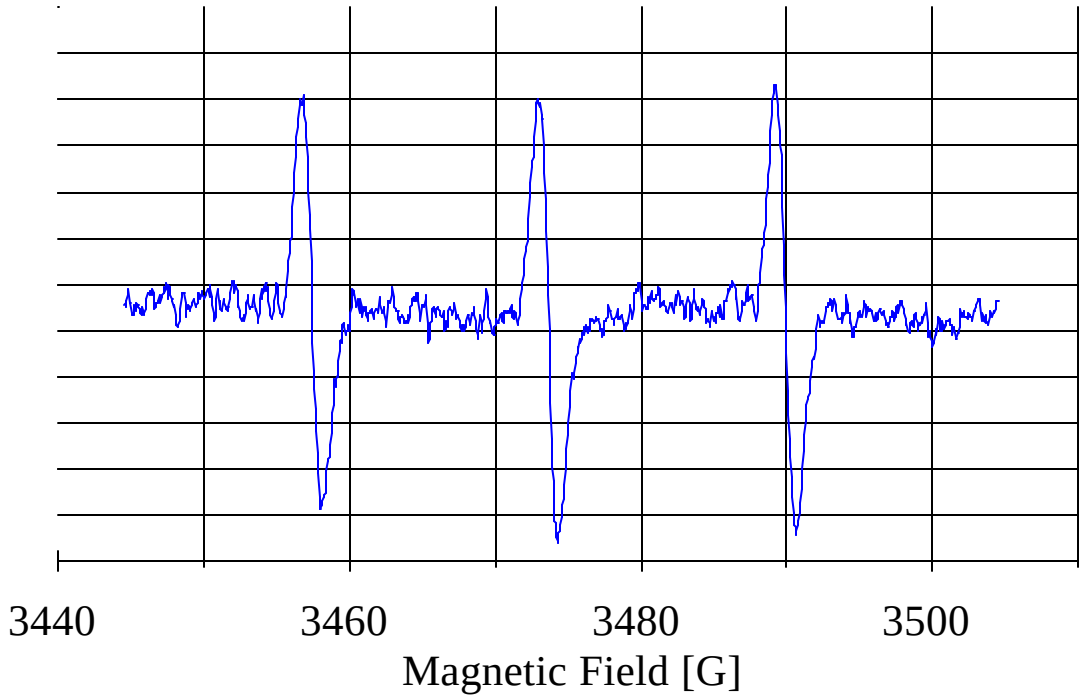

Figure 40. An EPR spectrum of a nitroxide signal obtained from FDO. Solutions contained: 500 μM FDO in water and EtOH (50:50). The EPR spectrometer settings: microwave power, 20 milliwatts; modulation amplitude, 0.7 G; time constant, 1.3 s; scan rate, 60 G/335 s; receiver gain, 5×10^5.

as well as acute UV radiation-induced POBN radical spin adduct formation (Figure 43). The maximum absorption for FDO is near 260 nm (ϵ = 27,000 $M^{-1} \bullet cm^{-1}$) with minimal absorption at wavelengths greater than 295 nm. Thus, FDO does not have significant UV absorbing potential and it's mechanism of protection is not due to blocking UV radiation.

FDO Protection in Chronic UV Radiation Exposed Skin

In a chronic exposure study, mice were treated with FDO and exposed to UV radiation for 23 weeks. The EPR ascorbate signal heights of the different treatment groups are given in Table 7. Those samples not previously exposed to UV radiation had the greatest increase in the ascorbate radical signal height, whereas those chronically exposed to UVB radiation and treated with vehicle alone had the least amount of ascorbate radical signal. The decrease in the ascorbate radical signal in the chronically exposed samples could be due to the depletion of baseline endogenous levels of ascorbate, UV radiation is known to deplete ascorbate during acute exposure [Shindo *et al.*, 1994]. The FDO-treated samples may have protected against this ascorbate depletion.

Discussion

Initiation of lipid peroxidation generally requires the presence of iron or other catalytic metals [Miller *et al.*, 1990; Yin *et al.*, 1992]. The initiation mechanism is a complex process that probably involves a hydrogen abstraction from polyunsaturated fatty acids by hydroxyl radicals generated by Fe(II), ferryl (FeO(II)), perferryl species

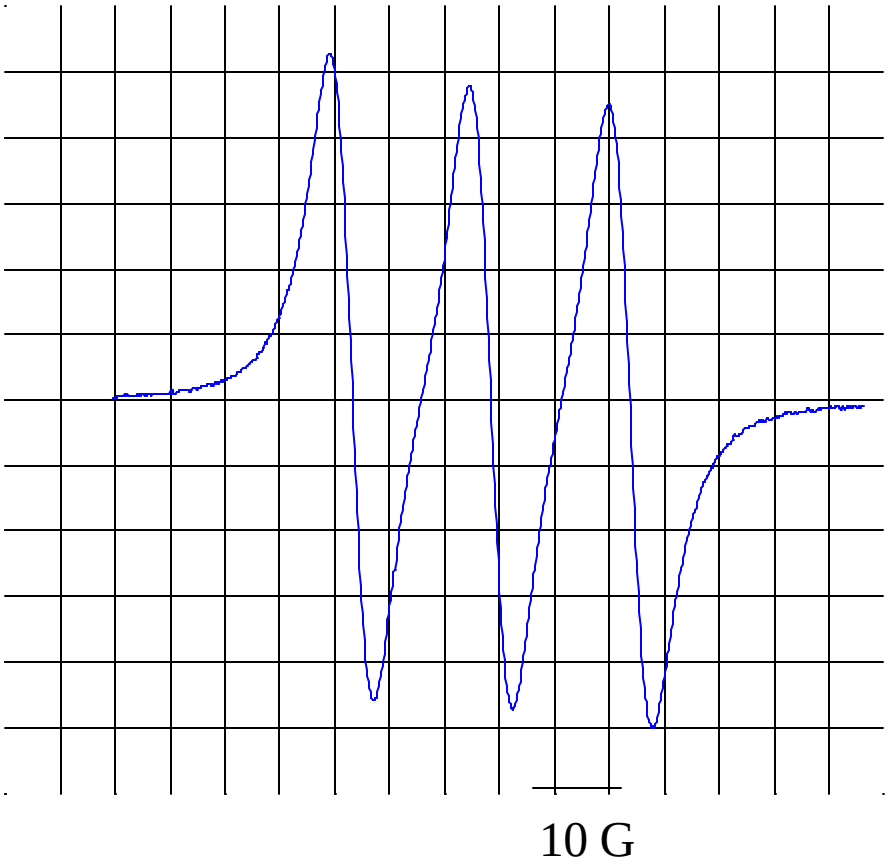

Figure 41. MGD-NO spectrum.
Solutions contained 75 mM MGD, 15 mM Fe(II), and 50 µL of 1 mM nitric oxide.

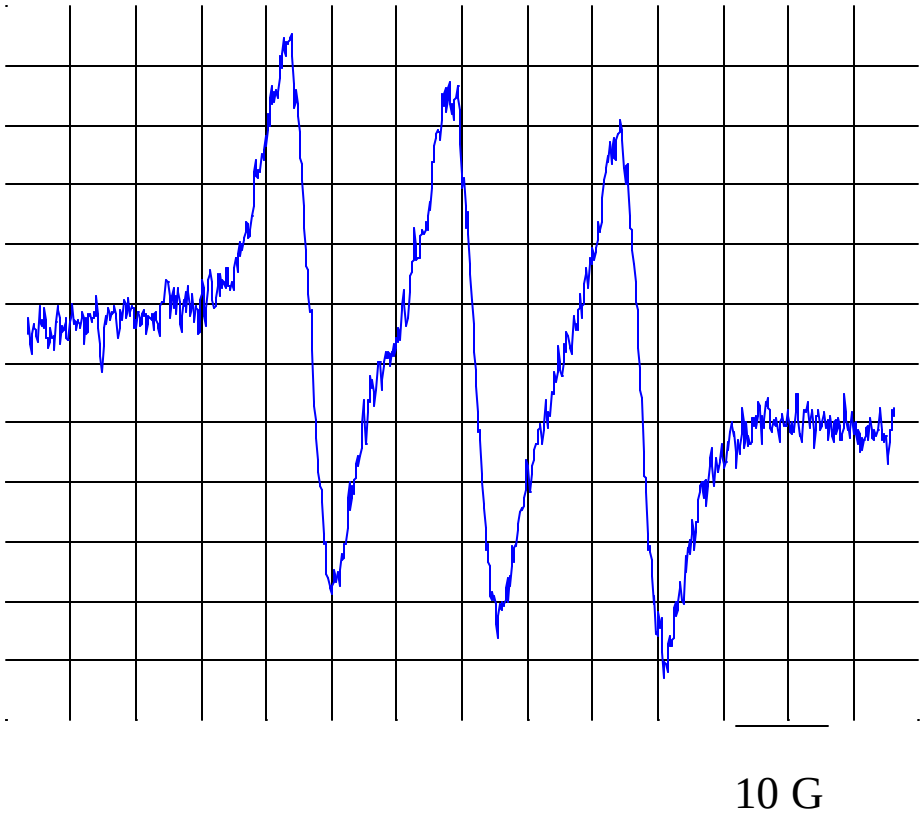

Figure 42. MGD-NO released from FDO in the presence of UV radiation. The spectra were signal averaged ten times.

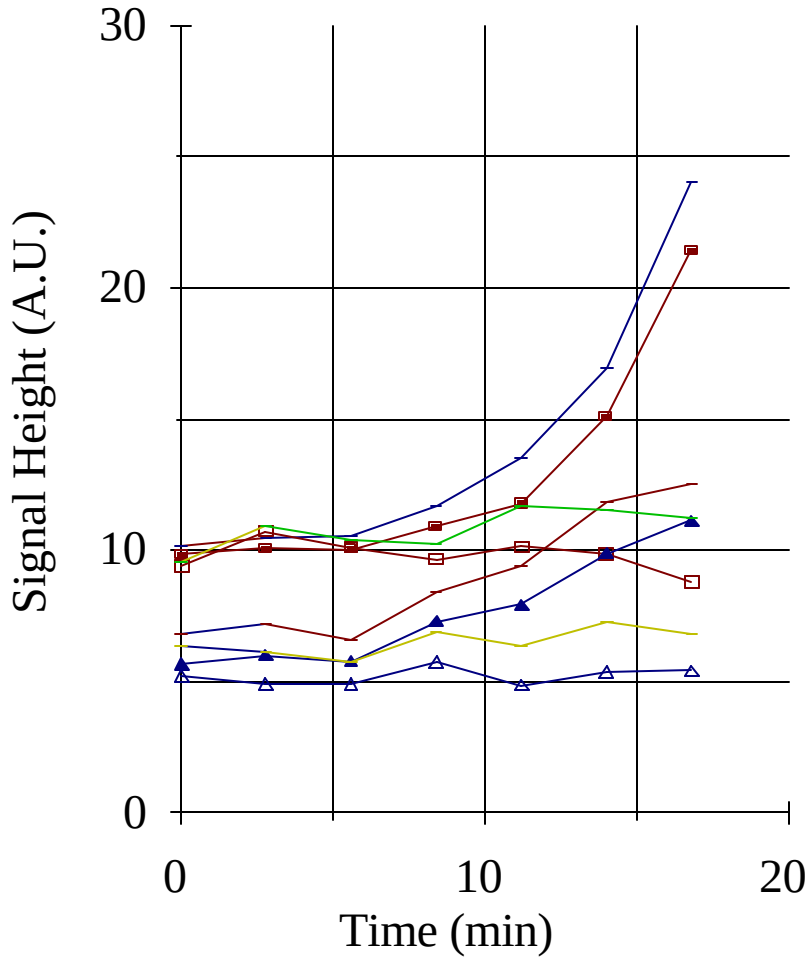

Figure 43. FDO decreases the UV radiation-induced POBN radical adduct signal. □, POBN radical EPR signal height in vehicle-treated skin with no UV exposure; ■, POBN radical EPR signal height in vehicle-treated skin during UV exposure; Δ, POBN radical EPR signal height in FDO-treated skin with no UV exposure; ♦, POBN radical EPR signal height in FDO-treated skin during UV exposure. The epidermal surface of the skin was exposed while in the EPR cavity to UV radiation after collection of the third data point. Each data point from radiation exposed samples represents the mean of four separate experiments. FDO treated skin samples were compared to vehicle samples, using a Student's t test assuming equal variance. There was a statistical difference between these samples for most time points ($p < 0.05$).

Table 7. Ascorbate radical signal height in UV radiation and FDO-treated mouse skin.

Treatment	Ascorbate Radical Signal Heights (A.U.)		
	Initial	UV-induced	% increase
Vehicle 31.8	64.9	97.8 ± 27.9%	
Vehicle + chronic UV	32.7	49.2	45.5 ± 11.7%
FDO + chronic UV	36.6	65.1	75.3 ± 17.3%

Note: The signal height data represents the mean ± SEM of four or more different experiments. The percentage increase was calculated from the mean increase.

($Fe(II)O_2$), or possibly an Fe(III)-O_2-Fe(II) complex [Yin *et al.*, 1992]. Superoxide can act as a reducing agent, reducing iron complexes to the ferrous state. Ferrous ions and hydrogen peroxide can react to generate hydroxyl radical ($^{\bullet}OH$) through the Fenton reaction:

$$Fe(II) + H_2O_2 \longrightarrow Fe(III) + {}^{\bullet}OH + OH^- \qquad \text{(V-1)}$$

Hydroxyl radical can react at an extremely high rate constant with almost every type of molecule in a living cell. Sites of $^{\bullet}OH$ attack are determined by the site of the bound iron, site-specific attack. Therefore, if iron is bound to membrane lipids, introduction of a reducing agent can lead to lipid peroxidation.

Since the formation of the oxidizing species in each case requires ferrous iron, it was not unexpected that topical application of $FeSO_4$ would increase UV radiation-induced free radical formation. Ferrous iron did not however, significantly increase ambient baseline levels of free radicals in our model; thus, the presence of oxidative stress (*i.e.*, UV radiation) or a reducing agent must also be required to initiate significant lipid peroxidation processes.

Skin is a normal site of iron excretion, and with chronic UV radiation exposure the concentration of this iron increases. The presence of increased iron could be due to simple hyperplasia, resulting from sun exposure, reducing the rate of normal iron excretion. Iron may also be leaked from skin vessels, released from inflammatory cells [Kellogg and Fridovich, 1975] or released from ferritin by superoxide [Monteiro and Winterbourn, 1988] or UVA irradiation [Aubailly *et al.*, 1994].

The metal chelator Desferal® is already being used in numerous clinical applications, such as in treatment of porphyria cutanea tarda [Rocchi *et al.*, 1991], aluminum intoxication [Douthat *et al.*, 1994], malaria [Thompson, 1994], *Pneumocystis carinii* [Weinberg, 1994], and in acute iron intoxication during pregnancy [Lacoste *et al.*, 1992]. In our results, Desferal® was found to significantly reduce UV radiation-induced free radical formation in skin and thus should be considered for use in photoprotective agents.

Topically applied FDO was also found to be photoprotective. FDO was found to reduce ambient as well as acute UV radiation-induced free radical formation and may protect against ascorbate depletion in chronic UV radiation exposure.

In other work, where mice were chronically exposed to UVB, FDO prevented induction of the enzyme ornithine decarboxylase (ODC), an enzyme that is an essential, but not sufficient, factor for tumor promotion. FDO was also found to retard formation of mouse skin wrinkles (4 weeks in untreated; 13 weeks treated with 5% FDO) and inhibit mouse skin tumor formation (16 weeks for untreated; 22 weeks for treated with 5% FDO) [Bissett *et al.*, 1994]. In UVB radiation exposed human skin, FDO was clinically effective against induction of erythema, histological changes, and ODC increase [Bissett *et al.*, 1994].

The exact mechanism by which FDO is a photoprotectant is unknown. It is proposed that FDO acts as a metal chelator. However, in our chemical chelation experiments the iron-FDO complex served as a rather effective catalyst for oxidations. If it is acting as a chelator, FDO may protect by removing iron from the site of damage in the skin. FDO may also remove

iron from ‘catalytically worse’ chelators (*i.e.*, citrate) that are endogenous to the skin or diminish the ability of Fe (II) (or Fe (III)) to directly donate (or withdraw electrons) to other biological targets.

Based on our MGD spin trapping experiments, we propose that instead of only being a chelator, FDO may also be protecting by acting as a nitric oxide donor antioxidant. Nitric oxide is known to be an excellent membrane antioxidant in protection against LDL oxidation [Hogg *et al.*, 1993]

The use of iron chelators and nitric oxide donors to reduce free radical formation is an entirely new approach to photoprotection and subsequently skin cancer prevention. Instead of only blocking the UV radiation from being absorbed by skin, as is done now with UV absorbers, such as *para*-aminobenzoic acid and cinnamate (common ingredients found in over-the-counter sunscreens), skin could also be protected by preventing propagation of iron-catalyzed free radical damage. UV radiation is implicated as the leading cause of skin cancer; depletion of the earth's natural sunscreen, the ozone layer, is predicted to escalate skin cancer incidence. Thus, the development of this iron chelator photoprotective concept is imperative.

CHAPTER VI

THE EFFECT OF TOPICALLY APPLIED TOCOPHEROL ON ULTRAVIOLET RADIATION-MEDIATED FREE RADICAL DAMAGE IN SKIN[11]

Abstract

Previously, we demonstrated by electron paramagnetic resonance spectroscopy that ultraviolet radiation induces free radical formation in Skh-1 hairless mouse skin. Because free radical oxidative stress is thought to play a principal role in skin photoaging and cancer, oxidative stress and subsequent photodamage should be decreased by supplementation of skin with antioxidants. Using both the ascorbate free radical and an EPR spin trapping system to detect short-lived radicals, we evaluated the effect of the topically applied antioxidants tocopherol sorbate, α-tocopherol, and tocopherol acetate on UV radiation-induced free radical formation. We show that tocopherol sorbate significantly decreases the UV radiation-induced radical flux in skin. Using our chronically exposed mouse model, tocopherol sorbate was also found to be significantly more protective against skin photoaging than α-tocopherol and tocopherol acetate. These results extend our previous observations of UV radiation-induced free radical generation in skin and indicate the utility of tocopherol sorbate as an antioxidant in providing significant protection against UV radiation-induced oxidative damage.

---

[11] A version of this chapter has been published. BA Jurkiewicz, DL Bissett, GR Buettner: The effect of topically applied tocopherol on ultraviolet-radiation mediated free radical damage in skin. *J Invest Dermatol*, 104: 484-488, 1995.

Introduction

Ultraviolet radiation is thought to produce free radical species in skin, leading to premature aging and cancer [Norins, 1962; Pathak and Stratton, 1968; Black, 1987; Fuchs *et al.*, 1989; Schallreuter and Wood, 1989; Meffert *et al.*, 1976; Miyachi *et al.*, 1989; Darr and Fridovich, 1994; Nishi *et al.*, 1991]. There are several reports providing evidence of this free radical production in skin [Norins, 1962; Pathak and Stratton, 1968;]. In experiments in Chapters IV and V, using room temperature EPR spectroscopy, we have detected a very low steady-state level of the ascorbate radical in mouse skin [Buettner *et al.*, 1987; Buettner and Jurkiewicz, 1993]. Upon UV radiation exposure of Skh-1 hairless mouse skin the ascorbate free radical signal intensity increased, indicating free radical-mediated oxidative stress [Jurkiewicz and Buettner, 1994; Buettner and Jurkiewicz, 1993]. The ascorbate radical is resonance stabilized and thus easily detected by EPR. However, the non-resonance stabilized radicals initially produced by UV radiation would have very short lifetimes at room temperature; thus, EPR spin trapping techniques were used. With these techniques, we previously observed a UV radiation-produced, carbon-centered free radical spin adduct in skin, characteristic of spin-trapped alkyl radicals generated from membrane lipids [Jurkiewicz and Buettner, 1994]. These findings indicate that UV light induces lipid peroxidation in skin.

The skin is constantly exposed to environmental oxidants (UV light, ozone, cigarette smoke) and naturally contains antioxidants to protect against this oxidative damage. However this scavenging cannot be 100% efficient. Chronic exposure of skin to UV radiation can

significantly decrease cellular and membrane antioxidants [Maeda *et al.*, 1991]; their depletion could lead to unregulated free radical formation. Therefore, if free radicals are involved, supplementation of skin with antioxidants should prevent radical-mediated oxidative damage. Indeed, Bissett *et al.* [Bissett *et al.*, 1990] have shown that application of antioxidants (tocopherol, ascorbate, propyl gallate, and Trolox®) prior to UV exposure delays UV-induced chronic skin damage in hairless mice. Topical and systemic supplementation with tocopherols has been found to be photoprotective by reducing erythema [Trevithick *et al.*, 1992; Roshchupkin *et al.*, 1979; Fryer, 1993] as well as by delaying the onset of UV radiation-induced skin tumor formation during chronic exposure [Bissett *et al.*, 1990; Bissett *et al.*, 1989; Bissett *et al.*, 1992; Black *et al.*, 1983; Black and Chan, 1975]. Both α-tocopherol (**I**) and its acetate derivative (**II**) have been shown to act as UV photoprotectants through antioxidant mechanisms, Figure 44 [Beijersbergen van Henegouwen *et al.*, 1992].

However, α-tocopherol itself could be photoactive by increasing free radical formation in skin. Tocopherols absorb in the UVB region of sunlight (280-320 nm, ϵ_{295} α-tocopherol = 3050 M^{-1} cm^{-1} [Windholz, 1983]). UV radiation absorption by α-tocopherol can result in direct conversion to its chromanoxyl radical form [Kagan *et al.*, 1992]. This free radical form of tocopherol may possibly serve as a pro-oxidant by propagating further deleterious free radical reactions [Bowry and Stocker, 1993; Mukai *et al.*, 1993], or it may be reduced by other antioxidant systems [Frei *et al.*, 1989]. Such regeneration of α-tocopherol would result in the depletion of other endogenous

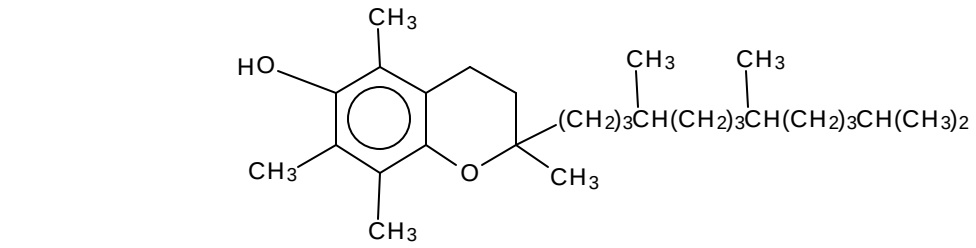

I

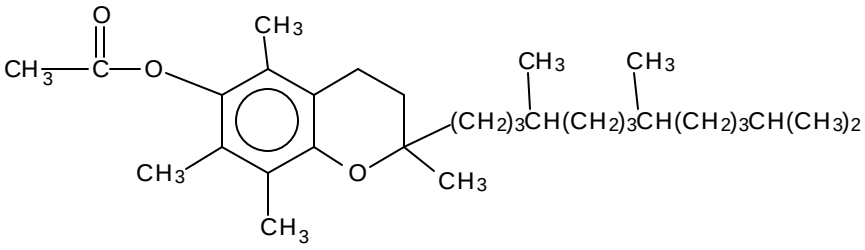

II

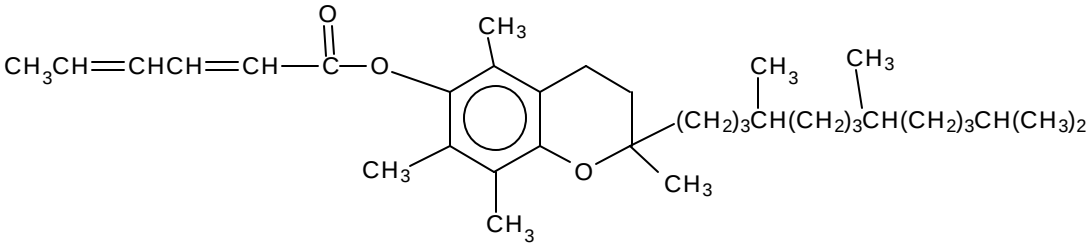

III

Figure 44. Structures of forms of tocopherol.
I is dl-α-tocopherol, II is tocopherol acetate, and III is tocopherol sorbate.

antioxidants. Consequently, there exists an apparent conflict between the role of tocopherol as a photoprotective antioxidant and as a possible harmful photoreactive agent.

In our study we examined the antioxidant capabilities of α-tocopherol and tocopherol acetate as well as another derivative of vitamin E, tocopherol sorbate (**III**). We investigated the UV radiation-induced radicals in intact mouse skin directly by measuring the ascorbate free radical EPR signal height and indirectly by EPR spin trapping techniques. We then examined the effects of these three different chemical forms of vitamin E on the reduction or enhancement of UV radiation-induced free radical production. In addition, we examined the effects of these antioxidants on prevention of skin wrinkling and tumor formation in chronic UVB exposed mice.

Materials and Methods

Animals

Female albino hairless Skh:HR-1 mice (Charles River Laboratories, Portage, MI) were group housed up to five to a cage. Mice were approximately ten weeks old at the start of experimental work. All animals were kept in rooms with controlled temperature, humidity, and a 12-hour light /darkness cycle. They were given standard laboratory chow diet and water *ad libitum*. The housing, feeding, and handling of animals was in compliance with standards set forth by the U.S. Animal Welfare Act or recommendations in National Institutes of Health "Guide for the Care and Use of Laboratory Animals." All procedures performed on animals were reviewed and approved by a veterinarian and an Institutional Animal Care and Use Committee.

Sample Preparation

Mice were topically treated over the dorsal skin with 0.1 mL of vehicle or a tocopherol solution for 3 weeks (3 times per week, Monday, Wednsday, Friday). α-Tocopherol acetate and *dl*-α-tocopherol were obtained from Sigma Chemical Co., St. Louis, MO. α-Tocopherol sorbate was synthesized as described previously [Bissett and Bush, 1989]. The test groups, each containing 10 animals, were as follows: isopropanol (IPA) vehicle alone; 5% α-tocopherol in IPA; 5% tocopherol acetate in IPA; and 5% tocopherol sorbate in IPA. The treatments provided approximately a 2 mg/cm^2 coverage of skin, a standard for sunscreen usage in the U.S. [Food and Drug Administration, 1978]. Following 3 weeks of treatment, each group was sacrificed by CO_2 asphyxiation, and the dorsal skins collected. All skin samples were kept at liquid nitrogen temperatures until EPR examination.

Ascorbate Radical Measurement

Whole mouse skin was cut into EPR usable pieces (≈1.0 cm^2, epidermis & dermis), placed in a Wilmad Glass Co. (Buena, NJ) tissue cell, and positioned in a TM_{110} EPR cavity [Jurkiewicz and Buettner, 1994]. EPR spectra were obtained at room temperature using a Bruker ESP 300 spectrometer (Bruker Instruments; Karlsruhe, Germany), operated at 9.74 GHz with 100-kHz modulation frequency. The EPR spectrometer settings for the ascorbate radical experiments were: microwave power, 40 milliwatts; modulation amplitude, 0.66 G; time constant, 0.3 s; scan rate, 8 G/41.9 s; receiver gain, 2 x 10^6. For both ascorbate and spin

trapping experiments the epidermal surface only was exposed to UV radiation while in the EPR cavity, using the same radiation source setup [Jurkiewicz and Buettner, 1994].

Spin Trapping

For the spin trapping experiments, α-[4-pyridyl 1-oxide]-N-*tert*-butyl nitrone (POBN) was obtained from Sigma Chemical Co., St. Louis, MO. A 50 μL solution of 250 mM POBN was applied to the epidermis for nine minutes; the skin was then blotted and placed in a Wilmad tissue cell. Relative radical concentrations were determined by measuring the signal height of the low field doublet of POBN spin adduct. No significant increase in background EPR signal occurred when POBN alone was exposed to UV radiation. EPR instrument settings for the spin trapping experiments for Figure 2 were: microwave power, 40 milliwatts; modulation amplitude, 0.6 G; time constant, 0.3 s; scan rate, 60 G/41.9 s; receiver gain, 1×10^6. The spin trapping data in Figure 4 represent four signal-averaged scans where the EPR settings were: microwave power, 40 milliwatts; modulation amplitude, 1.06 G; time constant, 0.6 s; scan rate, 10 G/41.9 s; receiver gain, 1×10^6.

UV Radiation Setup for EPR

The radiation source was a Photomax 150 W xenon arc lamp (Oriel Corporation, Stratford, CT). For the UV radiation experiments wavelengths below 300 nm were filtered out using a 3 mm Schott WG 305 filter (Duryea, PA) (2.9 milliwatts/cm^2 including visible; 1.5 milliwatts/cm^2 for 300-400 nm); for visible light experiments, wavelengths below 400 nm were filtered out using an Oriel 59472 filter (1.5 milliwatts/cm^2); infrared radiation was removed by a

5 cm water filter. Filtered fluence rates were measured with an International Light (Newburyport, MA) radiometer, assuming that the cavity grid transmits 75% of the incident light.

In Vivo Irradiation and Topical Treatment

The procedure for irradiation of the dorsal skin of mice with UVB radiation has been described previously [35]. Briefly, mice (n = 8 per treatment group) were irradiated individually under a bank of four Westinghouse FS-40 sunlamps (UVB radiation, peak emission near 315 nm). Mice were irradiated three times weekly (Monday, Wednesday, Friday) with 30 mJ/cm^2 UVB radiation per exposure (approximately 0.5 the mouse MED). For topical treatment, the dorsal skin of the mice was treated with 0.1 mL of test solution [isopropanol or 5% (w/v) antioxidant in isopropanol; prepared weekly] 2 hours prior to each irradiation.

Skin Wrinkling Evaluations

Skin wrinkling in hairless mice was assessed as described previously [Bissett *et al.*, 1987; Bissett *et al.*, 1990]. The grading scale is 0 to 3, in which 0 is no wrinkling and 3 is the maximum visible wrinkle development observed in our work. Visible evaluations were done blind by an individual not involved in the treatment and irradiation work.

Skin lesions were diagnosed and counted as tumors if they were circular, red, raised, and greater than 1 mm in diameter. In other work, these types of lesions were examined histologically and found them to be papillomas and squamous cell carcinomas [Bissett *et al.*, 1990].

Statistical Analyses

Means at individual time points for treated skin and corresponding vehicle control were calculated. Differences in the mean free radical production between treatments and vehicle were statistically assessed using a Student's t-test.

Results

Endogenous Ascorbate Radical Production

The level of free radical signal in tocopherol-treated mouse skin was examined in room light as well as in the presence of UV radiation. Using room temperature EPR, a very low steady-state level of the ascorbate free radical ($Asc^{\bullet-}$) was observed to be naturally present in skin (Figure 45, top). Due to ascorbate's role as the terminal small-molecule antioxidant [Frei *et al.*, 1989; Buettner, 1993], the ascorbate radical concentration can be used as a marker of oxidative stress [Buettner and Jurkiewicz, 1993]. Exposure of mouse skin to UV radiation while in the EPR cavity results in an increased $Asc^{\bullet-}$ signal height [Jurkiewicz and Buettner, 1994]. This increase indicates that during UV exposure the skin is undergoing free radical oxidative stress. Exposure to visible light (wavelengths >400 nm) had no affect on $Asc^{\bullet-}$ levels (data not shown).

The tocopherol acetate treatments were found to neither enhance nor protect against UV radiation-induced $Asc^{\bullet-}$ formation (Figure 46). Skin treated with α-tocopherol appears to have increased $Asc^{\bullet-}$ signal in the presence of radiation, indicating that the alpha form of

tocopherol could act as a weak photoreactive agent. However, this increase was not found to be significant by statistical analysis. Examining the calculated p values, only tocopherol sorbate treatment was found to provide a significant reduction in $Asc^{\bullet-}$ formation ($p < 0.05$). This reduction was found both in ambient, non UV-exposed samples as well as in the UV radiation-exposed skin samples.

The ascorbate radical EPR intensity[12] data were also converted into percentage change versus vehicle control. By taking the difference between control and antioxidant-treated skin $Asc^{\bullet-}$ signal heights at each time point before and after UV exposure, we were able to arrive at overall averages, Table 8. Both the baseline and UV radiation-exposed $Asc^{\bullet-}$ intensities for the tocopherol sorbate-treated samples were significantly lower than vehicle values, whereas in the UV radiation exposed α-tocopherol-treated samples the $Asc^{\bullet-}$ levels were found to be significantly higher than vehicle levels. The acetate form had no effect on $Asc^{\bullet-}$ levels.

UV Radiation-Induced POBN Adduct Signal

In the POBN experiments, when skin was exposed to UV radiation both $Asc^{\bullet-}$ as well as a POBN radical adduct signal are detectable by EPR (Figure 45, bottom). The UV radiation-induced formation of POBN radical adduct was unaffected by the tocopherol acetate treatments (Figure 47). The α-tocopherol appears to have enhanced the POBN signal as compared to control during UV radiation exposure; however, this was not found to be

[12] EPR signal intensity is linearly correlated with steady-state radical concentrations.

significant by statistical analysis. Only the tocopherol sorbate significantly reduced the POBN signal compared to control values.

Each tocopherol treatment time point was compared to vehicle control. Examining the calculated p- values for the tocopherol data, only the tocopherol sorbate treatment was found to provide a statistically significant reduction in POBN radical adduct formation. This reduction was found both in baseline samples as well as in the UV-exposed skin samples.

The POBN spin trapping data were then converted into percentage change versus vehicle control as done for the $Asc^{\bullet-}$ data (*vide supra*), Table 9. Again, the α-tocopherol and tocopherol acetate forms did not significantly reduce UV radiation-induced radical flux, whereas the tocopherol sorbate treatment was found to dramatically decrease radical levels.

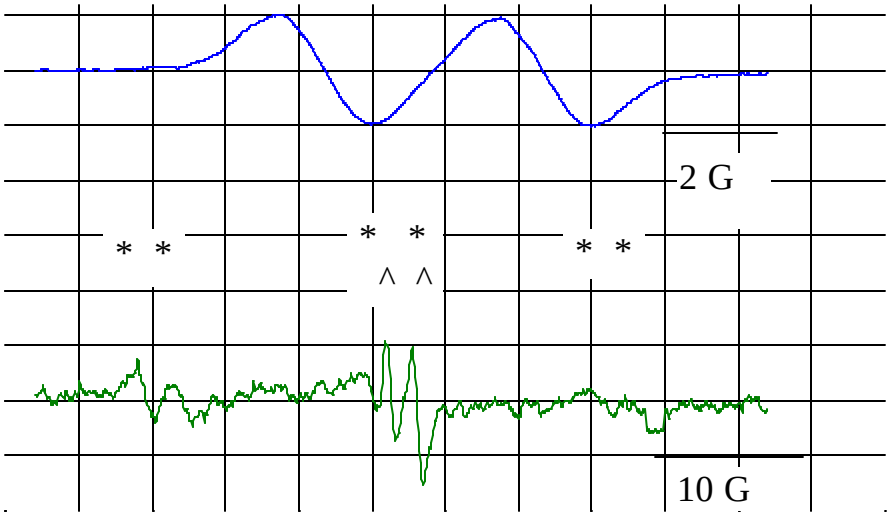

Figure 45. Ascorbate radical doublet and POBN adduct EPR signal in mouse skin. (Top) The EPR doublet signal of $Asc^{\bullet -}$ with hyperfine splitting $a^{H4} \cong 1.8$ Gauss is observed. (Bottom) POBN Spin Trapping of a Radical from UV Radiation Exposed Mouse Skin. The POBN adduct of a carbon-centered radical (*****), $a^N = 15.56$ G, $a^H = 2.70$ G, as well as the $Asc^{\bullet -}$ (^), are shown. The upper spectrum is from skin exposed to room light only, the lower spectrum is from skin exposed to the UV radiation source.

Table 8. Tocopherol sorbate reduces skin ascorbate radical.

Treatment	Endogenous (before UV)	UV-Induced
Alpha tocopherol	+3.7 ± 3.7	+17.6 ± 3.6*
Tocopherol acetate	-3.8 ± 5.5	+1.4 ± 2.3
Tocopherol sorbate	-16.2 ± 6.3*	-29.1 ± 4.4*

Note: The percentage change in skin ascorbate radical EPR signal height of tocopherol treated skin versus vehicle treated skin is given. Data is presented as mean ± SD. *Denotes significant (at $p < 0.05$) compared to endogenous or UV radiation-exposed vehicle values.

In Vivo Photoprotection

The photoprotective effect of topically applied tocopherols against chronic UVB radiation-induced skin damage was evaluated in a mouse model of photoaging [Bissett *et al.*, 1987; Bissett *et al.*, 1990a]. In previous testing using this model [Bissett *et al.*, 1990b], it was observed that tocopherol acetate was poorly photoprotective against chronic UVB radiation-induced skin wrinkling while α-tocopherol provided significant protection. In the present work, we compared the efficacy of these two materials against tocopherol sorbate (Figure 48). The results substantiate our previous observations and indicate that tocopherol sorbate is significantly more protective than the other two forms of vitamin E against skin wrinkling. The study was not continued to the point where all mice had skin tumors, so a thorough evaluation of protection against tumor formation was not possible. However, there were fewer tumors in the tocopherol sorbate group (1.8 tumors/mouse) and α-tocopherol group (2.0 tumors/ mouse) versus the vehicle control group (3.6 tumors/ mouse) at the end of the study (week 23). Since the tocopherol acetate did not provide significant photoprotection against skin wrinkling at 15 weeks into the study, that group was discontinued prior to the point of first tumor appearance (week 19 in the vehicle control animal group). While tocopherol sorbate and α-tocopherol appeared to reduce the average number of tumors per mouse, they did not delay onset of appearance of the first tumor relative to vehicle treated animals.

Table 9. Tocopherol sorbate reduces skin POBN radical adduct.

Treatment	Endogenous (before UV)	UV-Induced
Alpha tocopherol	-17.8 ± 2.8*	+6.5 ± 2.3
Tocopherol acetate	-8.5 ± 6.4	-11.3 ± 5.0
Tocopherol sorbate	-33.2 ± 2.0*	-39.8 ± 11.2*

Note: The percentage change in skin POBN radical adduct EPR signal height of tocopherol treated skin versus vehicle treated skin is given. Data is presented as mean ± SD. *Denotes significant (at $p < 0.05$) compared to endogenous or UV radiation-exposed vehicle values.

Discussion

In previous work, using the POBN spin trapping system, a UV radiation-produced carbon-centered free radical was detected from intact skin [Jurkiewicz and Buettner, 1994]. The EPR spectra exhibited hyperfine splittings that are characteristic of POBN/alkyl radicals, a^N = 15.56 G and a^H = 2.70 G, possibly generated from membrane lipids as a result of β-scission of lipid alkoxyl radicals. In lipid peroxidation, propagation is the rate limiting step:

$$LOO^{\bullet} + L'H \longrightarrow LOOH + L'^{\bullet} \quad \text{(VI-1)}$$

$k = 10 \text{ to } 50\ M^{-1}s^{-1}$ [Buettner, 1993]

where $LOO^{\bullet}$ and $L'^{\bullet}$ are lipid peroxyl and carbon-centered lipid radicals, while L′H and LOOH are unsaturated lipid and lipid hydroperoxides. This reaction is slow compared to the addition of oxygen to a lipid radical ($k = 3 \times 10^8\ M^{-1}s^{-1}$ [Hasegawa and Patterson, 1978]) thus, antioxidants such as tocopherols (TOH) have a chance to compete with oxidizable substrates for the lipid peroxyl radical and thereby break the chain of propagation.

$$LOO^{\bullet} + TOH \longrightarrow LOOH + TO^{\bullet} \quad \text{(VI-1)}$$

$k = 8 \times 10^4\ M^{-1}s^{-1}$ [Patterson, 1981]

Thus, by applying TOH and inhibiting the propagation of lipid peroxidation it may be possible to reduce or prevent skin damage associated with free radicals.

α-Tocopherol is the active free radical scavenging form of vitamin E. Norkus *et*

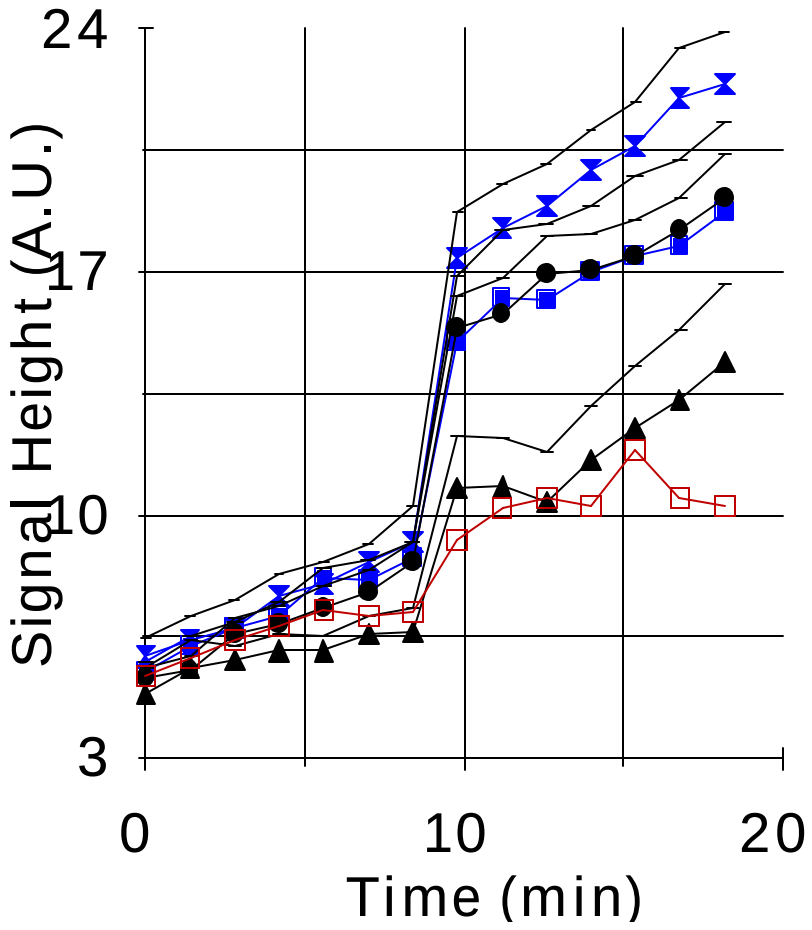

Figure 46. Ascorbate radical EPR signal height decreases in tocopherol sorbate treated skin.
□, $Asc^{\bullet-}$ signal height of IPA vehicle-treated skin exposed to room light only; ■, $Asc^{\bullet-}$ signal height of IPA vehicle treated skin; ●, tocopherol acetate treated skin; X, α-tocopherol treated skin; and ♦, tocopherol sorbate treated skin during UV exposure. The epidermal surface of the skin was exposed while in the EPR cavity to UV radiation after collection of the seventh data point. Standard error bars were determined for the UV radiation-exposed data. Each point from radiation-exposed samples represents the mean of at least six separate experiments.

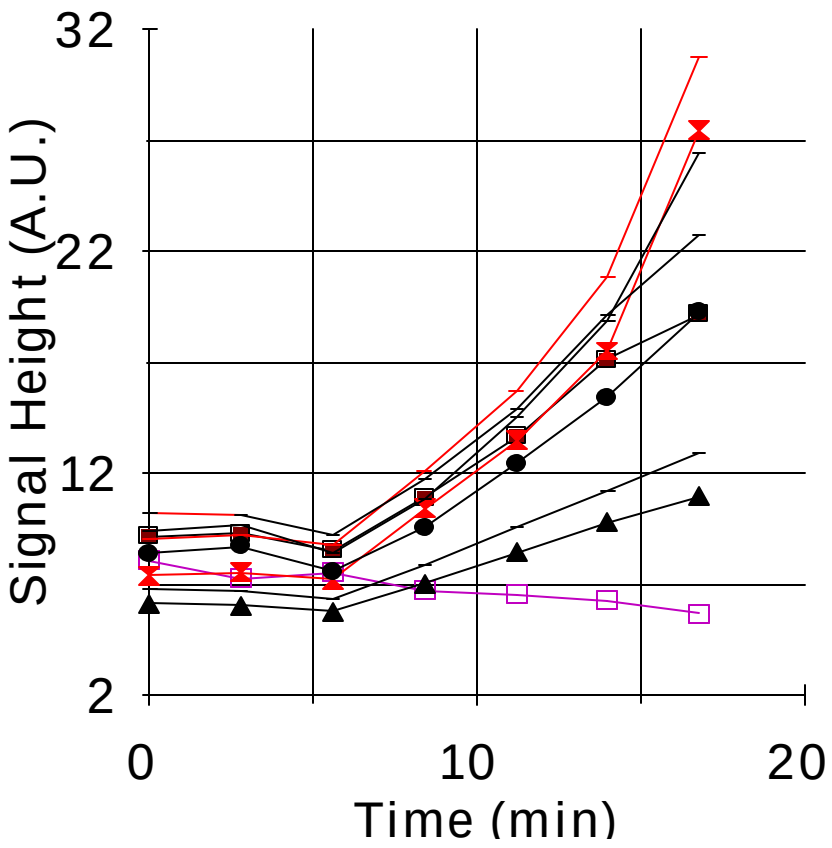

Figure 47. POBN radical adduct EPR signal height decreases in tocopherol sorbate treated skin.
□, POBN radical signal height in IPA vehicle treated skin exposed to room light only; ■, POBN radical signal height of IPA vehicle treated skin; ●, tocopherol acetate treated skin; X, α-tocopherol treated skin; and ♦, tocopherol sorbate treated skin during UV exposure. The epidermal surface of the skin was exposed while in the EPR cavity to UV radiation after collection of the third data point. Standard error bars were determined for the UV radiation-exposed data. Each point from radiation-exposed samples represents the mean of at least six separate experiments.

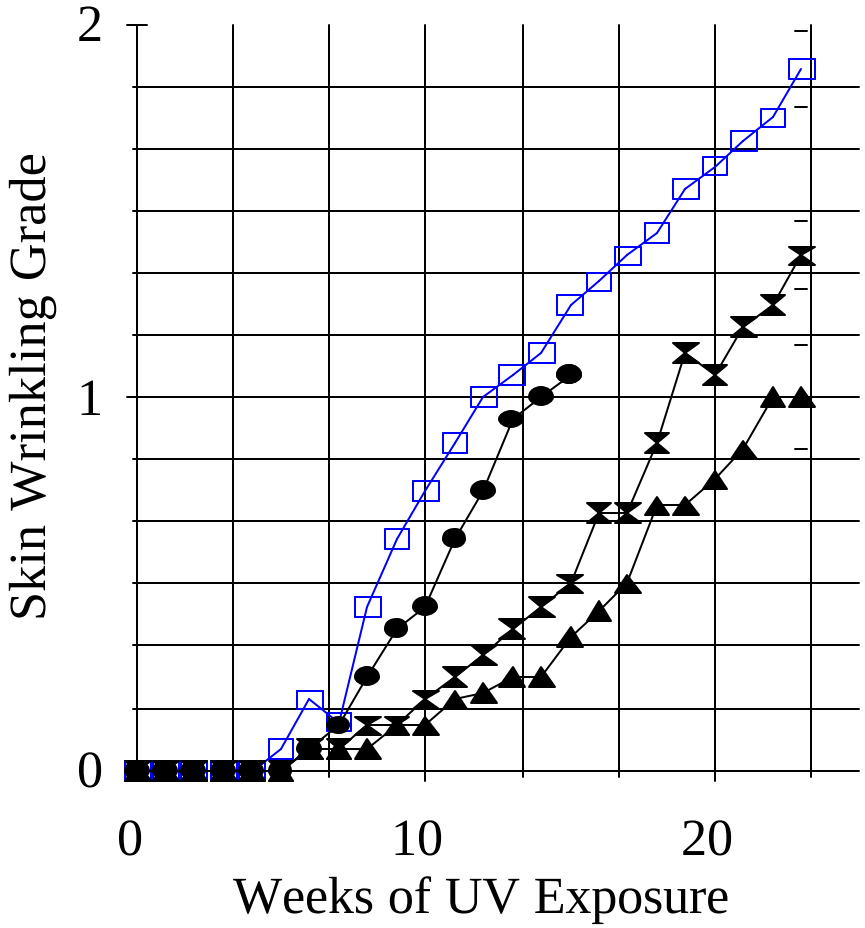

Figure 48. Tocopherols protect against UVB-induced mouse skin wrinkling. Tocopherol acetate, ●, was significantly different from vehicle, ❑, at only weeks 7-12. Alpha-tocopherol, X, and tocopherol sorbate, ♦, were significantly different from vehicle starting at week 7 and through the remainder of the study.

al., found that topical application of α-tocopherol acetate to mouse skin significantly increases skin α-tocopherol levels, suggesting that α-tocopherol acetate is bioconverted in the skin to free α-tocopherol [Norkus *et al.*, 1993]. In our study, tocopherol sorbate was found to be the most effective in preventing UV induced skin wrinkling, suggesting that its uptake and appropriate bioconversion is more efficient than the other tocopherol forms examined. Additionally, the sorbate moiety is expected to have an antioxidant activity (*e.g.*, singlet oxygen quenching) due to its conjugated double bond system [Bissett *et al.*, 1990c].

In the skin wrinkling study α-tocopherol was found to be protective. However in the EPR experiments, α-tocopherol was found to slightly enhance radical production while tocopherol acetate had no effect on radical levels with the methods used. The UV radiation dose used for the EPR free radical experiments was an acute exposure, whereas the *in vivo* skin wrinkling experiments involved chronic UV exposure. The increased free radical levels in the acute exposure experiments could be due to α-tocopherol absorbing UV radiation itself and being directly converted to its free radical form.

The tocopherol sorbate treatment was found to be highly photoprotective against UV radiation-induced free radical formation and photoaging in the hairless mouse model. There was almost 50% less detectable radical formation in UV radiation-exposed tocopherol sorbate treated than in α-tocopherol treated skin. In addition, tocopherol sorbate treatment decreased baseline radical formation in skin, suggesting a possible anti-aging role for this treatment. The exact reason for tocopherol sorbate effectiveness as a radical scavenger is unknown; the

tocopherol moiety may be scavenging lipid radicals while the sorbate moiety could be acting as a singlet oxygen scavenger, or the sorbate form of vitamin E may enhance membrane incorporation and bioconversion of the tocopherol. Further work is needed to elucidate the mechanism involved in protection.

The use of topical antioxidants to reduce free radical formation is a promising new approach to photoprotection and possibly skin tumor prevention. In addition to blocking the UV radiation from being absorbed by skin, as is typically done with UV absorbers, such as *para*-aminobenzoic acid and cinnamate (sunscreen ingredients), skin could also be protected by preventing propagation of free radical damage.

Currently, sunscreens and many cosmetics contain tocopherol in the acetate form which, based on the methods used here, has only a modest protective effect. Our data clearly demonstrate that the sorbate form of vitamin E significantly reduces the level of free radicals in UV radiation-exposed mouse skin. This reduction in measured free radical signal in tocopherol-treated skin correlates with a decrease in photo-induced skin wrinkling in animals similarly treated, suggesting a connection between free radicals and wrinkling. Thus, our data support the use of tocopherol sorbate in sunscreen preparations to reduce photoaging.

CHAPTER VII

UV RADIATION-INDUCED FREE RADICAL FORMATION IN HUMAN SKIN

Introduction

There are significant biochemical and structural differences between human and mouse skin that could affect their responses to UV radiation and other environmental insults. For example, mouse skin has an approximately three times greater penetration rate than human skin [Bissett *et al.*, 1990]; this is likely due to the three-fold difference in stratum corneum thickness between the two species [Bronaugh and Maibach, 1985]. This and other inherent differences must be taken into account when extrapolating results of a mouse model to problems dealing with human skin diseases [Mershon and Callahan, 1975]. Another potential drawback to using an animal model is the controversy regarding the ethical use of animals in research. Despite these impediments, the hairless mouse is currently the best model available to study photoaging of the skin. The goal of the research presented in this Chapter was to compare our standard mouse skin to the use of human skin graphs and biopsies as models for UV radiation-induced free radicals.

Materials and Methods

Human Tissues

Human skin grafts were obtained from Ohio Valley Tissue and Skin Center, (Cincinnati, OH). The skin was 1/6″ thick and graphed from undetermined locations. The gross

appearance of the skin was white, non-wrinkled, and hairless. Skin was frozen at 77 K in 10% glycerol. Glycerol is a preservative commonly found as an ingredient in over-the-counter cosmetics.

Human skin biopsies were obtained from three different anonymous plastic surgery patients. Intact skin sections (0.5 - 0.8 cm) were obtained from pre-auricular or post-auricular regions. Any observable hair was shaved off and blood was washed from samples. Because of limitations in sample size when using EPR, much of the dermis was cut away from the human skin samples prior to examination. The light source setup was the same as previously described in Chapters IV through VI. To detect the ascorbate radical EPR spectrometer settings were: microwave power, 40 milliwatts; modulation amplitude, 0.66 G; time constant, 1.3 s; scan rate, 8 G/84 s; receiver gain, 2×10^6. All ascorbate data represents two signal-averaged scans. The EPR spectrometer setting for the POBN spin trapping experiments were: microwave power, 40 milliwatts; modulation amplitude, 0.6 G; time constant, 0.3 s; scan rate, 50 G/42 s; receiver gain, 1×10^6; and for DMPO: microwave power, 40 milliwatts; modulation amplitude, 1.06 G; time constant 0.3 s; scan rate 80 G/84 s; receiver gain, 1×10^6.

Handling of Human Tissues

The procedures followed for the safe handling of potentially harmful human tissues were based on those recommended by the Cooperative Human Tissue Network, Columbus, Ohio. Gloves were worn at all times. All waste generated (including gloves, tissues, etc.) was placed in appropriate biohazard containers. All fat and tissue trimmed from the specimens were placed

in a plastic vial containing bleach and placed in appropriate biohazard containers. All surfaces which came in contact with tissue were rinsed in 100 % ethanol and then rinsed thoroughly with a dilute solution containing bleach.

Results

Human Skin Graft

Naturally observable by EPR in grafted skin was the ascorbate free radical. When the graft was exposed to UV radiation, the ascorbate radical signal significantly increased (Figure 49). Visible light also increased levels of ascorbate radical signal in the human skin graft samples, though not as dramatically as seen with the UV radiation exposure. The EPR signal of the UV radiation and visible light exposed samples were found to be statistically different than non-exposed samples ($p < 0.05$). These results are quite different from what was observed in our mouse skin samples. The mouse skin did not have an increased ascorbate radical signal when exposed to visible light (Chapter IV, Figure 25), however, the mouse skin samples had a significantly higher ambient baseline ascorbate radical signal than that observed in the human graphs.

Using EPR spin trapping techniques, the spin trap α-[4-pyridyl 1-oxide]-N-*tert*-butyl nitrone (POBN) was topically applied to skin. With POBN, a radical spin adduct with splitting $a^N = 15.55$ G and $a^H = 2.89$ G was observed, possibly a carbon dioxide radical [Riesz *et al.*, 1985] or a carbon-centered radical, possibly $(CH_3)_2C^{\bullet}OH$ [Farraggi *et al.*, 1984] generated by UV radiation-induced oxidation of the glycerol storage solution. Upon examination of

glycerol alone the same carbon-centered radical signal appeared (a^N = 15.54 G; a^H = 2.70 G), approximately 10 minutes after UV radiation exposure. These results indicate that the spin adduct signal observed in the skin is likely due to breakdown of glycerol.

In these spin trapping experiments the ascorbate radical signal began to diminish after approximately five minutes of UV radiation exposure. In the mouse model, the ascorbate was observable for up to 4 hours with continuous UV exposure. These results indicate that endogenous ascorbate levels may be low in the skin graphs or that glycerol-derived radicals are depleting the ascorbate.

Due to the apparent low level of ascorbate detected, human skin graphs may not be a suitable model for the examination of free radical processes. In addition, the glycerol in the graft storage solution produces radicals when exposed to UV radiation. Many over-the-counter cosmetics contain appreciable concentrations of glycerol, which upon exposure to UV radiation will produce radicals that may lead to skin damage. The use of this ingredient in cosmetics and sunscreen preparations may need to be reconsidered.

Human Skin Biopsy

Naturally observable by EPR in human skin biopsies is the ascorbate free radical at a very low steady-state concentration. As can be seen in Figure 50, there is an approximately four-fold increase in the ascorbate radical EPR signal when the human

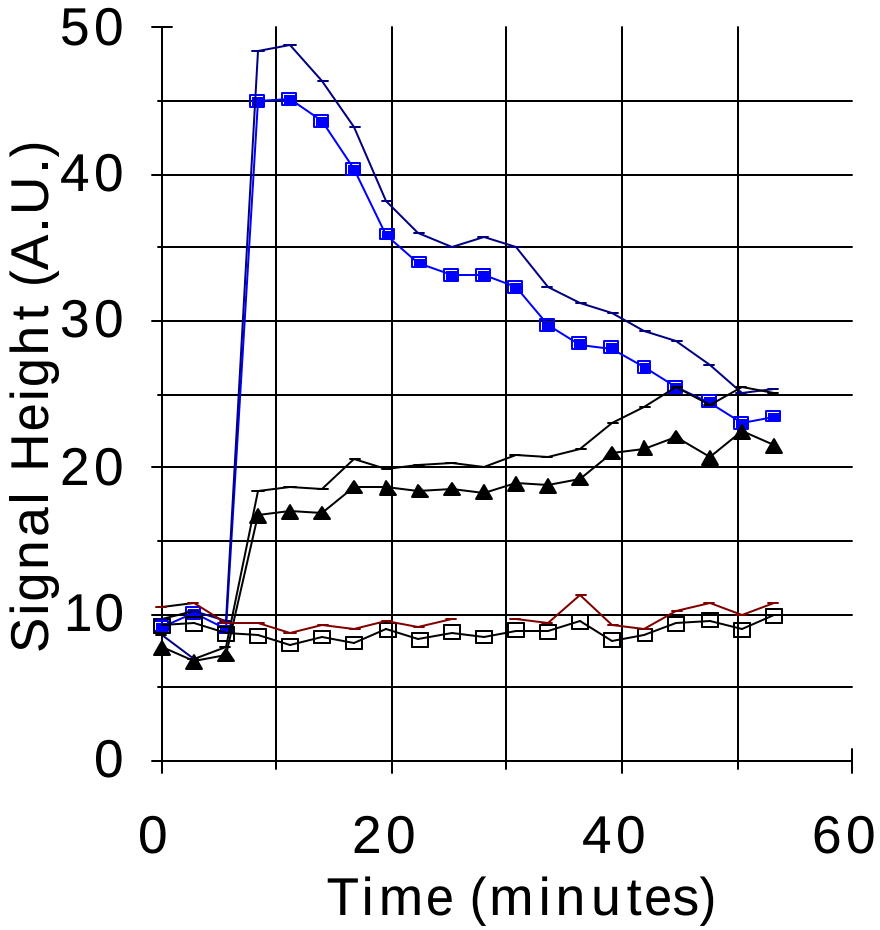

Figure 49. UV radiation increases the ascorbate radical signal in human skin graphs. ■, Ascorbate radical signal in graphs exposed to UV radiation (WG 305 nm cutoff and IR filters); ♦, Ascorbate radical signal in graphs exposed to visible light (400 nm cutoff and IR filters); □, Ascorbate radical signal in graphs exposed to room light only. The samples were exposed to light after collection of the third data point. Each data point represents the mean of four samples ± SEM.

skin is exposed to UV radiation. If after approximately 5 minutes of irradiation the UV radiation source is turned off, the ascorbate radical signal returns to near baseline, ambient levels immediately (Figure 51). In mouse skin, this signal decreased only ≈ 20% after the oxidative insult was removed, and did not return to baseline levels (data not shown).

Visible light was also found to increase the biopsy ascorbate radical signal; approximately a two-fold increase was observed (Figure 50). This induction of free radicals by visible light was also observed in the human graft samples. Visible light may be being absorbed by a human skin chromophore not found in our mouse skin, such as melanin, which can produce free radicals. Radical production would also increase if visible light were depleting or inactivating an antioxidant. For instance, skin catalase can be inactivated by visible radiation through an oxygen-dependent decomposition of one of the four porphyrin rings.

The production of short-lived free radicals in human skin was examined using spin trapping techniques. The spin trap POBN, 50 μL of a 250 mM solution, was topically applied to the human skin biopsy for 8-9 minutes, blotted and then examined by EPR.

No signal was observable in the absence of UV radiation. When the skin was exposed to UV radiation a triplet of doublets was observed as well as the ascorbate free radical signal (Figure 52). The hyperfine splittings were a^N = 15.62 G and

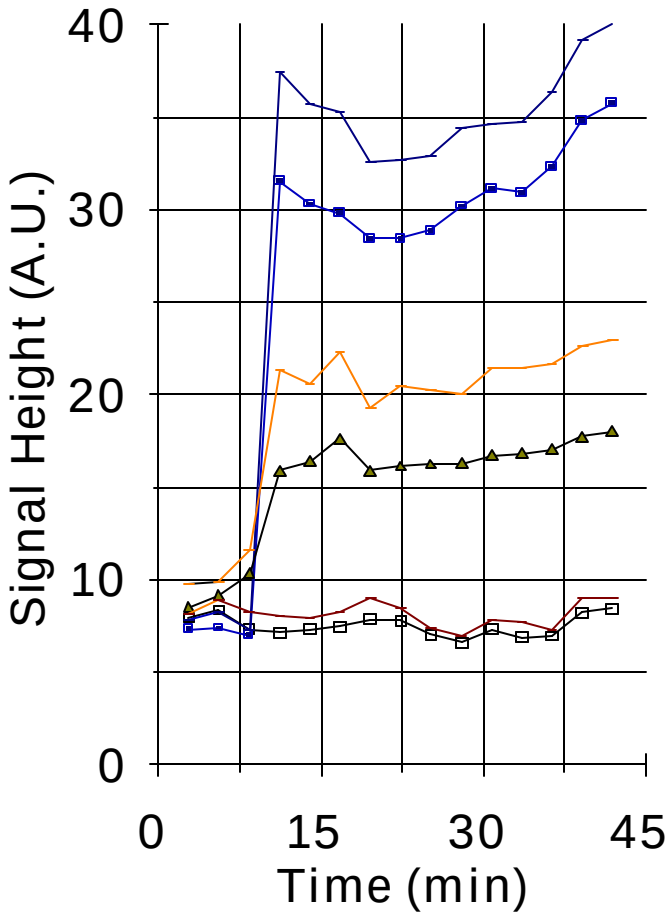

Figure 50. The ascorbate radical signal height in human skin increases on exposure to UV radiation.

■, Ascorbate radical signal in biopsies exposed to UV radiation (WG 305 nm and IR filters); ♦, Ascorbate radical signal in biopsies exposed to visible light (400 nm and IR filters); □, Ascorbate radical signal in biopsies exposed to room light only. The samples were exposed to light after collection of the third data point. Each data point represents the mean of four samples ± SEM.

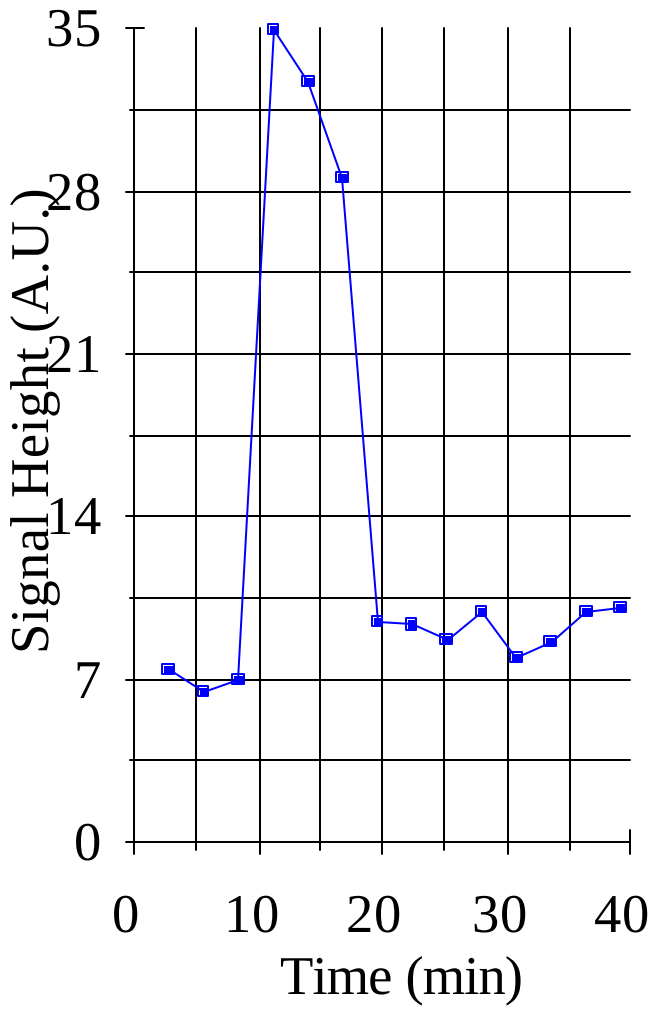

Figure 51. The ascorbate radical signal returns to baseline levels after oxidative stress is removed.
While in the EPR cavity, the biopsies were exposed to UV radiation after the third consecutive scan and turned off following collection of the sixth scan.

a^H = 3.1 G, which are consistent with the carbon dioxide radical [Riesz *et al.*, 1985]. This signal was very weak; thus other spin traps were examined.

Human skin biopsies were treated with 50 µL of a 1 M solution of DMPO for approximately 8 minutes, then blotted prior to EPR examination. No signal was detected in room light alone. After UV radiation exposure, the ascorbate free radical signal as well as a six line DMPO adduct signal was observable (Figure 53). The hyperfine splittings were a^N = 14.54 G and a^H = 16.0 G, characteristic of alkoxyl radicals, possibly formed by lipid peroxidation processes. This finding is consistent with the previous observation of UV radiation-induced lipid alkyl radicals in mouse skin. Thus, this work supports the use of human skin biopsies as a useful model for studying free radical formation.

Because lipid peroxidation products were observed in our spin trapping experiments, iron may be involved in these free radical processes. Thus, we have examined the effect of topically applied Desferal® on protection against this UV radiation-induced free radical production. Using DMPO spin trapping techniques, 15 µL of 10 mM Desferal® or 15 µL of water was topically applied two minutes prior to EPR examination. No signal was observable in the absence of radiation. After exposure to UV radiation the same six line DMPO adduct as well as the ascorbate free radical signal was observable in both treatment groups, Figure 54. Those samples treated with Desferal® had approximately 50 % less signal than the untreated samples. As previously seen in Figure 39, Desferal® does not absorb UV wavelengths, and thus must be

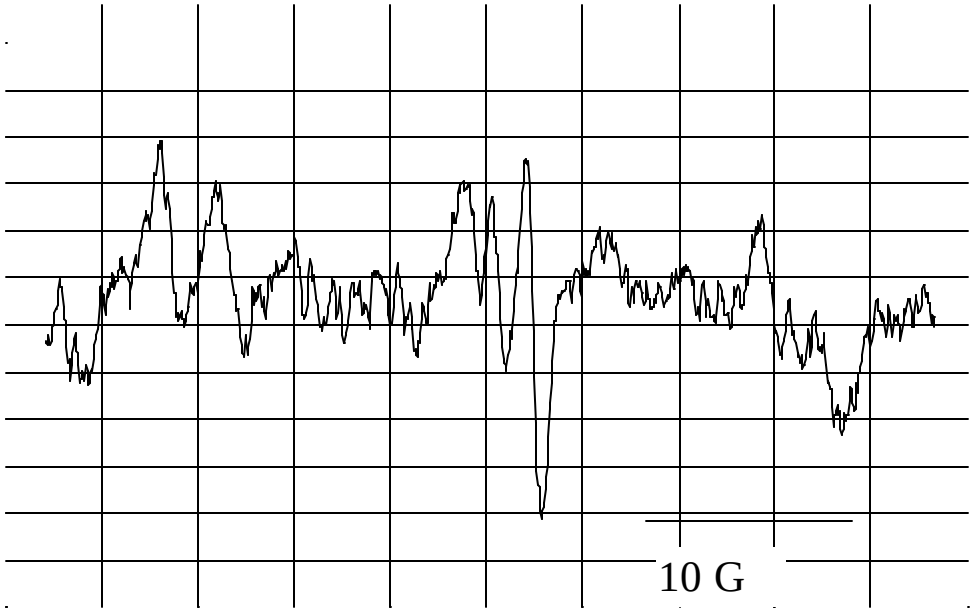

Figure 52. POBN spin trapping of carbon-dioxide radicals in human skin biopsies. The EPR spectrum represents 20 signal-averaged scans.

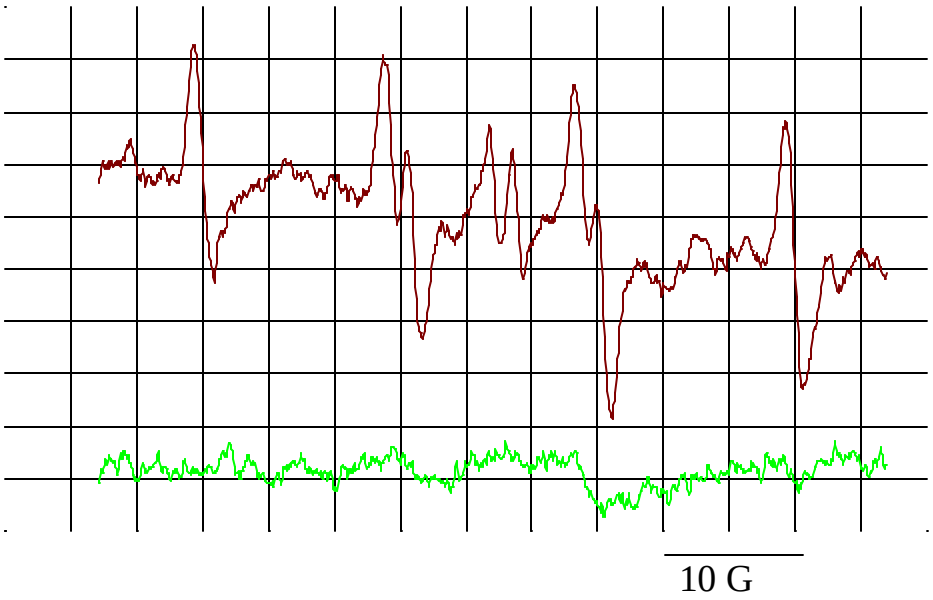

Figure 53. The EPR spectra of UV radiation-induced DMPO radical adducts in human skin biopsies.
The top spectrum is of human skin exposed to UV radiation, the lower spectrum is of human skin exposed to room light. Both spectra are the result of ten signal-averaged scans.

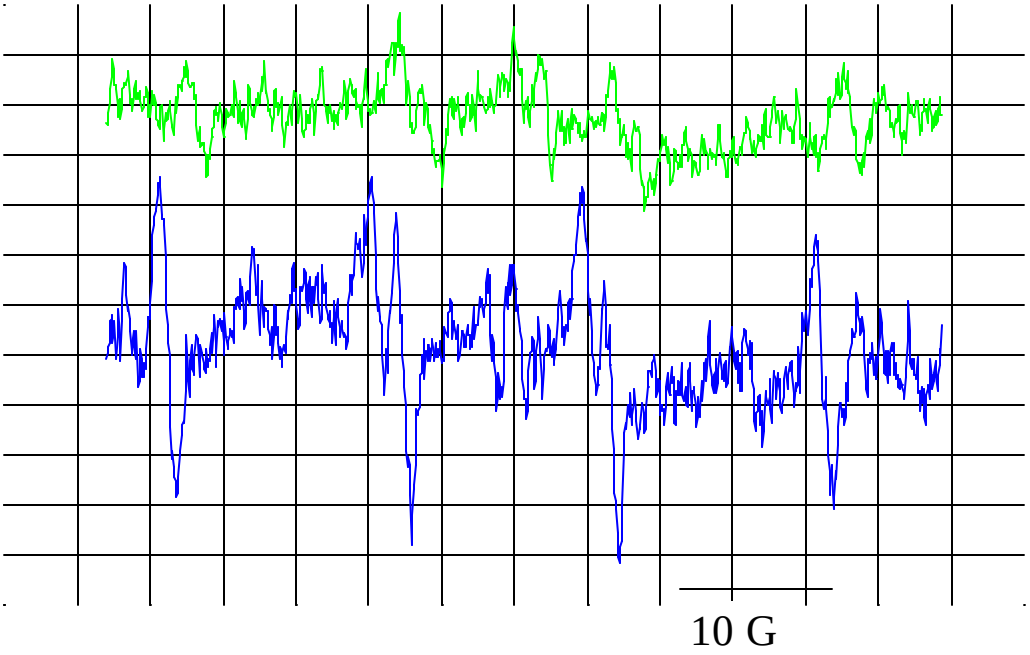

Figure 54. Desferal® decreases the UV radiation-induced DMPO adduct signal in human skin biopsies.
The lower spectrum is of the DMPO signal adduct in skin exposed to UV radiation. The upper spectrum is of human skin treated with Desferal® and exposed to radiation. Both spectra are the result of five signal-averaged scans.

protecting through chelation of skin iron. These results indicate a role for iron in the UV radiation-induced free radical formation in human skin. The protective effect of Desferal® in human skin was consistent with results obtained in our mouse experiments.

Discussion

The ultimate test animal for therapeutic experiments is humans, but even the use of humans in research has drawbacks. Using human subjects or obtaining biological samples from humans requires informed consent and always carries the risk of biohazard exposure to infectious agents such as hepatitis and HIV. Biopsy samples must be obtained from surgeries, where the time interval between resection and experimental examination or appropriate sample storage is highly variable. Thus, it is usually necessary to conduct extensive tests in animals before definitive human experiments should be undertaken.

The data presented in this work demonstrated that in both murine and human skin biopsies the ascorbate free radical signal intensity increases with UV radiation exposure, indicating oxidative stress. Visible light also caused an increase in free radical formation in the human graphs and biopsies, which is inconsistent with the findings in our mouse model. This may be due to the higher ambient, baseline ascorbate radical signal present in the mouse skin.

Mice naturally produce ascorbate, whereas it is a vitamin for humans that must be obtained through the diet. It would seem logical that under oxidative stress conditions mice would produce more ascorbate resulting in higher ascorbate radical signal. Mice are normally able to replete their ascorbate stores after an oxidative insult, whereas humans need to conserve

their ascorbate. Thus, the observation of the human ascorbate radical signal returning to baseline levels after removal of oxidative stress (the radiation source was turned off) may indicate a 'conservation' mechanism. In the mouse skin, conservation would not be necessary and thus, does not occur. The hypothesis that humans contain a mechanism for ascorbate conservation will need to be tested further.

Using EPR spin trapping techniques we have for the first time detected, *in situ,* a free radical spin adduct during UV radiation exposure of human skin. The trapped radical in human biopsies had different hyperfine splittings from those measured in the mouse skin, an alkoxyl versus an alkyl radical respectively, but still provides evidence for UV radiation-induced lipid peroxidation in both models. These results support the use of the Skh-1 hairless mouse model as a predictive tool for the study of human skin photochemistry. By applying these approaches, we have obtained a better understanding of how UV radiation induces skin damage and how this UV radiation exposure may be related to dermatopathological processes.

CHAPTER VIII

DENOUEMENT AND FUTURE DIRECTIONS

The skin is particularly vulnerable to free radical attack due to constant exposure to high oxygen tensions, frequent exposure to UV radiation, and the presence of considerable amounts of polyunsaturated fatty acids [Black, 1987; Darr and Fridovich, 1994]. Evidence for UV radiation-induced free radical formation and subsequent lipid peroxidation in skin has been circumstantial. The goal of this thesis project was to provide direct evidence for UV radiation-induced free radicals in skin. The first objective was to develop a method to examine oxidative stress in a chemical or biological system. In Chapter III the use of the ascorbate free radical as a marker of oxidative stress was examined by EPR in three different radical generating systems. In a paired comparison study with the spin trap DMPO, the ascorbate radical EPR signal height was found to increase as oxidative stress increases. Thus, it was hypothesized that the ascorbate radical could be used as a marker of oxidative stress in chemical and biological systems [Buettner and Jurkiewicz, 1993; Roginsky and Stegmann, 1994]. Because ascorbate is endogenously present in most biological tissues, the ascorbate radical signal may be useful for monitoring free radical oxidations *in vivo*. The future use of this EPR oxidative measurement technique should also be considered for use in human medicine as a diagnostic technique.

Direct EPR detection of ascorbate radical has been shown to be a reliable indicator of oxidative flux in the study of free radical oxidations in mouse skin [Buettner *et al.*, 1987;

Jurkiewicz and Buettner, 1994; Timmins and Davies, 1993], hepatocytes [Tomasi *et al.*, 1989], ischemia reperfusion of hearts [Arroyo *et al.*, 1987; Nohl *et al.*, 1991; Sharma *et al.*, 1994], and in a preliminary study presented in this Chapter, the lens of the eye.

Using the ascorbate radical, we were able to provide the first direct evidence for the production of free radicals by UV radiation in intact skin. The endogenous ascorbate free radical in both mouse and human skin was observed to increase in the presence of UV radiation. Using EPR spin trapping techniques it was possible to detect, *in situ*, a free radical spin adduct during UV radiation exposure of mouse or human skin. Alkyl radicals were observed in mouse skin and alkoxyl radicals were observed in human skin biopsies. The presence of these types of radicals is consistent with UV radiation-induced lipid peroxidation.

Another tissue that is routinely exposed to UV radiation is the lens of the eye. Cataract formation is related to UV radiation exposure [Taylor *et al.*, 1988], and evidence suggests that free radicals are involved in this damage [Weiter and Finch, 1975; Murakami *et al.*, 1989]. Ascorbic acid is clearly of importance as an antioxidant in the lens of the eye, present at steady-state concentrations of 1 to 2 mM in the human lens and adjacent aqueous and vitreous humors. We have done preliminary experiments to examine UV radiation-induced ascorbate radical production in the lens. Bovine lens tissue was placed in an EPR tissue cell and irradiated as previously described in the skin

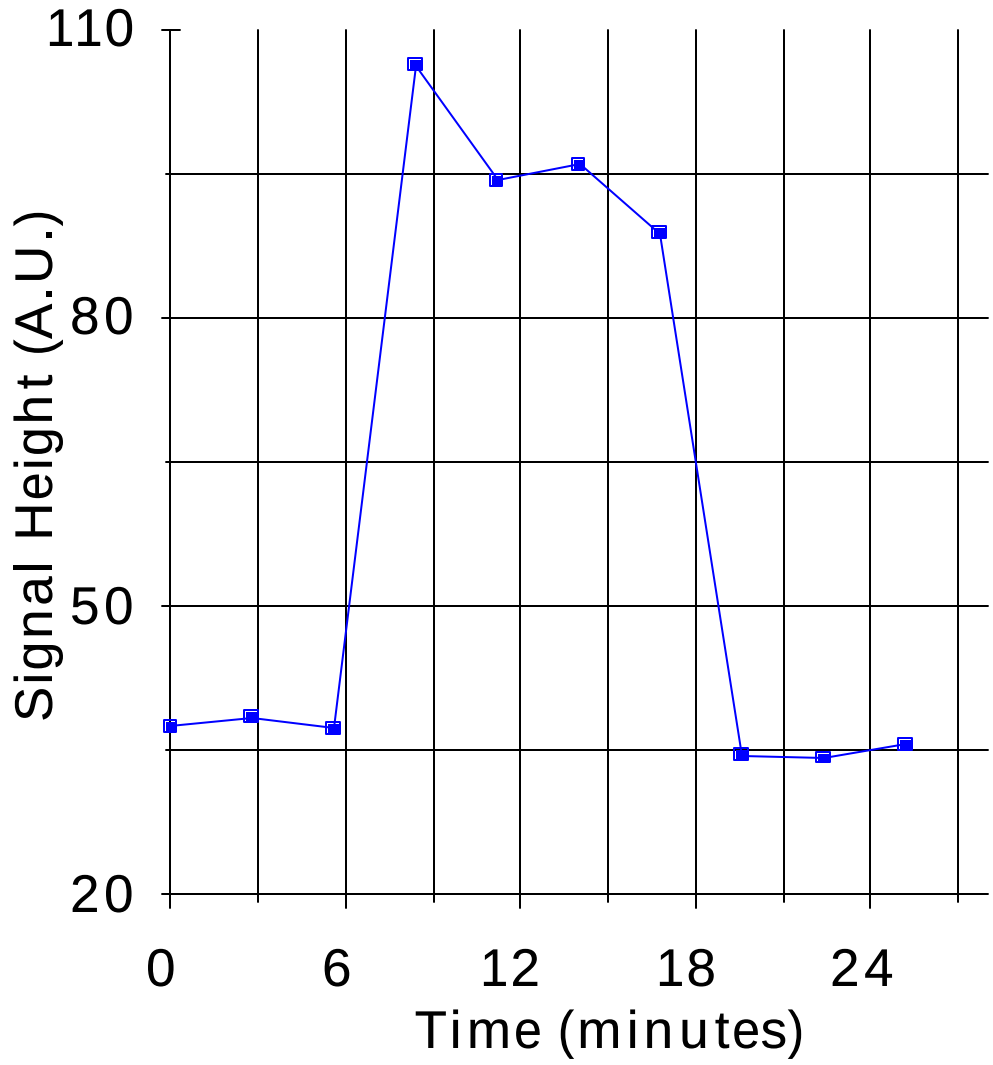

Figure 55. $Asc^{\bullet-}$ increases in UV radiation exposed lens.
Whole bovine lens was cut into EPR usable pieces (≈ 0.7 cm x 1.0 cm), placed in a Wilmad Glass Co. tissue cell, and positioned in a TM_{110} EPR cavity. EPR spectra were obtained at room temperature using a Bruker ESP 300 spectrometer, operated at 9.74 GHz with 100-kHz modulation frequency. The EPR spectrometer settings for the ascorbate radical experiments were: microwave power, 40 milliwatts; modulation amplitude, 0.63 G; time constant, 1.3 s; scan rate, 6 G/167.7 s; receiver gain, 2×10^6. While in the EPR cavity, the lens was exposed to UV radiation after the third consecutive scan and turned off following collection of the seventh scan. The light source and EPR experimental setup is depicted in Chapter IV, Figure 20.

experiments. A low steady-state level of the ascorbate free radical is detectable by EPR in bovine lens (Figure 55). During UV photooxidative stress the levels of ascorbate free radical signal significantly increases. When the radiation source is turned off, the ascorbate free radical signal returns to baseline levels. This return to baseline radical signal levels is consistent with those results obtained in our human skin biopsies.

Some lipid peroxidation products can diffuse, thus unlike the site-specific action of the hydroxyl radical, these species can cause damage throughout the cell and its surrounding environment. Uncontrolled lipid peroxidation can result in tissue damage, leading to membrane fluidity changes [Bruch and Thayer, 1983], altered activity of membrane bound enzymes and receptors [Field and Salome, 1982; L'Abbe *et al.*, 1991], changes in ion permeability, protein and DNA damage [Ames *et al.*, 1982], mutagenesis [Bachur *et al.*, 1979], and perhaps apoptosis [Ramakrishnan *et al.*, 1993; Ramakrishnan *et al.*, 1995; Ramakrishnan *et al.*, 1995]. These lipid peroxidation-induced alterations may lead to changes resulting in photoaging or may play a specific role in free radical induced dermatopathologies, such as skin cancer.

The traditional model of cancer involves an initiation event followed by a promotion sequence. In non-melanoma skin cancer, the initiating event has traditionally been thought to due to a direct hit to DNA by UV radiation, resulting in formation of dimers or other photoproducts. However, DNA does not have significant absorption in the solar radiation spectrum to which humans are exposed. UVB radiation, which is shown to be most effective in

producing DNA dimers, is almost entirely absorbed by the non-viable cells of the stratum corneum. It is difficult to elucidate how damage in a presumably 'dead' cell can result in an initiating carcinogenic event. As mentioned previously, some reactive oxygen species and lipid peroxidation products are diffusible; thus an insult that occurs in the non-viable layers of the skin may be propagated into the viable regions of the epidermis and dermis.

To have significant lipid peroxidation, iron is required. The role of iron in UV radiation-induced free radical production was examined in Chapter V. Topical application of ferrous but not ferric iron was found to increase UV radiation-induced free radical formation in the concentrations examined. We know that chronic exposure to UV radiation increases skin iron content [Bissett *et al.*, 1991], but the mechanism for this increase is unknown. It may be that UV radiation, UVA wavelengths specifically, is involved in photoaging and the promotion step of carcinogenesis through formation of free radicals in the lower layers of the epidermis and dermis. UVA can interact with blood vessels, possibly cause endothelial cell damage, and leakage of iron containing compounds from the blood constituents. Direct irradiation of ferritin with UVA radiation induces reduction of Fe(III) to Fe(II) [Aubailly *et al.*, 1991]. Thus, ferritin present in fibroblasts [Einstein *et al.*, 1991] and macrophages [Ackerman *et al.*, 1988] may be a potential source for the production of iron-related tissue damage. Once catalytically available, iron can diffuse to the DNA where it can be involved in the direct hit initiation, or may be involved in Fenton chemistry elsewhere in the skin leading to further free radical formation.

Thus, it was hypothesized that chelation of this iron should protect against free radical-induced lipid peroxidation. Indeed, topical application of the iron chelator Desferal® or FDO, a proposed iron chelator, reduced endogenous as well as UV radiation-induced free radical formation in skin. Topical application of iron chelators may protect the skin by reducing the rate of reduction of the iron complexes or by moving the iron to a 'safer' location, *i.e.*, away from the DNA or lipid membranes. Desferal® is an excellent iron chelator and when topically applied to human or mouse skin significantly reduces the UV radiation-induced radical signal in skin. FDO, although not an effective inhibitor of iron catalysis, also protects the skin by reducing free radical formation and may do so by removing the iron from the DNA. Our results provide direct evidence for a role of iron in free radical formation in skin and indicate that metal chelators should be considered as anti-aging and photoprotective products. FDO may also be protective by acting as a nitric oxide donor. Nitric oxide is known to be an excellent antioxidant in prevention of LDL oxidation [Hogg *et al.*, 1993], and in our skin model may be protecting against UV radiation-induced membrane damage.

Because UV radiation-induces free radicals in skin, antioxidants should also protect against this insult. In Chapter VI, the use of the antioxidant tocopherol was examined as a photoprotectant against UV radiation-induced free radical formation. Three different forms of tocopherol were studied, α-tocopherol, tocopherol acetate, and tocopherol sorbate. Topical application of tocopherol sorbate was found to significantly reduce ambient as well as the UV radiation-induced enhancement of free radical production, where as α-tocopherol and

tocopherol acetate had minimal effects. The reduction of free radical production in skin by tocopherols was found to directly correlate with decreased wrinkling and tumor formation in animals, chronically exposed to UV radiation. These results suggest an anti-aging as well as photoprotective role for tocopherol sorbate in mouse skin.

Topical application of the antioxidant tocopherol reduced free radical formation, skin wrinkling, and provided modest protection against the number of tumors formed. The tocopherols did not protect against the onset of tumor formation, indicating that they could not protect against the initiating carcinogenic event, but rather may act by delaying the promotion step. Thus, when free radical scavengers are present, free radical formation is decreased and there is a delayed progression in photoaging and skin cancer development.

Alpha-tocopherol is already being examined for beneficial effects in healing of scars, burns, eczema, psoriasis, dental pulp, and ulcers. In our work, tocopherol sorbate was found to be more protective against UV radiation-induced damage and may be beneficial in these dermatopathologies too. Tocopherol sorbate and Desferal® should be considered for application in human subjects to prevent UV-radiation induced free radical formation and reduce photodamage related to chronic UV radiation exposure, such as wrinkling, sagging, and tumor formation. In addition, the use of antioxidants and metal chelators should be considered for use in prevention of skin damage in patients receiving radiation therapy. In radiation therapy, skin absorbs a significant dose of ionizing radiation. A few hours after doses greater than 5 Gy there is an early erythema, similar to sunburn, characterized by vasodilation, edema, and leakage

of plasma constituents from the capillaries. This erythemal response can last for days. Topical application of antioxidants and chelators may blunt this skin damage, which can be the dose-limiting adverse effect during cancer therapy.

In addition to presenting an innovative approach to photoprotection, this research project presented a new experimental model for the study of photochemistry and biology of the skin. Albino mice have been used since 1928 to study UV radiation-induced damage in skin [Findlay, 1928]; however, there are differences between the skin of mice and humans suggesting a potential need for a more appropriate model for studying dermatopathology. In our results, the UV radiation-induced radical formation observed in human skin biopsies had similarities to what was observed in mouse skin. Thus, this work supports the use of hairless Skh-1 mice as predictive tools for human skin photochemistry, and also suggests the use of human skin biopsies in free radical research.

Future Directions

Although this work provides a better understanding of how UV radiation may induce skin damage and consequent dermatopathological processes, there are still unresolved questions. For instance, the exact identity of these radicals or the location of radical production in skin is not known, providing an impetus for further research. As for the exact identity of the apparent lipid-derived spin adducts obtained in UV radiation exposed mouse or human skin, the carbon-centered radicals could be from two sources: either a primary carbon-centered radical, where the adduct is formed from the polyunsaturated fatty acid through hydrogen abstraction, or

through secondary carbon-centered radicals. Alkoxyl radicals are secondary radicals that can undergo β-scission to form alkyl radicals, such as ethyl and pentyl radicals [Chamulitrat *et al.*, 1992]. The EPR hyperfine coupling constants alone cannot definitively distinguish the difference in the carbon-centered radicals. Therefore, high-pressure liquid chromatography and mass spectroscopy will need to be employed for further identification.

Although this research project provides evidence for the use of antioxidants as well as metal chelators against UV radiation-induced free radical formation and photodamage a combined modality as well as the potential use of other antioxidants and iron chelators should be examined. In our work topical application of tocopherol or metal chelators prior to UV irradiation was found to be protective against free radical formation. In work by Roshchupkin *et al*. topical application of tocopherol and BHT two minutes after UV radiation exposure was found to be protective against erythema in rabbits [Potapenko *et al.*, 1984]; however, in other work, tocopherol alone applied after UV irradiation had no protective effects [Roshchupkin *et al.*, 1979]. Clearly, the application of tocopherols and metal chelators after UV irradiation should also be examined.

One of the most exciting ideas proposed in this work is the potential use of nitric oxide donors as photoprotective antioxidant agents. According to preliminary data presented in this thesis FDO is a drug that releases nitric oxide when it is exposed to UV radiation. Thus, the antioxidant nitric oxide would be released when oxidative stress is present. This novel approach to photoprotection, and potentially antiaging, could revolutionize the way sunscreens developed.

Other directions that should be persued are the further examination of whether free radical formation correlates with damage, specifically, evidence for oxidative damage to DNA that may lead to cancer. This would provide a direct connection between UV radiation-induced free radical formation and carcinogenesis.

The use of antioxidants, iron chelators, and nitric oxide donors to reduce free radical formation is an entirely new approach to photoprotection and subsequently skin cancer prevention. Instead of only blocking the UV radiation from being absorbed, skin could also be protected by preventing propagation of free radical damage. UV radiation is implicated as the leading cause of skin cancer; projections indicate that 50% of Americans will have skin cancer at least once in their lifetime [Miller and Weinstock, 1994]. This results in considerable costs and impact on the health care system, with a million cancer patients a years, and considerably more seeking care for non-cancerous lesions and cosmetic changes to reduce signs of photoaging. Thus, the development of these photoprotective concepts is imperative.

REFERENCES

Ackerman Z, Seidenbaum M, Lowenthal E, Rubinow A: Overload of iron in the skin of patients with varicose ulcers. Possible contributing role of iron accumulation in progression of the disease. *Arch Dermatol* 124:1376-1378, 1988.

Ames BN, Hollstein MC, Cathcart R: Lipid peroxidation and oxidative damage in DNA. In: *Lipid Peroxides in Biology and Medicine* ed., Yagi K, Academic Press, New York, 339-351, 1982.

Andronik-Lion V, Boucher JL, Delaforge M, Henry Y, Mansuy D: Formation of nitric oxide by cytochrome P450-catalyzed oxidation of aromatic amidoximes. *Biochem Biophys Res Commun* 185:452-458, 1992.

Arroyo CM, Kramer JH, Dickens BF, Weglicki WB: Identification of free radicals in myocardial ischemia/reperfusion by spin trapping with nitrone DMPO. *FEBS Lett* 221:101-104, 1987.

Atherton NM: *Electron Spin Resonance*. Halsted Press, London, 1973.

Aubailly M, Salmon S, Haigle J, Bazin M, Maziere JC, Santus R: Peroxidation of model lipoprotein solutions sensitized by photoreduction of ferritin by 365 nm radiation. *J Photochem Photobiol B* 26:185-191, 1994.

Aubailly M, Santus R, Salmon S: Ferrous ion release from ferritin by ultraviolet-A radiations. *Photochem Photobiol* 54:769-773, 1991.

Bachur NR, Gorden SL, Gee MV, Kon H: NADPH cytochrome P-450 reductase activation of quinone anticancer agents to free radicals. *Proc Natl Acad Sci USA* 76: 954-957, 1979.

Basu AK, Marnett LJ: Unequivocal evidence that malondialdehyde is a mutagen. *Carcinogenesis* 4:331, 1983.

Beehler BC, Przybyszewski J, Box HB, Kulesz-Martin MF: Formation of 8-hydroxydeoxyguanosine within DNA of mouse keratinocytes exposed in culture to UVB and H_2O_2. *Carcinogenesis* 13:2003-2007, 1992.

Beijersbergen van Henegouwen GMJ, de Vries H, van den Broeke, LT, Junginger HE: RRR-Tocopherols and their acetates as a possible scavenger of free radicals produced in the skin upon UVA-exposure - An in vivo screening method. *Fat Sci Technol* 94:24-27, 1992.

Bielski BHJ, Cabelli DE, Arudi RL: Reactivity of HO_2/O_2^- radicals in aqueous solution. *J Phys Chem Ref Data* 14:1041-1100, 1985.

Bielski BHJ: Chemistry of ascorbic acid radicals. In: *Ascorbic Acid: Chemistry, Metabolism, and Uses*. eds., Seib PA, Tolbert BM, Washington DC: American Chemical Society 81-100, 1982.

Bissett DL, Bush RD: Photoprotection compositions comprising tocopherol sorbate. *U.S. Patent* 4,847,072, 1989.

Bissett DL, Chatterjee R, Hannon DP: Chronic ultraviolet radiation-induced increase in skin iron and the photoprotective effects of topically applied iron chelators. *Photochem Photobiol* 54: 215-223, 1991.

Bissett DL, Chatterjee R, Hannon DP: Photoprotective effect of superoxide-scavenging antioxidants against ultraviolet radiation-induced chronic skin damage in hairless mouse. *Photodermatol Photoimmunol Photomed* 7:56-62, 1990a.

Bissett DL, Chatterjee R, Hannon DP: Photoprotective effect of topical anti-inflammatory agents against ultraviolet radiation-induced chronic skin damage in the hairless mouse. *Photodermatol Photoimmunol Photomed* 7:153-158, 1990b.

Bissett DL, Chatterjee R, Hannon DP: Protective effects of a topically applied antioxidant plus an antiinflammatory agent against ultraviolet radiation-induced chronic skin damage in the hairless mouse. *J Soc Cosmet Chem* 43:85-92, 1992.

Bissett DL, Hannon DP, Orr TV: An animal model of solar aged skin: histological, physical, and visible changes in UV-irradiated hairless mice. *Photochem Photobiol* 46:367-378, 1987.

Bissett DL, Hannon DP, Orr TV: Wavelength dependence of histologic, physical, and visible changes in chronically UV-irradiated hairless mouse skin. *Photochem Photobiol* 50:763-769, 1989.

Bissett DL, Hillebrand GG, Hannon DP: The hairless mouse as a model of skin photoaging: its use to evaluate photoprotective materials. *Photodermatol* 6:228-233, 1989.

Bissett DL, Majeti S, Fu J-JL, McBride JF, Wyder WE: Protective effect of topically applied conjugated hexadienes against ultraviolet radiation-induced chronic skin damage in the hairless mouse. *Photodermatol Photoimmunol Photomed* 7:63-67, 1990c.

Bissett DL, McBride JF: Iron content of human epidermis from sun-exposed and non-exposed body sites. *J Soc Cosmet Chem* 43:215-217, 1992.

Bissett DL, Oelrich DM, Hannon DP: Evaluation of a topical iron in animals and in human beings: Short-term photoprotection by 2-furildioxime. *J Am Acad Dermatol* 31:572-578, 1994.

Bissett DL, Oelrich DM, Hannon DP: Evaluation of a topical iron chelator in animals and in human beings: Short-term photoprotection by 2-furildioxime. *J Am Acad Dermatol* 31:572-578, 1994.

Black HS: Potential involvement of free radical reactions in ultraviolet light- mediated cutaneous damage. *Photochem Photobiol* 46:213-221, 1987.

Black HS, Chan JT: Suppression of ultraviolet light-induced tumor formation by dietary antioxidants. *J Invest Dermatol* 65:412-414, 1975.

Black HS, Lenger W, McCann V, Thronby J: Relation of UV dose to antioxidant modification of photocarcinogenesis. *J Am Coll Toxicol* 2:201-207, 1983.

Blois MS, Zahlan AB, Muling JE: Electron spin resonance studies on melanin. *Biophys J* 4:471-490, 1964.

Borg DC, Schaich KM, Elmore JJ, Bell JA: Cytotoxic reactions of free radical species of oxygen. *Photochem Photobiol* 28:887-907, 1978.

Boring CC, Squires TS, Tong T: Cancer statistics. *Cancer Abs* 43:7-26, 1993.

Borsook H, Davenport HW, Jeffreys CEP, Warner RC: The oxidation of ascorbic acid and its reduction in vitro and in vivo. *J Biol Chem* 117:237-279, 1937.

Bowry VW, Stocker R: Tocopherol-mediated peroxidation. The prooxidant effect of vitamin E on the radical-initiated oxidation of human low-density lipoprotein. *J Am Chem Soc* 115:6029-6044, 1993.

Bowser PA, Nugteren DH, White RJ, Houtsmuller UMT, Prottey C: Identification, isolation and characterized of epidermal lipids containing linoleic acid. *Biochim Biophys Acta* 834:419-428, 1985.

Brody I: The epidermis. In: *Normale und Pathologische Anatomie der Haut*. ed., Gans O, Steigleider GK, Springer, Berlin, New York, 1-142, 1968.

Bronaugh RL, Maibach HI: In vitro models for human percutaneous absorption. In: *Models in Dermatology*. eds., Maibach HI, Lowe NJ, New York, Krager, 1985.

Bruch RC, Thayer WS: Differential effect of lipid peroxidation on membrane fluidity as determined by electron spin resonance probes. *Biochim Biophys Acta* 733:216-222, 1983.

Bruls WAG, Slaper H, van der Leun JC, Berrens L: Transmission of human epidermis and stratum corneum as a function of thickness in the ultraviolet and visible wavelengths. *Photochem Photobiol* 40:485-489, 1984.

Buettner GR: Ascorbate autoxidation in the presence of iron and copper chelates. *Free Rad Res Comms* 1:349-353, 1986.

Buettner GR: Ascorbate oxidation: UV absorbance of ascorbate and ESR spectroscopy of the ascorbyl radical as assays for iron. *Free Rad Res Comms* 10:5-9, 1990.

Buettner GR: In the absence of catalytic metals ascorbate does not autoxidize at pH 7: ascorbate as a test for catalytic metals. *J Biochem Biophys Meth* 16:27-40, 1988.

Buettner GR: The pecking order of free radicals and antioxidants: lipid peroxidation, α-tocopherol, and ascorbate. *Arch Biochem Biophys* 300:535-543, 1993.

Buettner GR: Spin Trapping: ESR parameters of spin adducts. *Free Radic Biol Med* 3:259-303, 1987.

Buettner GR, Chamulitrat W: The catalytic activity of iron in synovial fluid as monitored by the ascorbate free radical. *Free Radic Biol Med* 8:55-56, 1990.

Buettner GR, Jurkiewicz BA: Ascorbate free radical as a marker of oxidative stress: an EPR study. *Free Radic Biol Med* 14:49-55, 1993.

Buettner GR, Kiminyo KP: Optimal EPR detection of weak nitroxide spin adduct and ascorbyl free radical signals. *J Biochem Biophys Meth* 24:147-151, 1992.

Buettner GR, Motten AG, Hall RD, Chignell CF: ESR detection of endogenous ascorbate free radical in mouse skin: Enhancement of radical production during UV irradiation following topical application of chlorpromazine. *Photochem Photobiol* 46:161-164, 1987.

Burkitt MJ, Gilbert BC: Model studies of the iron-catalyzed Haber-Weiss cycle and the ascorbate driven Fenton reaction. *Free Rad Res Commun* 10:265-280, 1990.

Burton GW, Ingold KU: Vitamin E: Application of the principles of physical organic chemistry to the exploration of its structure and function. *Acc Chem Res* 9:194-201, 1986.

Burton GW, Ingold KU: β-Carotene: An unusual type of lipid antioxidant. *Science* 224:569-573, 1984.

Buxton GV, Greenstock CL, Helman WP, Ross AB: Critical review of rate constants for reactions of hydrated electrons, hydrogen atoms and hydroxyl radicals ($^{\bullet}OH/^{\bullet}O^{-}$) in aqueous solution. *J Phys Chem Ref Data* 17:513-886, 1988.

Cabelli DE, Bielski BHJ: Kinetics and mechanism for the oxidation of ascorbic acid/ascorbate by HO_2/O_2^- radicals. A pulse radiolysis and stopped-flow photolysis study. *J Phys Chem* 87:1809-1812, 1983.

Cabrini L, Pasquali P, Tadolini B, Sechi AM, Landi L: Antioxidant behavior of ubiquinone and β-carotene incorporation on model membranes. *Free Radic Res Comm* 2:85-92, 1986.

Cadet J, Berger M, Decarroz C, Wagner JR: Photosensitized reactions on nucleic acids. *Biochimie* 68:813-834, 1986.

Campbell I, Divek R: Electron Paramagnetic Resonance Spectroscopy. In: *Biological Spectroscopy*. Benjamin/Cummings Publishing Company, Menlo Park, CA 179-215, 1984.

Caprini L, Pasquali P, Tadolini B, Sechi AM, Landi L: Antioxidant behaviour of ubiquinone and beta-carotene incorporated in model membranes. *Free Radic Res Commun* 2:85-92, 1986.

Carrington A, McLachlan AD: *Introduction to Magnetic Resonance*. Harper & Row, New York, 1967

Cerutti PA: Prooxidant states and cancer. *Science* 227:375-381, 1985.

Chamulitrat W, Jordan SJ, Mason RP: Fatty acid formation in rats administered oxidized fatty acids: *In vivo* spin trapping investigation. *Arch Biochem Biophys* 299:361-367, 1992.

Chatterjee SN, Agarwal S: Liposomes as membrane model for study of lipid peroxidation. *Free Radic Biol Med* 4:51-72, 1988.

Chatterjee SN, Agarwal S, Bose B: An approach towards understanding the genesis of sunlight-induced skin cancer. *Ind J Biochem Biophys* 27:254-263, 1990.

Connor MJ, Wheeler LA: Depletion of cutaneous glutathione by ultraviolet radiation. *Photochem Photobiol* 47:239-245, 1987.

Corey EJ, Mehrota MM, Khan AU: Water induced dismutation of superoxide anion generates singlet molecular oxygen. *Biochem Biophys Res Commun* 145:842-846, 1987.

Creutz C: The complexities of ascorbate as a reducing agent. *Inorg Chem* 20:4449-4452, 1981.

Crist KC: *Comprehensive regional scale air pollution/radiative modeling: an analysis of the relationships between changes in radiative transfer and atmospheric trace gas species*. The University of Iowa, Ph.D. Thesis, 1994.

Darr D, Fridovich I: Free radicals in cutaneous biology. *J Invest Dermatol* 102:671-675, 1994.

Davies MB, Austin J, Partridge DA: *Vitamin C: Its Chemistry and Biochemistry*. Royal Society of Chemistry, Cambridge, 1991.

Davies RE, Forbes PD: Effect of UV radiation on survival of non-haired mice. *Photochem Photobiol* 43:267-274, 1986.

Davis HF, McManus HJ, Fessenden RW: An ESR study of free-radical protonation equilibria in strongly acid media. *J Phys Chem* 90:6400-6404, 1986.

De Gruijl FR, Van der Meer J, Van der Leun J: Follow up on systemic influence of partial pre-irradiation on UV-tumorigenesis. *Photochem Photobiol* 38: 381-384, 1983.

De Simone C, Rusciani L, Venier A, Larussa FM, Littaruru GP, Oradei A, Lippa S, Serri F: Vitamin E and coenzyme Q10 content in epidermis and basal cell epithelioma. *J Invest Dermatol* 89:317, 1987.

Douthat WG, Acuna Aguerre G, Fernandez Martin JL, Mouzo R, Cannata Andia JB: Treatment of aluminum intoxication: a new scheme for desferrioxamine administration. *Nephrology Dialysis Transplant.* 9:1431-4, 1994.

Draper HH, Squires EJ, Mahmoodi H, Wu J, Agarwal S, Hadley M: A comparative evaluation of thiobarbituric acid methods for the determination of malondialdehyde in biological materials. *Free Radic Biol Med* 15:353-363, 1993.

Einstein RS, Garcia-Mayol D, Pettingel W, Munro HN: Regulation of ferritin and heme oxygenase synthesis in rat fibroblasts by different forms of iron. *Proc Natl Acad Sci USA* 88:688-692, 1991.

Eisenstark A, Perrot G: Catalase has minor role in protection against near ultraviolet radiation damage in bacteria. *Mol Gen Genet* 207:68-72, 1987.

Emerit I, Khan SH, Esterbauer H: Hydroxynonenal, a component of clastogenic factors? *Free Radic Biol Med* 10:371-377, 1991.

Erben-Russ M, Michel C, Bors W, Saran M: Absolute rate constants of alkoxyl radical reactions in aqueous solution. *J Phys Chem* 91:2362-2365, 1987.

Esterbauer H, Eckl P, Ortner A: Possible mutagens derived from lipids and lipid precursors. *Mut Res* 238:223-233, 1990.

Farraggi M, Carmichael A, Riesz P: OH radical formation by photolysis of aqueous porphrin solutions. A spin trapping e.s.r. study. *Int J Radiat Biol* 46:703-713, 1984.

Field FJ, Salome RG: Effect of dietary fat saturation, cholesterol and cholestyramine on acyl-CoA: cholesterol acyltransferase activity in rabbit intestinal microsomes. *Biochim Biophys Acta* 712:557-570, 1982.

Findlay GM: Ultraviolet light and skin cancer. *Lancet* 2:1070-1073, 1928.

Floche L, Otting F: Superoxide dismutase assays. In: *Methods Enzymol*, Vol. 105. ed., Packer L, Academic Press, 93-105, 1984.

Foerster G, Weis W, Staudinger H: Messung der elektronenspinresonanz an semidehydroascorbinsaure. *Annalen Der Chemie* 690:166-169, 1965.

Food and Drug Administration. Sunscreen drug products for over-the-counter drugs. *Fed Reg* 43, 38259, 1978.

Foote CS, Denny RW: Chemistry of singlet oxygen. VII. Quenching by β-carotene. *J Am Chem Soc* 90:6233-6235, 1968.

Forni LG, Monig J, Mora-Arellano VO, Willson RL: Thiyl free radicals: Direct observations of electron transfer reactions with phenothiazines and ascorbate. *J Chem Soc Perkin Trans II* 961-965, 1983.

Forslind B, Grundin TG, Lindberg M, Roomans GM, Werner Y: Recent advances in X-ray microanalysis in dermatology. *Scanning Electron Microsc* II:687-695, 1985.

Freeman BA, Carpo JD: Biology of disease: Free radicals and tissue injury. *Lab Invest* 47:412-426, 1982.

Frei B, England L, Ames BN: Ascorbate is an outstanding antioxidant in human blood plasma. *Proc Natl Acad Sci USA* 86:6377-6381, 1989.

Frei B, Stocker R, Ames BN: Antioxidant defenses and lipid peroxidation in human blood plasma. *Proc Nat Acad Sci USA* 85:9748-9752, 1988.

Fryer M: Evidence for the photoprotective effects of vitamin E. *Photochem Photobiol* 58, 304-312, 1993.

Fuchs J: *Oxidative Injury in Dermatopathology*. New York: Springer-Verlag, 1992.

Fuchs J: Validity of the 'bioassay' for thioredoxin reductase activity. *Arch Dermatol* 124:849-851, 1988.

Fuchs J, Huflejt M, Rothfuss L, Carcamero G, Packer L: Acute effects of near ultraviolet and visible light on cutaneous antioxidant defense system. *Photochem Photobiol* 50:739-744, 1989a.

Fuchs J, Huflejt ME, Rothfuss LM, Wilson DB, Gerardo C, Packer L: Impairment of enzymatic and nonenzymatic antioxidants in skin by photooxidative stress. *J Invest Dermatol* 93:769-773, 1989b.

Fuchs J, Mehlhron RJ, Packer L: Free radical reduction mechanisms in mouse epidermis skin homogenates. *J Invest Dermatol* 93:633-640, 1989c.

Fuchs J, Schurer N: Lipid peroxidation in dermatopathology. In: *Membrane Lipid Oxidation*, vol. 3, ed. C. Vigo-Pelfrey, CRC Press, Boca Raton, 165-189, 1991.

Furchgott RF, Zawadzki JV: The obligatory role of endothelial cells in the relaxation of arterial smooth muscle of acetylcholine. *Nature* 288:373-376, 1980.

Giovannini L, Bertelli AAE, Scalori V, Dell'Osso L, Alessandi MG, Mian M: Skin penetration of CoQ in the rat. *Int J Tissue Reac* 103-105, 1988.

Goldschmidt BM: Role of aldehydes in carcinogenesis. *J Environ Sci Health* C2:231, 1984.

Goldsmith L: *Biochemistry and Physiology of the Skin*. London, Oxford University Press, 1982.

Green R, Charlton R, Seftel H, Bothwell T, Mayet F, Adams B, Finch C, Layrisse M: Body iron excretion in man: a collaborative study. *Am J Med* 45: 336-353, 1968.

Gutteridge JMC: Aspects to consider when detecting and measuring lipid peroxidation. *Free Radic Res Commun* 1:173-184, 1986.

Guzman Barron ES, DeMeio RH, Klemperer F: Studies of biological oxidations. Copper and hemochromogens as catalysts for the oxidation of ascorbic acid. The mechanism of the oxidation. *J Biol Chem* 112:625-640, 1936.

Halliwell B: How to characterize a biological antioxidant. *Free Rad Res Comms* 9:1-32, 1990.

Halliwell B, Foyer CH: Ascorbic acid, metal ions and the superoxide radical. *Biochem J* 155:697-700, 1976.

Halliwell B, Gutteridge JMC: *Free Radicals in Biology and Medicine*. Oxford, Clarendon Press, 1989.

Halliwell B, Gutteridge JMC: The importance of free radicals and catalytic metal ions in human diseases. *Molec Aspects Med* 8:89-193, 1985.

Hanada K, Gange RW, Connor MJ: Effects of glutathione depletion on sunburn cell formation in the hairless mouse. *J Invest Dermatol* 96:838-840, 1991.

Harmon D: Free radical theory of aging. *Mut Res* 275:257-266, 1992.

Hasegawa K, Patterson LK: Pulse radiolysis studies in model lipid systems: Formation and behavior of peroxyl radicals in fatty acids. *Photochem Photobiol* 28:817-823, 1978.

Hogg N, Kalyanaraman B, Joseph J, Struck A, Parthasarathy S: Inhibition of low-density lipoprotein oxidation by nitric oxide. Potential role in atherogenesis. *FEBS* 334:170-174, 1993.

Ito T: Cellular and subcellular mechanisms of photodynamic action: the $^1O_2$ hypothesis as a driving force in recent research. *Photochem Photobiol* 28:493-508, 1978.

Iwaoka T, Tabat F, Takahashi T: Lipid peroxidation and lipid peroxide detected by chemiluminescence. *Free Radic Biol Med* 3:329-333, 1987.

Janzen EG: Spin trapping. *Accounts Chem Res* 4:31-40, 1971.

Janzen EG: Spin trapping and associated vocabulary. *Free Radic Res Comms* 19:163-167, 1990.

Jurkiewicz BA, Buettner GR: Ultraviolet light-induced free radical formation in skin: An electron paramagnetic resonance study. *Photochem Photobiol* 59:1-4, 1994.

Jurkiewicz BA, Bissett DL, Buettner GR: The effect of topically applied tocopherol on ultraviolet-radiation mediated free radical damage in skin. *J Invest Dermatol* 104:484-488, 1995.

Kagan V, Witt E, Goldman G, Scita G, Packer L: Ultraviolet light-induced generation of vitamin E radicals and their recycling. A possible photosensitizing effect of vitamin E in skin. *Free Radical Res Commun* 16, 51-64, 1992.

Kahn MMT, Martell AE: Metal ion and metal chelate catalyzed oxidation of ascorbic acid by molecular oxygen. I. Cupric and ferric ion catalyzed oxidation. *J Am Chem Soc* 89:4176-4185, 1967.

Kalyanaraman B, Darley-Usmar VM, Wood J, Joseph J, Parthasarathy S: Synergistic interaction between the probucol phenoxyl radical and ascorbic acid in inhibiting the oxidation of low density lipoprotein. *J Biol Chem* 267:6789-6795, 1992.

Kasha M, Kahn AU: The physics, chemistry, and biology of singlet oxygen. *Ann NY Acad Sci* 171:1-23, 1970.

Kellogg EW, Fridovich I: Superoxide, hydrogen peroxide, and singlet oxygen in lipid peroxidation by xanthine oxidase system. *J Biol Chem* 250:8812-8817, 1975.

Khan MMT, Martell AE: Metal ion and metal chelate catalyzed oxidation of ascorbic acid by molecular oxygen. II. Cupric and ferric chelate catalyzed oxidation. *J Am Chem Soc* 89:7104-7111, 1967.

Klepp O, Magnus K: Some environmental and bodily characteristics of melanoma patients. A case-control study. *Int J Cancer* 23:482-486, 1979.

Klingman LH, Akin FJ, Klingman AM: The contribution of UVA and UVB to connective tissue damage in hairless mice. *J Invest Dermatol* 84:272-276, 1985.

Klingman LH, Akin FJ, Klingman AM: Sunscreens prevent ultraviolet photocarcinogenesis. *J Am Acad Dermatol* 3:30-35, 1980.

Klingman LH, Gebre M: Biochemical changes in hairless mouse skin collagen after chronic exposure to ultraviolet-A radiation. *Photochem Photobiol* 54:233-237, 1991.

Kobayashi T, Matsumoto M, Iizuka H, Suzuki K, Taniguchi N: Superoxide dismutase in psoriasis, squamous cell carcinoma, and basal cell epithelioma: an immuno-histochemical study. *Br J Dermatol* 124:555-559, 1991.

Komarov A, Mattson D, Jones MM, Singh PK, Lai CS: In vivo spin trapping of nitric oxide in mice. *Biochem Biophys Res Comm*. 195(3):1191-8, 1993.

Koppenol WH: A thermodynamic appraisal of the radical sink hypothesis. *Free Radic Biol Med* 14:91-94, 1993.

Koppenol WH, Butler J: Energetics of interconversion reactions of oxy radicals. *Adv Free Radical Biol* 1:91-131, 1985.

Kozlov AY, Yegorov DY, Vladimirov YA, Azizova OA: Intracellular free iron in liver tissue and liver homogenate: studies with electron paramagnetic resonance on the formation of paramagnetic complexes with desferal and nitric oxide. *Free Radic Biol Med* 13:9-16, 1992.

Krinsky NI: Mechanism of action of biological antioxidants. *Proc Soc Exp Biol Med* 200:248-254, 1992.

Krinsky NI, Deneke SM: Interaction of oxygen and oxy-radicals with caratenoids. *J Natl Cancer Inst* 69:205-209, 1982.

L'Abbe MR, Trick KD, Beare-Rogers JL: Dietary (n-3) fatty acids affect rat heart, liver and aorta protective enzyme activities and lipid peroxidation. *J Nutr* 121:1331-1340, 1991.

Lacoste H, Goyert GL, Goldman LS, Wright DJ, Schwartz DB: Acute iron intoxication in pregnancy: case report and review of the literature. *Obstetrics Gynecology* 80:500-1, 1992.

Lai CS, Komarov AM: Spin trapping of nitric oxide produced in vivo in septic-shock mice. *FEBS Letters* 345:120-4, 1994.

Laroff GP, Fessenden RW, Schuler RH: The electron spin resonance spectra of radical intermediates in the oxidation of ascorbic acid and related substances. *J Am Chem Soc* 94:9062-9073, 1972.

Larson RA, Lloyd RE, Marley KA, Tuveson RW: Ferric-ion-photosensitized damage to DNA by hydroxyl and non-hydroxyl radical mechanisms. *J Photochem Photobiol B* 14:345-357, 1992.

Laub R, Schneider YJ, Octave JN, Crichton RR, Tronet A: Iron mobilization studies-uptake and release of radiolabelled derivatives of desferrioxamine B by the rat hepatocytes and macrophages. In: *Structure and Function of Iron Storage Transport Proteins*, Proc Int Conf, 6th, Amsterdam, 469-471, 1983.

Lewin S: Vitamin C: *Its Molecular Biology and Medical Potential*. New York: Academic Press, 1976.

Lopez-Torres M, Shindo Y, Packer L: Effect of age on antioxidants and molecular markers of oxidative damage in murine epidermis and dermis. *J Invest Dermatol* 102:476-480, 1994.

Maeda K, Naganuma M, Fukuda M: Effects of chronic exposure ultraviolet-A including 2% ultraviolet-B on free radical reduction systems in hairless mice. *Photochem Photobiol* 54:737-740, 1991.

Maisuradze VN, Platonov AG, Gudz TI, Goncharenko EN, Kudriashov IUB: Effect of ultraviolet rays on lipid peroxidation and various factors of its regulation in the rat skin. *Biol Nauki* 5:31-35, 1987.

Mason RP, Mottley C: Nitroxide radical adducts in biology: Chemistry, applications, and pitfalls. In: *Electron Spin Resonance*. ed., Symonds MCR, Royal Society of Chemistry, London, 10B, 185, 1987.

McCay PB: Vitamin E: Interactions with free radicals and ascorbate. *Ann Rev Nutr* 5:323-340, 1985.

Meffert H, Diezel W, Sonnichsen N: Stable lipid peroxidation products in human skin: detection, ultraviolet light-induced increase, pathogenic importance. *Experientia* 32:1397-1398, 1976.

Mershon MM, Callahan JF: Exploiting the differences. In: *Animal Models in Dermatology*. ed., Maibach HI, Churchill Livingstone, New York, 36-52, 1975.

Miller DL, Weinstock MA: Nonmelanoma skin cancer in the United States: Incidence. *J Am Acad Dermatol* 30:774-778, 1994.

Miller DM, Aust SD: Studies of ascorbate-dependent, iron catalyzed lipid peroxidation. *Arch Biochem Biophys* 271:113-119, 1989.

Miller DM, Buettner GR, Aust SD: Transition metals as catalysts of 'autoxidation' reactions. *Free Radic Biol Med* 8:95-108, 1990.

Minakata K, Suzuki O, Saito S, Harada N: Ascorbate radical levels in human sera and rat plasma intoxicated with paraquat and diquat. *Arch Toxicol* 67:126-130, 1993.

Minetti M, Forte T, Soriani M, Quaresima V, Menditoo A, Ferrari M: Iron-induced ascorbate oxidation in plasma as monitored by ascorbate free radical formation. *Biochem J* 282:459-465, 1992.

Miyachi Y, Imamura S, Niwa Y: Decreased superoxide dismutase activity by a single exposure to ultraviolet radiation is reduced by liposomal superoxide dismutase pretreatment. *J Invest Dermatol* 89:111-112, 1987.

Miyachi Y, Toda K, Nishigori C, Imamura S: Reactive oxygen species in cutaneous photobiology. *Photomed Photobiol* 11:71-79, 1989.

Miyachi Y, Yoshioka A, Imamura S, Niwa Y: The cumulative effect of continual oxidative stress to skin and cutaneous aging. In: *Cutaneous Aging*, eds. AM Klingman. and Y Takase, University of Tokyo Press, Tokyo, 435-447, 1988.

Moan J: UV-A radiation, melanoma induction, sunscreens, solaria and ozone reduction. *J Photochem Photobiol B* 24:210-203, 1994.

Moan J, Dahlback A, Henriksen T, Magnus K: Biological amplification factor for sunlight-induced nonmelanoma skin cancer at high latitudes. *Cancer Res* 49:207, 1989.

Molin L, Wester PO: Iron content in normal and psoriatic epidermis. *Acta Dermato Venerol* 53:473-476, 1973.

Monboisse JC, Borel JP: Oxidative damage to collagen. In: *Free Radicals and Aging*. ed. I. Emerit and B. Chance, Birkhauser Verglag Basel, Switzerland, 323-327, 1992.

Monteiro HP, Winterbourn CC: The superoxide-dependent transfer of iron from ferritin to transferrin and lactoferrin. *Biochem J* 256:923-928, 1988.

Mukai FH, Goldstein BD: Mutagenicity of malondialdehyde, a decomposition product of peroxidized polyunsaturated fatty acids. *Science*. 191:868-869, 1976.

Mukai K, Sawada K, Kohno Y, Terao J: Kinetic study of the prooxidant effect of tocopherol: hydrogen abstraction from lipid hydroperoxides by tocopheroxyls. *Lipids* 28:747-752, 1993.

Murakami J, Okazaki M, Shiga T: Near UV-induced free radicals in ocular lens, studies by ESR and spin trapping. *Photochem Photobiol* 49:465-473, 1989.

Navas P, Villalba JM, Cordoba F: Ascorbate function at the plasma membrane. *Biochim Biophys Acta* 1197:1-13, 1994.

Neta P, Huie RE, Ross AB: Rate constants for reactions of peroxyl radicals in fluid solutions. *J Phys Chem Ref Data* 19:413-513, 1990.

Newcomb SA, Culling-Berglund AJ, Davis TP: Endogenous levels of beta-carotene in human buccal mucosa cells by reversed-phase high-performance liquid chromatography. *J Chromatography* 526:47-58, 1990.

Nielsen H: Covalent binding of peroxidized lipid to protein: III. Reaction of individual phospholipids with different proteins. *Lipids* 16:215, 1981.

Niki E: Free radical initiators as source of water- or lipid-soluble peroxyl radicals. *Methods Enzymol* 186:100-108, 1990.

Niki E: Vitamin C as an antioxidant. *World Rev Nutr Diet* 64:1-30, 1991.

Nishi J, Ogura R, Sugiyama M, Hidaka T, Kohno M: Involvement of active oxygen in lipid peroxide radical reaction of epidermal homogenate following ultraviolet light exposure. *J Invest Dermatol* 97:115-119, 1991.

Nishikimi M: Oxidation of ascorbic acid with superoxide anion generated by the xanthine-xanthine oxidase system. *Biochem Biophys Res Comms* 63:463-468, 1975.

Niwa Y: Superoxide dismutase. *Biomed Ther* 19:30-34, 1987.

Noble WC: Microbiology of human skin. *Acta Dermatolovenerologica* (Stockholm) 54:49, 1991.

Nohl H, Stolze K, Napetschnig S, Ishikawa T: Is oxidative stress primarily involved in reperfusion injury of the ischemic heart? *Free Radic Biol Med* 11:581-588, 1991.

Norins AL: Free radical formation in the skin following exposure to ultraviolet light. *J Invest Dermatol* 39:445-448, 1962.

Norkus EP, Bryce GF, Bhagavan HN: Uptake and bioconversion of α-tocopheryl acetate to α-tocopherol in skin of hairless mice. *Photochem Photobiol* 57:613-615, 1993.

Oberley LW, Oberley TD: Free radicals, cancer, and aging. In: *Free Radicals, Aging, and Degenerative Diseases*. ed. AR Liss, 325-371, 1981.

Oberley TD, Oberley LW, Slattery AF, Lauchner LJ, Elwell JH: Immunohistochemical localization of antioxidant enzymes in adult syrian hamster tissues and during kidney development. *Amer J Path* 137:199-214, 1990.

Ogura R, Sugiyama M, Nishi J, Haramaki N: Mechanism of lipid radical formation following exposure of epidermal homogenate to ultraviolet light. *J Invest Dermatol* 97:1044-1047, 1991.

Ogura R, Sugiyama M, Sakanashi T, Hidaka T: Role of oxygen in lipid peroxide formation of skin exposed to ultraviolet light. In: *The Biological Role of Reactive Oxygen Species in Skin*. eds. O Hayaishi, S Imamura, Y Miyachi. Elsevier, New York, pp. 55-63, 1987.

Ohara T, Sasaki R, Shibuya D, Asaki S, Toyota T: Effect of omeprazole on ascorbate free radical formation. *Tohoku J Exp Med* 167:185-188, 1992.

Orr WC, Sohol RS: Extension of life-span by overexpression of superoxide dismutase and catalase in *Drosophila melanogaster*. *Science* 263:1128-1130, 1994.

Packer JE, Willson RL, Bahnemann P, Asmus KD: Electron transfer reactions of halogenated aliphatic peroxyl radicals: measurement of absolute rate constant by pulse radiolysis. *J Chem Soc Perkin Trans II* 2:296-299, 1980.

Packer L: Vitamin E- biological activity and health benefits: summing-up overview. *German International Workshop on α-tocopherol*. Kluvensiek, Germany, Jan. 31-Feb 5, 1991.

Palmer RMJ, Ferrige AG, Moncada S: Nitric oxide release accounts for the biological activity of endothelium-derived relaxing factor. *Nature* 327:524-526, 1987.

Pathak MA, Stratton K: Free radicals in human skin before and after exposure to light. *Arch Biochem Biophys* 123:468-476, 1968.

Patterson LK: Studies of radiation-induced peroxidation in fatty acid micelles. In: *Oxygen and Oxy-Radicals in Chemistry and Biology*. eds. MAJ Rodgers, EL Powers. Academic Press: New York, 89-96, 1981.

Pauling L: Effect of ascorbic acid on incidence of spontaneous mammary tumors and UV light-induced skin tumors in mice. *Am J Clin Nutr* 54:1252S-5S, 1991.

Pelizzetti E, Meisel D, Mulac WA, Neta P: On the electron transfer from ascorbic acid to various phenothiazine radicals. *J Am Chem Soc* 101:6954-6959, 1979.

Pence BC, Naylo MF: Effects of single dose ultraviolet radiation on skin superoxide dismutase, catalase, and xanthine oxidase in hairless mice. *J Invest Dermatol* 95:213-216, 1990.

Picardo M, Zompetta C, De Luca A, Faggioni A, Nazzaro-Porro M, Passi S: Squalene peroxides may contribute to ultraviolet light-induced immunologic effects. *Photodermatol Photoimmunol Photomed* 8:105-110, 1991.

Pietri S, Culcasi M, Stella L, Cozzone PJ: Ascorbyl free radical as a reliable indicator of free-radical-mediated myocardial ischemic and post-ischemic injury. *Eur J Biochem* 193:845-854, 1990.

Pietri S, Seguin JR, D'Arbigny P, Culcasi M: Ascorbyl free radical: A noninvasive marker of oxidative stress in human open-heart surgery. *Free Radic Biol Med* 16:523-528, 1994.

Pollitt N: β-Carotene and photodermatoses. *Br J Dermatol* 93:721-724, 1975.

Poole CP Jr, Farach HA: *Handbook of Electron Spin Resonance*. Data Sources, Computer Technology, Relaxation, and ENDOR. American Institute of Physics, New York, 1994.

Potapenko AY, Abijev GA, Pitsov MY, Roschchupkin DI, Vladirov YA, Pliquett F, Ermolayev AV, Sarycheva IK, Evstigneeva RP: PUVA induced erythema and changes in mechanoelectrical properties of skin. Inhibition of tocopherols. *Arch Dermatol Res* 276:12-16, 1984.

Priestley JO, Foster RC: Amount of ascorbic acid in normal epidermis. *J Invest Dermatol* 32:3, 1959.

Pugliese PT, Lampley CB: Biochemical assessment of the anti-aging effects of cosmetic products. *J Appl Cosmet* 3:129-138, 1985.

Punnonen K, Puntala A, Jansen CT, Ahotupa M: UVB irradiation induces lipid peroxidation and reduces antioxidant enzyme activities in human keratinocytes in vitro. *Acta Derm Venereol* (Stockholm) 71:239-273, 1991.

Raes M, Michiels C, Remacle J: Comparative study of the enzymatic defense systems against oxygen-derived free radicals: The key role of glutathione peroxidase. *Free Radic Biol Med* 3:3-7, 1987.

Ramakrishnan N, Kalinich JF, McClain DE: Membrane lipid peroxidation initiates radiation-induced apoptosis. *FASEB J* in press:1995b.

Ramakrishnan N, Kalinich JF, McClain DE: Membrane lipid peroxidation initiates radiation-induced apoptosis. Radiation Research Society Meeting 43rd, 225, 1995a.

Ramakrishnan N, McClain DE, Catravas GN: Membranes as sensitive targets in thymocyte apoptosis. *Int J Rad Biol* 63:693-701, 1993.

Record IR, Dreosti IE, Konstantinopoulos M, Buckley RA: The influence of topical and systemic vitamin E on ultraviolet light-induced skin damage in hairless mice. *Nutr Cancer* 16:219-225, 1991.

Rees S, Slater TF: Ascorbic acid and lipid peroxidation: The cross-over effect. *Acta Biochim Biophys Hung* 22:241-249, 1987.

Retsky KL, Freeman MW, Frei B: Ascorbic acid oxidation product (s) protect human low density lipoprotein against atherogenic modification. *J Biol Chem* 268:1304-1309, 1993.

Richard S, de Rigal J, de Lacharriere O, Berardesca E, Leveque JL: Noninvasive measurement of the effect of lifetime exposure to the sun on the aged skin. *Photodermatol Photoimmunol Photomed* 10:164-9, 1994.

Riesz P, Berdahl D, Christman CL: Free radical generation by ultrasound in aqueous and nonaqueous solutions. *Environ Health Perspective* 64:233-252, 1985.

Rocchi E, Cassanelli M, Borghi A, Paolillo F, Pradelli M, Pellino S, Vezzosi A, Gallo E, Baccarani Contri M, Ventura E: Liver overload and desferrioxamine treatment of porphria cutanea tarda. *Dermatologica* 182:27-31, 1991.

Roffo AH: Cancer and sun: Carcinomas and sarcomas caused by the action of sunlight on skin. *Bull Cancer* 23:590-616, 1934.

Roginsky VA, Stegmann HB: Ascorbyl radical as natural indicator of oxidative stress: Quanititative regularities. *Free Radic Biol Med* 17:93-103, 1994.

Rosario R, Mark GJ, Parrish JA, Mihm MC Jr: Histological changes produced in skin by equally erythemogenic doses of UV-A, UV-B, UV-C and UV-A with psoralens. *Br J Derm* 101:299-308, 1979.

Rose RC, Bode AM: Biology of free radical scavengers: An evaluation of ascorbate. *FASEB J* 7:1135-1142, 1993.

Roshchupkin D, Pistsov M, Potapenko A: Inhibition of ultraviolet light-induced erythema by antioxidants. *Arch Dermatol Res* 266:91-94, 1979.

Ross AB, Mallard WG, Helman WP, Buxton, Huie RE, Neta P: NDRL-NIST Solution Kinetics Database: -Ver. 2.0. Gaithersburg; NIST, 1994.

Rozell B, Hansson HA: Immunohistochemical localization of thioredoxin and thioredoxin reductase in adult rats. *Eur J Cell Biol* 38:79-86, 1985.

Samuni A, Mitchell JB, DeGraff W, Krishna CM; Samuni U; Russo A: Nitroxide SOD-mimics: Modes of action. *Free Rad Res Comms* 12-13:187-194, 1991.

Sasaki R, Kobayasi T, Kurokawa T, Shibuya D, Tero-Kubota S: Significance of the equilibrium constant between serum ascorbate radical and ascorbic acids in man. *Tohoku J Exp Med* 144:203-210, 1984.

Sasaki R, Kurokawa T, Shibuya D: Factors influencing ascorbate free radical formation. *Biochem Intl* 10:155-163, 1985.

Sasaki R, Kurokawa T, Tero-Kubota S: Ascorbate radical and ascorbic acid level in human serum and age. *J Gerontology* 1:26-30, 1983.

Sasaki R, Kurokawa T, Tero-Kubota S: Nature of serum ascorbate radical and its quantitative estimation. *Tohoku J Exp Med* 136:113-119, 1982.

Scarpa M, Stevanato R, Viglino P, Rigo A: Superoxide ion as active intermediate in the autoxidation of ascorbate by molecular oxygen. *J Biol Chem* 258:6695-6697, 1983.

Schallreuter KU, Hordinsky MK, Wood JM: Thioredoxin reductase. *Arch Dermatol* 123: 615-619, 1978.

Schallreuter KU, Wood JM: Free radical reduction in the human epidermis. *Free Radic Biol Med* 6, 519-532, 1989.

Sharma MK, Buettner GR: Interaction of vitamin C and vitamin E during free radical stress in plasma: An ESR study. *Free Radic Biol Med* 14:649-653, 1993.

Sharma MK, Buettner GR, Spencer KT, Kerber RE: Ascorbyl free radical as a real-time marker of free radical generation in briefly ischemic and reperfused hearts. *Circ Res* 74:650-658, 1994.

Sheehan DC; Harpchak BB: *Theory and Practice of Histotechnology*. 2nd ed. Battelle Press: Columbus, OH 1987.

Shibamoto T: The role of lipid peroxidation caused by ultraviolet light in skin diseases. *J Toxicol* 13:193-202, 1994.

Shindo Y, Witt E, Han D, Epstein W, Packer L: Enzymatic and non-enzymatic antioxidants in epidermis and dermis of human skin. *J Invest Dermatol* 102:122-124, 1994.

Shindo Y, Witt E, Han D, Packer L: Dose-response effects of acute ultraviolet irradiation on antioxidants and molecular markers of oxidation in murine epidermis and dermis. *J Invest Dermatol* 102:470-475, 1994.

Simic MG, Jovanovic SV: Antioxidation mechanisms of uric acid. *J Am Chem Soc* 111:5778-5782, 1989.

Stark JM, Jackson SK, Rowlands CC, Evans JC: Increases in ascorbate free radical concentration after endotoxin in mice. In: *Free Radicals: Methodology and Concepts*, ed., Rice-Evans C, Halliwell B., Richelieu, London; 201-209, 1988.

Stegmann HB, Schuler P, Westphal S, Wagner E: Oxidative stress of crops monitored by EPR. *Z Naturforsch C* 48:766-772, 1993.

Stuttgen G, Schaefer E: Vitamine und haut. In: *Funktionelle Dermatologie*. eds. G. Stuttgen, E. Schaefer, Springer, Berlin Heidelberg New York, 78-79, 1974.

Sugiura K, Iida Y, Ohgoshi H, Ueda H, Hirano K, Adachi T: Studies on superoxide dismutase in human skin. Contents of superoxide dismutase and lipoperoxide in skin of patients with atopic dermatitis. *Jpn J Dermatol* 96: 165-170, 1986.

Sugiura K, Ueda H, Hirano K, Adachi T: Studies on superoxide dismutase in human skin. Contents of superoxide dismutase and lipoperoxide in normal human skin. *Jpn J Dermatol* 95:1541-1545, 1985.

Sugiyama M, Kaneko N, Kagiyama A, Morakata S, Ogura R: Lipid peroxide and free radical formation in the epidermis following single exposure of ultraviolet light. *J Kurume Med Assoc* 47:346-350, 1984.

Symons MRC: *Chemical and Biological Aspects of Electron Paramagnetic Resonance Spectroscopy*. Van Norstrand Reinhold, London, 1978.

Taira J, Mimura K, Yoneya T, Hagi A, Murakami A, Makino K: Hydroxyl radical formation by UV-irradiated epidermal cells. *J Biochem* 111:693-695, 1992.

Tamba M, O'Neill P: Redox reactions of thiol free radicals with the antioxidants ascorbate and chlorpromazine: Role in radioprotection. *J Chem Soc Perkin Trans II* 1681-1685, 1991.

Taylor HR, West SK, Rosenthal FS, Munoz B, Newland H, Abbey H, Emmett EA: Effect of ultraviolet radiation on cataract formation. *New Eng J Med* 319:1429-33, 1988.

Thomas JP, Maiorino M, Ursis F, Girotti AW: Protective action of phospholipid hydroperoxide glutathione peroxidase against membrane-damaging lipid peroxidation. *J Biol Chem* 265:454-461, 1990.

Thompson DF: Deferoxamine treatment of malaria. *Annals Pharmacotherapy* 28:602-3, 1994.

Thompson SC, Jolley D, Marks R: Reduction of solar keratoses by regular sunscreen use. *N Engl J Med* 329:1147-1151, 1993.

Thornally PJ: Theory and biological application of the electron spin resonance technique of spin trapping, *Life Chem Rep* 4:57-112, 1986.

Timmins GS, Davies MJ: Free radical formation in murine skin treated with tumour promoting organic peroxides. *Carcinogensis* 14:1499-1503, 1993.

Tomasi A, Albano E, Bini A, Iannone AC, Vannini V: Ascorbyl radical is detected in rat isolated hepatocytes suspensions undergoing oxidative stress: and early index of oxidative damage in cells. *Advances in the Biosciences* 76:325-334, 1989.

Trenam CW, Blake DR, Morris CJ: Skin inflammation: Reactive oxygen species and the role of iron. *J Invest Dermatol* 99:675-682, 1992.

Trevithick JR, Xiong H, Lee S, Shun DT, Sanford SE, Karlik SJ, Norley C, Dilworth GR: Topical tocopherol acetate reduces post-UVB, sunburn-associated erythema, edema and skin sensitivity in hairless mice. *Arch Biochem Biophys* 269:575-582, 1992.

Unna PG: *The Histopathology of the Diseases of the Skin*. Edinburgh, 1894.

Vahlquist A, Lee JB, Michaelsson G, Rollman O: Vitamin A in human skin: II concentrations of carotene, retinol, and dehydroretinol in various components of normal skin. *J Invest Dermatol* 79:94-97, 1982.

van Welden H, de Gruijl FR, van der Putte SCJ, Toonstra J, van der Leun JC: The carcinogenic risks of modern tanning equipment: Is UV-A safer than UVB? *Arch Dermatol Res* 280:300-307, 1988.

Vessey DA, Lee KH: Inactivation of enzymes of the glutathione antioxidant system by treatment of cultured human keratinocytes with peroxide. *J Invest Dermatol* 100:829-833, 1993.

Wardman P: Reduction potentials of one-electron couples involving free radicals in aqueous solution. *J Phys Chem Ref Data* 18:1637-1755, 1989.

Weinberg GA: Iron chelators as therapeutic agents against Pneumocystis carinii. *Antimicrobial Agents Chemotherapy* 38:997-1003, 1994.

Weintraub LR, Demis DJ, Conrad ME, Crosby WH: Iron excretion by the skin. Selective localization of iron in epithelial cells. *J Lab Clin Med* 46:121-126, 1965.

Weissberger A, LuValle JE, Thomas DS: Oxidation processes. XVI. The autoxidation of ascorbic acid. *J Am Chem Soc* 65:1934-1939, 1943.

Weiter JJ, Finch ED: Paramagnetic species in cataractous human lenses. *Nature* 254:536-537, 1975.

Wertz JE, Bolton JR: *Electron Spin Resonance*. McGraw-Hill, New York, 1972.

Williams NH, Yandell JK: Outer-sphere electron-transfer reaction of ascorbate anions. *Aust J Chem* 35:1133-1144, 1982.

Williams NH, Yandell JK: Reduction of oxidized cytochrome c by ascorbate ion. *Biochim Biophys Acta* 810:274-277, 1985.

Windholz M: Tocopherol. In: *The Merck Index*, 10th edn. Merck & Co., Rahway, NJ, 1983.

Winterbourn CC: Superoxide as an intracellular radical sink. *Free Radic Biol Med* 14:85-90, 1993.

Wolf P, Donawho CK, Kripke ML: Effect of sunscreens on UV radiation-induced enhancement of melanoma growth in mice. *J Natl Cancer Inst* 86:99-105, 1994.

Yin D, Lingnert H, Ekstrand B, Brunk UT: Fenton reagents may not initiate lipid peroxidation in an emulsified linoleic acid model system. *Free Radic Biol Med* 13:543-556, 1992.

Yohn JJ, Norris DA, Yrastorza DG, Buno IJ, Leff JA, Hake SS, Repine JE: Disparate Antioxidant enzyme activities in cultured human cutaneous fibroblasts, keratinocytes, and melanocytes. *J Invest Dermatol* 97:405-409, 1991.

Zheng P, Klingman LH: UVA-Induced changes in hairless mouse skin: A comparison to UVB-induced damage. *J Invest Dermatol* 100:194-199, 1993.

Zurer PS: Ozone depletion's recurring surprises challenge atmospheric scientists. *Chem Eng News* 71:8-18, 1993.